UNIVERSIDADE DE LISBOA

FACULDADE DE MEDICINA DE LISBOA

Inhibitory Circuitry in Motor Neuron Disease: Changes in Spinal and Corticospinal Mechanisms in Amyotrophic Lateral Sclerosis and its Variants

José Filipe Oliveira Castro

Supervisor: Mamede Alves de Carvalho, MD, Ph.D.

Tese especialmente elaborada para obtenção do grau de Doutor em Ciências Biomédicas, especialidade de Neurociências

2024

UNIVERSIDADE DE LISBOA

FACULDADE DE MEDICINA DE LISBOA

Inhibitory Circuitry in Motor Neuron Disease: Changes in Spinal and Corticospinal Mechanisms in Amyotrophic Lateral Sclerosis and its Variants

José Filipe Oliveira Castro

Supervisor: Mamede Alves de Carvalho, MD, Ph.D.

Tese especialmente elaborada para obtenção do grau de Doutor em Ciências Biomédicas

Especialidade de Neurociências

Júri

Presidente:

- Doutora Helena Maria Ramos Marques Coelho Cortez Pinto, Professora Catedrática e Presidente do Conselho Científico da Faculdade de Medicina da Universidade de Lisboa

Vogais:

- PhD Hatice Tankisi, Full Professor da Aarhus University (Dinamarca)
- Doutora Liliana Rita Velindro Letra, Professora Auxiliar Convidada da Faculdade de Medicina da Universidade de Coimbra
- Doutor Mamede Alves de Carvalho, Professor Catedrático da Faculdade de Medicina da Universidade de Lisboa (Orientador)
- Doutor João Nuno Marques Parracho Guerra da Costa, Professor Associado da Faculdade de Medicina da Universidade de Lisboa
- Doutor Tiago Vaz Maia, Professor Associado da Faculdade de Medicina da Universidade de Lisboa
- Doutora Carla Cristina Paulo Gabriel Bentes, Professora Auxiliar Convidada da Faculdade de Medicina da Universidade de Lisboa

2024

Todas as afirmações efetuadas no presente documento são da exclusiva responsabilidade do autor, não cabendo qualquer responsabilidade à Faculdade de Medicina de Lisboa pelos conteúdos nele apresentados.

A impressão desta tese foi aprovada pelo Conselho Científico da Faculdade de Medicina de Lisboa em reunião de 23 de janeiro de 2024.

TABLE OF CONTENTS

List of Publications

The following manuscripts were published in international peer-reviewed journals derived from the work involved in the development of this thesis.

Accepted

Study I: Castro J, Swash M, de Carvalho M. **The cutaneous silent period in motor neuron disease.** Clinical Neurophysiology 2021, 132(2), pp.660-665. JIF – 4.861 [Q1] https://doi.org/10.1016/j.clinph.2020.10.033

Study II: Castro J, Swash M, de Carvalho M. **The cutaneous silent period as a measure of upper motor neuron dysfunction in amyotrophic lateral sclerosis.** Neurophysiologie Clinique 2023, 53 (4), 102843. JIF – 3.1 [Q2] https://doi.org/10.1016/j.neucli.2022.102843

Study III: Castro J, Pedrosa T, de Castro I, Swash M, de Carvalho M. **Mirror movements – A simple algorithm for mirror activity signal processing and normative values.** Neuroscience Letters 2023, 803 137186. JIF – 3.197 [Q2] https://doi.org/10.1016/j.neulet.2023.137186

Study IV: Castro, J., Pedrosa, T., Alves, I., Simão, S., Swash, M., & de Carvalho, M. **A neurophysiological approach to mirror movements in amyotrophic lateral sclerosis.** Clinical Neurophysiology 2023, 158, 27–34. Advance online publication. JIF – 4.861 [Q1] https://doi.org/10.1016/j.clinph.2023.12.002

Study V: Castro, J., Oliveira Santos, M., Swash, M., & de Carvalho, M. **Segmental motor neuron dysfunction in amyotrophic lateral sclerosis: Insights from H reflex paradigms.** Muscle & nerve 2024, Advance online publication. JIF – 3.4 [Q2] https://doi.org/10.1002/mus.28035

Acknowledgments

This thesis is the result of a collective effort, and I am deeply appreciative of the support and guidance I received from all those who have been a part of this academic journey. Your contributions have left an indelible mark on the development of this work. My deep appreciation goes to all who have contributed, in one way or another, but there are a few I wish to mention.

This work has been supported by Biogen Inc. I express my gratitude to my funders for their support, which has enabled me to conduct this research aimed at advancing our understanding of amyotrophic lateral sclerosis.

I want to express my heartfelt gratitude to all the patients and their families who graciously participated in our research. Your willingness to share your stories and undergo extensive neurophysiological studies made this doctoral thesis possible.

I also extend my sincere gratefulness to all the friends and coworkers who have volunteered as healthy controls for all the experiments. Your disposition and patience to endure the countless sessions of tests was invaluable.

Professor Mamede de Carvalho, my supervisor, who throughout these many years has taught, guided, encouraged, and allowed me to grow and develop my skills as a neurophysiologist and as a clinical investigator. I am both humbled and proud to have you as my mentor.

Everyone in the EMG Laboratory, which has been my “home away from home” for the past 20 years. Thank you for all the support, encouragement, and friendship.

João Costa, a friend who, through many years, has always had encouraging and teaching advice to give, be it in life, work, or academic questions.

My parents, who have always supported and encouraged me to always give my best in everything I do. Their love and caring have been a constant presence in life.

My wife and partner in life Vanda, who is always there, for better or worse, and without whom I would have been lost. Thank you for putting up with my ramblings during the long nights and weekends of these past years, and for taking care of everything in real life when I was deeply lost in all this process.

To Hugo, the son all parents dream of having. Thank you for making me want to do and be better as a person, husband, and parent.

Summary

Introduction

Amyotrophic Lateral Sclerosis (ALS) is a relentlessly progressive and devastating neurodegenerative disorder that primarily affects motor neurons within the spinal cord, brainstem and brain. This debilitating condition culminates in the gradual loss of motor function, leading to muscle weakness, atrophy, and eventually paralysis, typically with a fatal outcome within a few years after the first symptoms. Despite decades of research, the precise etiology of ALS remains elusive, and there is currently no cure for this devastating disease.

The pathophysiology of ALS is extraordinarily complex, involving an intricate interplay of genetic, environmental, and cellular factors. Among the multifaceted aspects contributing to the disease's onset and progression, the role of inhibitory spinal and supraspinal mechanisms is a compelling area of investigation. These mechanisms play a pivotal yet still not completely understood role in modulating the excitability of motor neurons and the integrity of motor circuits, thereby influencing the manifestation and progression of ALS.

There is an accumulated amount of evidence from animal, in vitro, histopathological, imaging, and neurophysiological studies implying cortical inhibitory mechanisms, mainly controlled by GABAergic and glycinergic interneurons, in ALS pathophysiology. The pathological decrease in inhibitory control of motoneurons excitability contributes, and possibly leads, to characteristic degeneration of the motor system. Regarding segmental spinal control of motor function, these mechanisms are much less studied in ALS, despite their possible significant role to the pathophysiology of this disease.

Objectives

The overall objective of this thesis was to advance our comprehension of the physiological and pathophysiological aspects of spinal and supraspinal inhibitory pathways in ALS. To achieve this goal, a series of carefully designed experiments employing diverse neurophysiological methods were undertaken. We used techniques such as the cutaneous silent period (CutSP), electromyographic quantification of mirror movements, and the H reflex, as well as several conditioning paradigms of this

reflex response, to interrogate inhibitory interneuron function, with a particular emphasis in segmental spinal mechanisms. We also aimed to link changes in these parameters to the clinical picture of patients, in particular to the dysfunction of upper motor neurons.

Materials and Methods

The studies here described were performed at the *Laboratório de EMG e Potenciais Evocados do Centro Hospitalar Universitário Lisboa Norte*, and at the *Instituto de Fisiologia da Faculdade de Medicina da Universidade de Lisboa - Instituto de Medicina Molecular João Lobo Antunes* (MCarvalho unit).

For the CutSP, measurements were made both in upper and lower limbs. In the upper limb, the target muscle was the abductor digiti minimi (ADM), and stimulation of cutaneous fibres was applied to the ipsilateral V^{th} finger using ring electrodes. In the lower limb, the target muscle was the tibialis anterior (TA), and stimulation of cutaneous fibres was applied to the sural nerve, posteriorly to the lateral malleolus. We performed measurements in two different conditions regarding the contralateral muscle to the one assessed: at rest, and during a maximal isometric contraction. Transcranial magnetic stimulation (TMS) was also performed to obtain an objective marker of corticospinal changes. We recruited patients with different phenotypes of motor neuron disease (typical ALS, primary lateral sclerosis (PLS) and progressive muscle atrophy (PMA)).

For the quantification of mirror activity (MA), we first developed a mathematical algorithm for automatic analysis of EMG signal. We validated the algorithm in a group of healthy subjects. Mirror activity was assessed in upper (ADM) and lower limbs (TA), on both sides, during a brief isometric full force contraction in one muscle and measuring muscle activity from the homonymous contralateral muscle. Afterward we recruited a group of ALS subjects and applied the same protocol of mirror activity quantification. We also used conventional TMS, including the quantification of the ipsilateral cortical silent period.

For the study of the H reflex we devised 3 sets of experiments, using paradigms of modulation of the test reflex response in ALS. We assessed recurrent inhibition, using a paired pulse technique stimulating the posterior tibial nerve. Presynaptic

inhibition of Ia afferents was evaluated by conditioning the H reflex with stimulation of the common peroneal nerve and assessing the D1 phase of inhibition. Finally, we studied the modulation of the H reflex after cutaneous stimulation of the lateral dorsum of the foot (distal sural nerve), a modulation inhibitory paradigm that is considered as postsynaptic and mediated by glycine.

Results

The onset latency of the cutaneous silent period was significantly increased in patients, when compared to healthy subjects, both in upper and lower limbs. This change was present in all disease phenotypes, including PMA patients. In parallel, a significant reduction of the amount of EMG suppression was also seen in limbs with marked UMN involvement. Interestingly, the changes seen in the first condition (contralateral muscle at rest) were partially reverted in the second condition (maximal contralateral contraction) in patients without clinical signs of UMN dysfunction. Furthermore, the onset latency of the CutSP was significantly related to the amount of clinical signs of UMN dysfunction and to changes in TMS. In the upper limb, the onset latency and duration of the CutSP were significant predictors of the amount of UMN signs.

The algorithm developed for quantification of MA was very well suited for latency markings, with an ICC of 0.998 ($p < 0.001$) with markings defined by two experienced neurophysiologists. In healthy subjects, there was a moderate positive correlation between age and MA in the ADM and in the TA. There was also significantly more MA on the dominant side. In ALS subjects, there was a significant increase in MA compared to healthy subjects, in all 4 muscles assessed. Interestingly, the side-to-side difference seen in healthy subjects is not present in ALS patients. Additionally, patients with normal TMS results had more mirror activity than healthy subjects, while patients with abnormal TMS results had more mirror activity than patients with normal TMS results. This pattern was also observed for the ipsilateral silent period.

There were no significant differences between ALS patients and healthy controls regarding the parameters of the standard H reflex, particularly in the H_{max}/M_{max} ratio. As for the conditioning paradigms, ALS patients exhibited significantly less recurrent inhibition (0.35 vs 0.11; $p = 0.036$), presynaptic inhibition of Ia terminals (1.0 vs 5.0; $p = 0.001$), and inhibition after cutaneous stimulation (0.0 vs 2.5; $p = 0.031$),

when compared to healthy controls. Interestingly, the amount of UMN signs was a significant predictor of both recurrent inhibition ($p = 0.010$) and presynaptic inhibition ($p < 0.001$), but not of inhibition after cutaneous stimulation ($p = 0.661$).

Discussion

The protocol implemented for the study of the CutSP is simple, well tolerated, and easily implemented in the routine neurophysiological assessment of ALS patients. In ALS patients, the onset latency of the CutSP is consistently increased, and the amount of EMG suppression decreased in limbs with signs of UMN dysfunction. Both these changes seem related to the severity of UMN dysfunction, as measured by clinical assessment and TMS responses. This confirms the presence of dysfunction in segmental spinal inhibitory circuits associated with supraspinal modulation of motoneuron excitability.

The quantification of MA using the algorithm developed is simple and practical. It allows for objective measurement and comparison between subjects. The amount of MA is significantly increased in ALS, both in upper and lower limbs. In upper limbs, MA is particularly increased in subjects with abnormal ipsilateral silent period, which depend on the integrity of transcallosal inhibitory pathways. The amount of MA is higher in patients with abnormal TMS, suggesting a link between callosal and corticospinal dysfunction.

The changes disclosed by all H reflex modulation paradigms tested underscore that extensive changes of segmental spinal inhibitory circuits are present in ALS. This is of particular interest given that the group of patients studied had very mild LMN involvement. These alterations were noticeable in both recurrent, presynaptic, and postsynaptic inhibitory mechanisms, rendering the corticomotoneuronal synapse notably vulnerable to hyperexcitation. In particular our results support glycinergic spinal cord dysfunction in ALS patients, as suggested by studies in the animal model.

Conclusions

Several inhibitory mechanisms, both at the cortical and at the segmental spinal level are altered in ALS. These changes are present in the early stages of the disease and are intrinsically linked to involvement of the UMN. These findings suggest that dysfunctional inhibitory interneurons, both at the cortical (as shown elsewhere) and at

the segmental spinal levels is a major feature in ALS, and potentially one of the drivers of the neurodegeneration characteristic of this devastating disease.

Keywords (6)

Amyotrophic lateral sclerosis; motor neuron disease; interneurons; inhibitory circuits; segmental spinal inhibition; cortical inhibition

Resumo

Introdução

A Esclerose Lateral Amiotrófica (ELA) é uma doença neurodegenerativa rapidamente progressiva que principalmente afeta os neurónios motores da medula espinal, do tronco cerebral, e do córtex. Deste processo resulta a gradual perda da função motora e da capacidade respiratória, em geral originando a morte poucos anos após os primeiros sintomas. Apesar de décadas de intensa investigação, a etiopatogenia desta doença permanece elusiva, não existindo atualmente cura para esta doença devastadora.

A origem da ELA é extraordinariamente complexa, envolvendo uma intricada interação de fatores genéticos, ambientais e celulares. Entre os aspetos multifacetados que contribuem para o início e progressão da doença, o papel dos mecanismos inibitórios espinhais e supraespinhais é uma área de investigação fascinante. Estes mecanismos desempenham um papel crucial, mas ainda não completamente compreendido, na modulação da excitabilidade dos neurónios motores e na integridade dos circuitos motores, influenciando assim o início e progressão da ELA.

Há uma significativa quantidade de evidências de estudos em animais, in vitro, histopatológicos, imagem e neurofisiológicos que implicam mecanismos inibitórios corticais, principalmente controlados por interneurónios GABAérgicos e glicinérgicos, na fisiopatologia da ELA. A disfunção do controle inibitório da excitabilidade dos motoneurónios contribui para, e possivelmente origina, a típica degeneração do sistema motor. Em relação ao controle da função motora a nível segmentar da medula espinhal, esses mecanismos estão menos estudados na ELA, apesar de seu potencial relevante papel na fisiopatologia desta doença.

Objetivos

O objetivo geral desta tese foi aumentar a compreensão dos aspetos fisiológicos e fisiopatológicos das vias inibitórias espinhais e supraespinhais na ELA. Para alcançar este objetivo, uma série de estudos cuidadosamente projetados, utilizando diversas técnicas neurofisiológicas, foram realizados. Em particular, foram utilizadas técnicas como o período de silêncio cutâneo (CutSP), a quantificação

eletromiográfica de movimentos em espelho e o reflexo H, assim como vários paradigmas de condicionamento deste reflexo, de forma a investigar a função dos interneurónios inibitórios, com ênfase especial nos mecanismos segmentares da medula espinhal. Também procuramos relacionar as alterações desses parâmetros com o quadro clínico, em particular quanto à disfunção do 1º neurónio motor.

Materiais e Métodos

Os estudos aqui descritos foram realizados no Laboratório de EMG e Potenciais Evocados do Centro Hospitalar Universitário Lisboa Norte e no Instituto de Fisiologia da Faculdade de Medicina da Universidade de Lisboa - Instituto de Medicina Molecular João Lobo Antunes (MCarvalho unit).

Para o estudo do CutSP, foram realizados registos nos membros superiores e inferiores. No membro superior, o músculo alvo foi o Abdutor do 5º dedo (ADM), e a estimulação das fibras cutâneas foi aplicada no quinto dedo ipsilateral usando elétrodos de anel. No membro inferior, o músculo alvo foi o tibial anterior (TA), e a estimulação das fibras cutâneas foi aplicada no nervo sural, posteriormente ao maléolo lateral. Foram realizados registos em duas condições diferentes em relação ao músculo contralateral ao avaliado: em repouso e durante contração isométrica máxima. Também foi efetuada estimulação magnética transcraniana (TMS), por forma a obter um marcador objetivo de alterações da via corticoespinhal. Foram incluídos doentes com diferentes fenótipos de doença do neurónio motor (ELA típica, esclerose lateral primária (PLS) e atrofia muscular progressiva (PMA)).

Para a quantificação da atividade em espelho (AE), primeiro desenvolvemos um algoritmo matemático para análise automática do sinal EMG. Validamos o algoritmo num grupo de indivíduos saudáveis. A AE foi avaliada nos membros superiores (ADM) e inferiores (TA), em ambos os lados, durante uma breve contração isométrica máxima de um músculo e medindo a atividade muscular do músculo homónimo contralateral. Posteriormente, estudamos um grupo de doentes com ELA com o mesmo protocolo de quantificação da AE. Também usamos TMS convencional, incluindo a avaliação do período de silêncio cortical ipsilateral.

Para o estudo do reflexo H, elaboramos três paradigmas de modulação deste reflexo na ELA. Avaliamos a inibição recorrente, usando uma técnica de dupla

estimulação do nervo tibial posterior. A inibição pré-sináptica dos aferentes Ia foi avaliada condicionando o reflexo H pela estimulação do nervo peroneal comum e avaliando a fase D1 da inibição. Finalmente, estudamos a modulação do reflexo H após estimulação cutânea do dorso lateral do pé (segmento distal do nervo safeno externo), um paradigma de inibição de modulação que é considerado como pós-sináptico e glicinérgico.

Resultados

Nos doentes com ELA, a latência de início do período de silêncio cutâneo estava significativamente aumentada, quando comparada com indivíduos saudáveis, tanto nos membros superiores como nos membros inferiores. Esta alteração estava presente em todos os fenótipos da doença, incluindo pacientes com PMA, e foi mais pronunciada naqueles com maior envolvimento do 1º neurónio motor. Uma menor supressão do EMG também foi observada nos doentes com mais marcado envolvimento piramidal. Nos doentes com PMA, as alterações observadas na primeira condição (músculo contralateral em repouso) foram parcialmente revertidas na segunda condição (contração contralateral máxima). Adicionalmente, a latência inicial do período de silêncio cutâneo associa-se, significativamente, com a a severidade do compromisso do 1º neurónio motor, tal como avaliado pelos sinais clínicos e pelas alterações observadas na TMS. No membro superior, a latência inicial e a duração do período de silêncio cutâneo foram preditores significativos da disfunção do 1º neurónio motor.

O algoritmo desenvolvido para quantificação da AE foi eficaz na marcação de latências, com um ICC de 0,998 ($p < 0,001$) comparando com marcações definidas por dois neurofisiologistas experientes. Em indivíduos saudáveis, houve uma correlação positiva moderada entre a idade e a AE, tanto no ADM como no TA. A AE foi significativamente mais intensa no lado dominante. Em pacientes com ELA, houve um aumento significativo da AE em comparação com indivíduos saudáveis, em todos os 4 músculos avaliados. Nos doentes, não foi observada esta diferença entre o lado dominante e o não-dominante. Para mais, a AE foi significativamente mais intensa nos doentes com resultados normais na TMS que os controlos, e nos doentes com resultados anormais na TMS quando comparados com aqueles com valores normais

na TMS. Estas diferenças foram replicadas quando considerando o valor do período de silêncio cortical ipsilateral.

Não se observaram diferenças significativas entre pacientes com ELA e controles saudáveis em relação aos parâmetros convencionais do reflexo H, incluindo na razão Hmax/Mmax. Quanto aos paradigmas de condicionamento, os pacientes com ELA apresentaram significativamente menos inibição recorrente (0,35 vs 0,11; p = 0,036), inibição pré-sináptica pela estimulação dos aferentes Ia (1,0 vs 5,0; p = 0,001) e na inibição após estimulação cutânea (0,0 vs 2,5; p = 0,031), em comparação com controles saudáveis. Notavelmente, a severidade dos sinais do 1º neurónio foi um preditor significativo tanto da inibição recorrente (p = 0,010) quanto da inibição pré-sináptica (p < 0,001), mas não da inibição após estimulação cutânea (p = 0,661).

Discussão

O protocolo proposto para o estudo do período de silêncio cutâneo é simples, bem tolerado e facilmente implementado na avaliação neurofisiológica de rotina de pacientes com ELA. Nestes, a latência inicial do período de silêncio cutâneo está atrasada e a supressão do EMG diminuída. O grau destas alterações associa-se com a severidade dos sinais clínicos e neurofisiológicos da disfunção do 1º neurónio motor. Estes resultados suportam a existência de uma disfunção nos circuitos inibitórios segmentares da medula espinhal, em função da sua modulação por vias supraespinhais.

A quantificação da AE usando o algoritmo desenvolvido é simples e prática. Esta abordagem permite uma medição objetiva, assim como fácil comparação entre sujeitos. Nos doentes, a quantidade de AE está significativamente aumentada, quer nos membros superiores, quer nos membros inferiores. Nos membros superiores, a AE está particularmente aumentada naqueles com um anormal período de silêncio cortical ipsilateral, o qual depende da integridade das vias inibitórias transcalosas. Os doentes com resultados anormais na TMS evidenciaram maior intensidade da AE, indicando uma associação entre a disfunção calosa e a lesão da via corticoespinhal.

As alterações observadas nos paradigmas estudados de modulação do reflexo H, suportam uma disfunção nos circuitos inibitórios segmentares da medula espinhal na ELA. Isso é de particular interesse dado que o grupo estudado de doentes tinha

envolvimento ligeiro do 2º neurónio motor. Estas alterações foram observadas nos mecanismos inibitórios recorrentes, pré-sinápticos e pós-sinápticos, incluindo a via glicinérgica, como sugerido pelo modelo animal, tornando a sinapse corticomotoneuronal vulnerável a fenómenos de hiperexcitabilidade,

Conclusões

Vários mecanismos inibitórios, tanto ao nível cortical quanto ao nível segmentar da medula espinhal, estão alterados na ELA. Estas mudanças estão presentes nas fases iniciais da doença e estão fortemente associadas ao envolvimento do 1º neurónio motor. As alterações aqui descritas suportam a presença de interneurónios inibitórios disfuncionais, tanto ao nível segmentar da medula espinhal, como supraespinhais, que podem favorecer o processo neurodegenerativo.

Palavras-chaves (6)

Esclerose lateral amiotrófica; doença do neurónio motor; interneurónios; circuitos inibitórios; inibição espinhal segmentar; inibição cortical

List of Figures

List of Tables

List of abbreviations

AAV	Adeno-associated virus
ADM	Abductor digiti minimi
ALS	Amyotrophic Lateral Sclerosis
ALSFRS	Amyotrophic Lateral Sclerosis Functional Rating Scale
ATP	Adenosine triphosphate
BiPAP	Bi-level positive pressure devices
CMAP	Compound muscle action potential
CMCT	Central motor conduction time
CNS	Central nervous system
CPAP	Continuous positive pressure
CRISPR	Clustered Regularly Interspaced Short Palindromic Repeats
CS	Corticospinal
CSF	Cerebrospinal fluid
CSP	Cortical silent period
CST	Corticospinal tract
CutSP	Cutaneous silent period
DTR	Deep tendon reflexes
EAATs	Excitatory amino acid transporters
ECAS	Edinburgh Cognitive and Behavioral ALS Screen
EEG	Electroencephalography
EMG	Electromyography
fALS	Familial amyotrophic lateral sclerosis
fMRI	Functional magnetic resonance imaging
FTD	Frontotemporal dementia
FUS/TLS	Fused in sarcoma/translated in liposarcoma
FVC	Forced vital capacity
H’	Conditioned H reflex
H'_{Pos}	Amount of inhibition after cutaneous stimulation
H'_{Pre}	Amount of presynaptic inhibition
H'_{RI}	Amount of recurrent inhibition
H_{max}	H reflex of maximum intensity
HRE	Hexanucleotide repeat expansion
ICC	Intraclass Correlation Coefficient
ICF	Intracortical facilitation
IHI	Interhemispheric inhibition
IQR	Interquartile range
ISI	Interstimulus interval
iSP	Ipsilateral silent period

LICI	Long interval intracortical inhibition
LMN	Lower motor neuron
MA	Mirror activity
MEP	Motor evoked potentials
MM	Mirror movements
M_{max}	M wave of maximum amplitude
MND	Motor Neuron Disease
MRC	Medical Research Council
MT	Motor threshold
NFs	Neurofilaments
NIV	Non-invasive ventilation
NMDA	N-methyl-D-aspartate
PAD	Primary afferent depolarization
PBA	Progressive bulbar atrophy
PBP	Progressive Bulbar Palsy
PEG	Percutaneous endoscopic gastrostomy
PET	Positron Emission Tomography
PLS	Primary Lateral Sclerosis
PMA	Progressive Muscular Atrophy
PTN	Posterior tibial nerve
RMT	Resting motor threshold
ROS	Reactive oxygen species
RS	Reticulospinal
rTMS	Repetitive TMS
sALS	Sporadic amyotrophic lateral sclerosis
SICI	Short interval intracortical inhibition
SMA	Secondary motor areas
SOD1	Superoxide dismutase 1
SVC	Slow vital capacity
TA	Tibialis anterior
TDP-43	TAR-DNA binding protein 43
TES	Transcranial electrical stimulation
TMS	Transcranial Magnetic Stimulation
TUDCA	Tauroursodeoxycholic acid
UMN	Upper motor neuron
VS	Vestibulospinal

1. Introduction

The famous French neurologist Jean-Martin Charcot coined the term Amyotrophic Lateral Sclerosis (ALS) in the late 19th century (Charcot, 1874), to characterize individuals experiencing "paralysis with spasms of the arms and primarily the legs (without any sensory impairment), accompanied by gradual muscle wasting, predominantly affecting the upper limbs and trunk" (Eisen, 2007). Over the past 150 years, significant advances have been made in the understanding of ALS since Charcot's initial observations.

The classic and most prevalent form of the disease, which is the most common form of Motor Neuron Disease (MND), involves the degeneration of the primary motor cortex, brainstem, and spinal cord, collectively referred to as ALS. This term also encompasses different syndromes, such as Primary Lateral Sclerosis (PLS), Progressive Muscular Atrophy (PMA), and Progressive Bulbar Palsy (PBP). The recent Gold Coast criteria (Shefner et al., 2020) incorporates PMA as similar to ALS.

Currently, the exact cause of sporadic ALS (sALS) remains unknown, although certain environmental risk factors have been associated with an increased likelihood of developing the disease (Gordon, 2013). Probably the most important disease origin determinant is the personal genetic background, many times associated with a specific mutation, but most of the times related to incompletely known changes in the complex genetic architecture. The pathophysiology of ALS involves various mechanisms, including oxidative damage, mitochondrial dysfunction, defects in axonal transport, and glutamate excitotoxicity (Rothstein, 2009).

Clinical presentation varies significantly due to the distinct involvement of upper motor neurons (UMN) and/or lower motor neurons (LMN). Common symptoms and signs include muscle weakness, muscle wasting, cramps, fasciculations, dysarthria, dysphagia, brisk deep tendon reflexes (DTR), clonus, and spasticity. In some cases, ALS may also be accompanied by frontotemporal dementia (Leigh, 2007). Despite the variability in the onset location, a contiguous spread of the degenerative processes has been suggested (Ravits and La Spada, 2009, Gromicho et al., 2020).

Neurophysiology plays a crucial role not only in diagnosing and monitoring ALS, but also in providing valuable insights into the pathophysiology of the disease.

Transcranial Magnetic Stimulation (TMS) has extensively documented changes in UMN function (Huynh et al., 2016), with a particular focus on cortical inhibition (Ziemann et al., 1997, Zanette et al., 2002a, Shibuya et al., 2017). Some authors have used changes in motor unit firing frequencies as an indicator of UMN dysfunction (de Carvalho et al., 2012). However, identifying UMN changes in the presence of significant LMN dysfunction can be challenging (Pinto et al., 2012). Inhibitory circuits, particularly segmental spinal circuits, have received little attention in ALS research. The role of spinal interneurons, including Renshaw cells, in the pathophysiology of ALS remains largely unknown. While some studies have suggested dysfunction of these specialized neurons (Raynor and Shefner, 1994, Shefner and Logigian, 1998, Howells et al., 2020), there is currently no consensus on their role in ALS (Mazzocchio and Rossi, 2010).

In this thesis, we explore spinal and supraspinal inhibitory mechanisms in ALS/MND patients using different neurophysiological techniques to obtain a deeper understanding of the associated pathophysiological mechanisms.

2. Literature review

2.1. Epidemiology

Epidemiologic studies in rare diseases are subject to significant variability due to differences in study design (prospective vs. retrospective), number and quality of data sources, diagnostic criteria (e.g., inclusion of only classic ALS or inclusion of other variants like PMA and PLS), and delineation of catchment area (province or region level vs. country level vs. continental area). There are also considerable differences in the number of ALS epidemiological studies according to region. In a recent systematic review of the global prevalence and incidence of ALS (Xu et al., 2020), more than half of the studies included in the analysis were from European countries. Nevertheless, geography may contribute to different findings in different countries and regions, consistent with the distribution of genetic risk factors in ALS. In Europe, for example, there is a trend for higher incidence rates in northern countries, which is in line with the higher genetic risk in Scandinavia (Chio et al., 2013).

2.1.1. Incidence and Prevalence

Recently, the worldwide crude incidence rate of ALS was estimated to be 1.59 per 100,000 persons-year (Xu et al., 2020). These values are similar to the ones reported in a previous study that estimated an incidence rate of 1.9 per 100,000 persons-year (Chio et al., 2013). The slight decrease in the incidence rate reported by Xu et al. is probably explained by the inclusion of recent studies from Asia, which typically have lower incidence rates. The variation in incidence rates worldwide is still a matter of debate. The highest incidence rates have been reported in European countries (2.76), while lower incidence rates have been reported in Asia (0.42) (Xu et al., 2020). A lower prevalence of ALS genes in Asian populations (Kim et al., 2016) may contribute to a better understanding of this issue.

Worldwide crude prevalence was estimated between 4.48 (Chio et al., 2013) and 4.42 (Xu et al., 2020) per 100,000 population. These prevalence values are relatively low, considering the incidence of the disease, which can be explained by a short survival period, usually between 2-5 years (Mehta et al., 2017).

2.1.2. Aetiology and risk factors

ALS has been proposed to follow complex progression, evolving gradually as a result of a genetic predisposition interacting with one or more environmental risk factors (Al-Chalabi et al., 2014).

Around 10-15% of ALS cases have a known family history of the disease (fALS), with monogenic mendelian-like transmission (Ryan et al., 2019). However, other types of genetic architecture with oligogenic and polygenic inheritance may contribute to ALS etiology (Goutman et al., 2022). To date, at least 40 genes have been linked to ALS, although four genes seem to account for approximately 50% of familial cases and 5% of sporadic cases reported (Zou et al., 2017).

Hexanucleotide repeat expansion (HRE) of *the C9orf72* gene (DeJesus-Hernandez et al., 2011) is the most frequent mutation in familial ALS and in patients with frontotemporal dementia (FTD), in Western countries (Smeyers et al., 2021). Pathogenic mechanisms linked to this mutation include two related gain-of-function effects (aggregation of expanded RNA and dipeptide repeat proteins) and haploinsufficiency of the related C9orf72 protein (Smeyers et al., 2021).

Superoxide dismutase 1 (SOD1) was the first gene associated with ALS (Rosen et al., 1993) and encodes the copper/zinc isoform of superoxide dismutase. Both loss of dismutase function and toxic gain of SOD1 function have been linked to pathophysiological mechanisms of ALS (Brasil et al., 2019). Nowadays, the presence of toxic SOD1 cytoplasmic aggregates is considered the most probable cause of neuron degeneration (Matsumoto et al., 2005).

ALS and its most common FTD subtype are characterized by ubiquitin-positive neuronal and glial cytoplasmic central nervous system inclusions. The chief protein in these inclusions is ubiquitinated TAR-DNA binding protein 43, known as TDP-43 (Neumann et al., 2006). TDP-43 is a multifunctional RNA- and DNA-binding protein encoded by the *TARDBP* gene located on chromosome 1 (Van Deerlin et al., 2008). Although principally nuclear, in ALS TDP-43 is mislocalized in the cytoplasm being heavily post-translationally modified and/or truncated (Goutman et al., 2022). Most genetic mutations cause this aggregation process, including patients with *TARDBP* gene mutations.

The fused in sarcoma/translated in liposarcoma (FUS/TLS) gene has also been linked to ALS (Kwiatkowski et al., 2009). FUS/TLS, like TDP-43, is also a multifunctional RNA-binding and DNA-binding protein that also originates pathological cell aggregates originating from this mutated protein.

Despite the constant evolution in our understanding of genetics, most ALS cases (85-90%) are still considered sporadic. Established risk factors for developing ALS are older age (mean age of onset 58-63 years; peak incidence in the 7th decade of life (Ingre et al., 2015)), being male, being smoker and having a family history of ALS and/or FTD (Armon, 2003). Recently, military service and moderate to high physical activity have also been associated with a higher risk of developing ALS (McKay et al., 2021, Zheng et al., 2023), in particular the practice of contact sports (Henriques et al., 2023).

Other environmental factors have also been linked to ALS development. Notably, the historical cluster of high incidence and prevalence of amyotrophic lateral sclerosis/Parkinsonism dementia complex in the Western Pacific has been shown to be related to the distribution of living cycad plants (Spencer et al., 2019), which has been associated with several neurodegenerative disorders (Rivadeneyra-Domínguez and Rodríguez-Landa, 2014). However, the origin of this past geographical focus of disease has also been explained by local water cyanobacteria contamination (Bradley et al., 2013).

2.1.3. Pathophysiology

Loss of the neuromuscular link, axonal retraction, and eventual cell death of the UMN and LMN, along with astrogliosis and microgliosis, are the hallmarks of ALS. In general, ubiquitin-positive inclusions are also observed in the remaining neurons. It is essential to first outline the underlying molecular mechanisms by which motor neurons degrade in ALS, to understand disease development and find new therapeutic solutions. We still do not fully understand the mode of action of the different mutated proteins currently known, or the ensuing neurodegeneration or neurotoxicity processes. However, it is believed that multiple pathways, rather than just one

mechanism, can cause neurodegeneration in ALS, suggesting a complex pathophysiology (Figure 1).

Figure 1 - Several proposed pathogenic mechanisms in ALS and their linked gene variants currently known

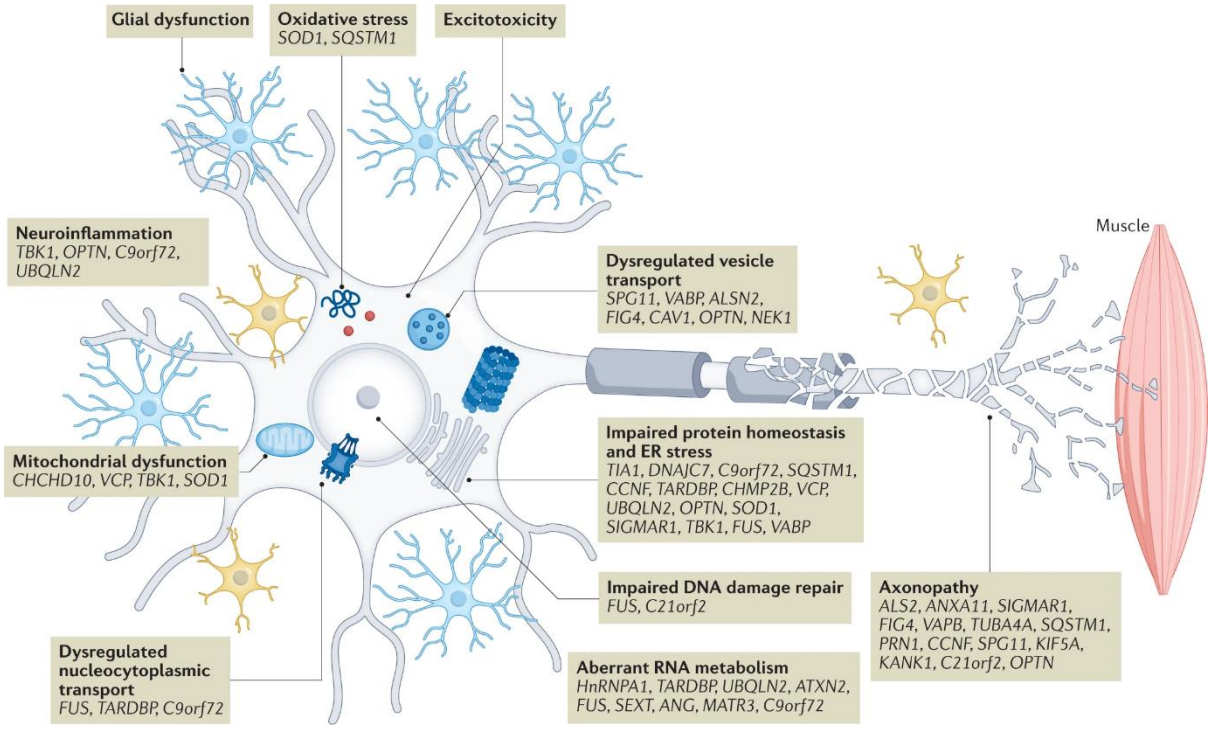

Note: Adapted from Mead et al. (2023), with permission.

Glutamate Excitotoxicity

The central nervous system's (CNS) primary excitatory neurotransmitter is glutamate. It is created in the presynaptic terminal and activates specific postsynaptic receptors, which results in neurotransmission through voltage-gated calcium channels. Excitatory amino acid transporters (EAATs), which are mainly glial and neuronal cell transporter proteins, remove unused glutamate from the synaptic cleft after being released from the presynaptic neuron. According to previous reports, a high glutamate concentration in the synaptic cleft causes excitotoxicity due to excessive or widespread activation of glutamate receptors, which might result in neurodegeneration of the affected neurons (Shaw and Eggett, 2000). Therefore, to avoid neuronal damage, glutamate must be quickly removed. Isoform 2 of the astroglial glutamate transporter, EAAT2, is specifically responsible for maintaining

glutamate levels within the nervous system below excitotoxic levels (Ilieva et al., 2009).

One of the earliest hypothesized pathways for the pathophysiology of ALS is glutamate excitotoxicity (Bendotti and Carri, 2004). In ALS, there are lower EAAT2 levels in the CNS, most likely due to the presence of aberrant EAAT2 mRNA or EAAT2 transporter breakage. This causes an increase in synaptic glutamate concentration and overstimulation of postsynaptic glutamate receptors, resulting in excitotoxic neuronal degeneration (Zarei et al., 2015).

Oxidative Stress

Free radicals or reactive oxygen species (ROS) are produced by oxygen metabolism. Oxidative stress is a state in which the amount of ROS produced exceeds the ability of cells to eliminate them. ROS buildup permanently harms the cell and its macromolecules, including proteins, DNA, and RNA. The primary enzyme that prevents oxidative damage and reduces superoxide leakage from mitochondria is SOD1. Therefore, SOD1 mutations might cause cytotoxicity. Early investigations hypothesized that SOD1 pathology may involve both a dominant toxic gain of function and a decline or loss in enzyme activity (Borchelt et al., 1994). According to a particular hypothesis, mutated SOD1 can resume its usual antioxidant action and produce harmful superoxide. Mutant SOD1 may transfer electrons to molecular oxygen from other cellular antioxidants, generating superoxide and making SOD1 the cause of oxidative stress (Liochev and Fridovich, 2003). Cerebrospinal fluid (CSF), serum, and urine samples from patients with ALS show elevated free radical levels and oxidative damage (Zarei et al., 2015). This might be caused by the mutant SOD1's altered active site geometry, which reduces the number of substrates. Defective oxidative phosphorylation may also contribute to oxidative stress in ALS, as shown by studies on the CSF of transgenic mice and patients, where high concentrations of ROS resulting from deficient oxidative phosphorylation, such as 3-nitrotyrosine, were found (Tohgi et al., 1999, Bacman et al., 2006). Increased ROS levels are correlated with mitochondrial dysfunction and serve as an illustration of how the ALS pathogenesis pathways may be coupled.

Mitochondrial Dysfunction

One distinctive feature of ALS is mitochondrial damage. ROS and other metabolic and structural changes in the cell cause neuronal injury, which is the primary cause of this dysfunction. Both spinal motor neurons and skeletal muscle of sporadic and familial ALS patients, as well as the disease mouse model, exhibit structural alterations in the mitochondria (Boillee et al., 2006, Sasaki and Iwata, 2007, Magrane and Manfredi, 2009). Deposition of the misfolded mutant SOD1 protein may change the physiological activity of mitochondria in ALS transgenic mice and humans (Menzies et al., 2002). Additionally, mutant SOD1 is responsible for the decreased activity of respiratory chain complexes I and IV, which are connected to malfunctioning energy metabolism. Because of the presence of mutant SOD1, it has been shown that motor neurons in patients with ALS lose their ability to bind Ca2+, which reduces calcium absorption from the cytoplasm and ultimately increases vulnerability to excitotoxicity (Bernard-Marissal et al., 2012). Additionally, mitochondria are essential components of synaptic terminals, which have high adenosine triphosphate (ATP) and calcium homeostasis needs. Neuronal metabolic changes and cell death may result from defects in mitochondrial axonal transport in these regions (Magrane and Manfredi, 2009).

Protein Aggregates

When misfolded proteins build up, they oligomerize and aggregate, creating protein aggregates that promote a hazardous environment in the neurons. Both sALS and fALS tissues from patients with SOD1 pathogenic mutations, as well as mutant SOD1 transgenic animals, have been observed to contain mutated SOD1 protein-rich inclusions in the neuron cytoplasm (Boillee et al., 2006). Aggregates made up of mutant SOD1 and other nuclear proteins, such as abnormal phosphorylated TDP43 or FUS, are formed as a result of the abnormal accumulation of defective proteins that prevent their degradation (Dormann and Haass, 2011). In more than 80% of ALS cases, TDP43 abnormal protein inclusions are present in the cytoplasm (Coan and Mitchell, 2015). These aggregates are strongly cytotoxic.

Accumulation of Neurofilaments

The accumulation of neurofilaments (NFs) in cell bodies and axons is a typical pathological feature of ALS. NFs are intermediate filaments of nerve cells and are an important part of the nerve cell cytoskeleton (Julien, 1999). The process leading to the

formation of NF aggregates in ALS remains unclear. Very rare mutations in NF genes occur in both fALS and sALS and may be correlated with abnormal phosphorylation of NFs, which affects the axonal transport of NFs, leading to their accumulation in the cell bodies and proximal axons. This accumulation may lead to defects in the axonal transport of other cellular components, such as mitochondria, which are essential for cell survival (Xiao et al., 2006). Another cause for the aggregation of NFs may be their altered stoichiometry, which plays a pivotal role in their distribution and aggregation. Abnormal organization of NF is an important part of ALS pathogenesis; however, the exact relationship between its accumulation and motor neuron degeneration remains unclear.

Neuroinflammation

Motor neurons that are not mutated but are surrounded by glial cells with a SOD1-mutated gene develop a pathological phenotype. Moreover, replacement of mutated glial cells with wild-type glia delays disease progression and prolongs survival in ALS mice. Thus, damaged glia and neurons are involved in neurodegeneration and disease progression (Lee et al., 2012). A neuroinflammatory response, including activated microglia, astrogliosis, and infiltrating immune cells at sites of neuronal injury, is one of the primary features of ALS. In ALS, the interaction between motor neurons and microglia, which are resident macrophages in the CNS, initially protects neurons. As the damage worsens, misfolded proteins, such as mutated SOD1, and other toxic molecules are released from motor neurons and astrocytes, which stimulate the activation of microglial cells, which switch from a neuroprotective to a neurotoxic phenotype (Gao et al., 2023). Thus, activated microglia increases during disease progression as a result of their interaction with the cellular microenvironment, leading to a cytotoxic neuroinflammatory effect on neurons.

Final common pathway

Although it is known that several processes contribute to the toxicity linked to each mutation, and that these pathways probably intersect, the pathogenesis of ALS appears to be heavily dependent on the initial cause of the disease. In the case of SOD1 mutations, for example, this convergence is very clear (Brasil et al., 2019).

The end result, regardless of the precise processes at work, is that motor neurons are unable to maintain their axonal projections. In LMNs, axonal retraction and denervation of the target cell result from this (Hardiman et al., 2017), causing muscle denervation. In the UMN, this process will cause improper regulation of LMNs, resulting in hypertonicity and weakness. Important neuronal networks are lost in the motor and extra-motor domains (Iyer et al., 2015). It is yet unknown why motor neurons are particularly vulnerable to the negative effects of these mutations, even though many of the proteins encoded by genes linked to ALS are broadly expressed throughout the body. One possible explanation is that motor neurons may be more vulnerable to metabolic problems than other neuron types because of their larger size and requirement to maintain longer axonal projections. Of note, however, there are other neuron subtypes, such as sensory neurons, that have much longer axonal extensions. The high expression of matrix metalloproteinase 9 and ephrin type-A receptor 4, as well as the poor expression of osteopontin and insulin-like growth factor 2 by motor neurons, are additional factors that may increase the susceptibility of motor neurons (Hardiman et al., 2017). These elements might inhibit the processes of axonal sprouting and repair.

Of particular interest is the observation that among LMNs, those forming fast-fatigable motor units tend to degenerate first in ALS (Saxena and Caroni, 2011). Nonetheless, the relationship between this phenomenon and other vulnerability factors remains to be fully elucidated.

2.2. Clinical presentation

ALS presents in its classic form with two prominent features: amyotrophy, characterized by muscle atrophy and weakness, and lateral sclerosis, which involves degeneration of the corticospinal tract in the lateral columns of the spinal cord (Figure 2). This classic presentation is observed in approximately 85% of ALS cases (Hardiman et al., 2017). There are, however, less common subtypes of ALS, based on the relative UMN versus LMN involvement and the regional distribution of involvement (Table 1).

It is crucial to distinguish between these ALS subtypes because the prognosis tends to be more favorable in syndromes with isolated UMN or LMN degeneration compared to classic ALS, which involves a combination of both upper and lower motor neuron involvement.

Figure 2 - Involvement of the lower and upper motor neurons is a crucial aspect of ALS

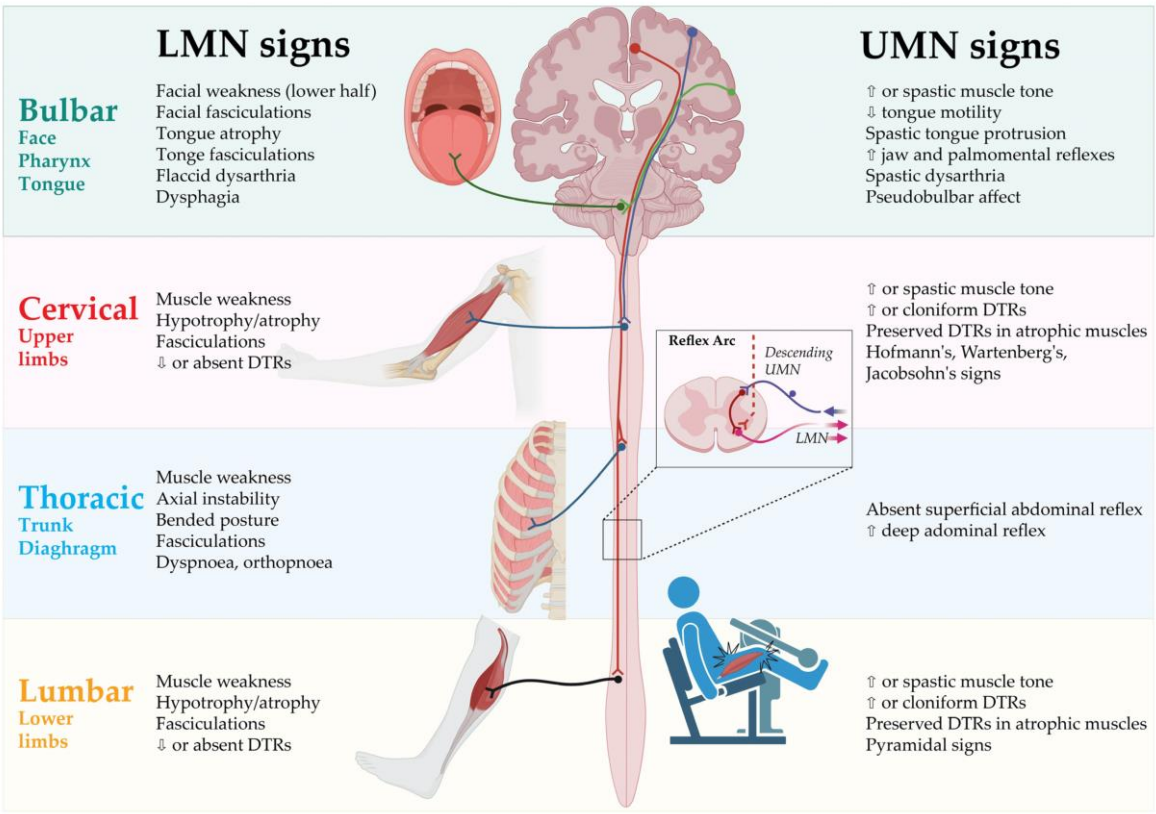

Each body area (bulbar, cervical, thoracic, and lumbar) exhibits distinct clinical symptoms as a result of upper and lower motor neuron dysfunction. LMN – lower motor neuron; UMN – Upper motor neuron; DTR – deep tendon reflex. Note: Adapted from Vidovic et al. (2023), under CC-BY attribution license.

2.2.1. Phenotypes

Classical amyotrophic lateral sclerosis

ALS is characterized by progressive muscle weakness, often accompanied by muscle atrophy, fasciculations, cramps, and a slowing of movements with muscle stiffness. The initial muscle weakness in ALS typically begins in a specific area and then spreads to neighboring body regions. This pattern suggests the spread of disease pathology within the motor system, involving both spinal cord segments and the motor cortex (Gromicho et al., 2020). In certain cases, muscle weakness may be preceded by a period in which patients notice fasciculations, muscle cramps, or mild weight loss.

The disease typically starts with either unilateral distal muscle weakness and atrophy in upper or lower limb muscles (spinal ALS, seen in roughly two-thirds of patients) or in the muscles related to speech and swallowing (bulbar ALS, seen in about one-third of patients). When ALS begins in the upper limbs, it most commonly affects the dominant hand (Turner et al., 2011). Thenar muscles are more severely affected than those in the hypothenar region, a phenomenon known as the split-hand syndrome (Eisen and Kuwabara, 2012, Corcia et al., 2021a). In lower limb onset cases, the anterior tibial muscle is usually affected earlier in the disease progression compared to the gastrocnemius muscle, and the hamstrings show signs of weakness before the quadriceps muscles (Jenkins et al., 2020). Approximately 3-5% of the patients present with symptoms of respiratory impairment due to initial respiratory muscles weakness, in particular of the diaphragm. This phenotype is typically characterized by middle-age old man with predominant LMN involvement and marked weight loss (Pinto et al., 2023).

Bulbar onset ALS often presents with dysarthria and/or dysphagia. Less commonly, patients may experience dysphonia, difficulty closing the mouth, or chewing problems. As the disease progresses, some individuals may develop limitations in maintaining head and trunk (Wijesekera and Leigh, 2009). Rarely, these postural problems can be the initial symptoms. About one-third of ALS patients may also experience episodes of uncontrollable laughter or crying, a phenomenon referred to as a pseudobulbar affect (Thakore and Pioro, 2017).

On neurological examination, a combination of signs indicating involvement of both UMNs and LMNs is typically observed. Signs of LMN involvement include muscle weakness, muscle atrophy, fasciculations, and decreased muscle tone. Signs of UMN involvement include hyperreflexia (or the presence of reflexes in atrophic muscles), spasticity (particularly noticeable in upper limb flexors and lower limb extensors), and a slowing of movements (such as tongue movement) (Masrori and Van Damme, 2020). In approximately 50% of patients with ALS, the degenerative process can extend beyond the motor neurons and affect the frontal and anterior temporal lobes of the brain. This can lead to a range of cognitive and behavioral changes, including executive dysfunction, language impairment, and behavioral changes (Neary et al., 2000). Cognitive changes can anticipate motor involvement (in general bulbar symptoms) in about 1-2% of the ALS patients (Gromicho et al., 2021).

Progressive muscle atrophy

PMA is a rare sporadic disorder characterized by progressive LMN loss without clinical signs of UMN involvement (Aran, 1850). Patients develop progressive flaccid weakness, muscular atrophy, fasciculations, and hypo- or areflexia. Asymmetrical involvement of distal limb muscles is the most common presentation (Statland et al., 2015), then spreading to other anatomic regions over the course of months or even years. Progression is, usually, slow with respiratory and bulbar involvement appearing in later stages (de Carvalho et al., 2007). The mean age of patients with PMA is higher than in patients with classic ALS, for this reason we have observed a more frequent number of patients with phenotype related to population ageing (Alves et al., 2023). Roughly 20 to 30% of patients with PMA will eventually present UMN signs, and thus, by definition, had LMN onset ALS (Kim et al., 2009). Even in patients that did not develop UMN clinical signs, evidence of UMN degeneration is commonly observed on autopsies (Lawyer and Netsky, 1953, Ince et al., 2003). Neurophysiological signs of UMN abnormalities have also been shown in PMA patients (Triggs et al., 1999, Vucic and Kiernan, 2007, Floyd et al., 2009, Castro et al., 2021).

Figure 3 – Example of an ALS patient, showing generalized muscle atrophy

Note: Picture kindly given by Mamede de Carvalho.

Primary lateral sclerosis

PLS is a slowly progressive condition characterized by a pure UMN syndrome, and it is diagnosed when no other disease process can account for these symptoms (Pringle et al., 1992, Turner et al., 2020). There is an ongoing debate as to whether PLS is a distinct disorder or simply a variant of ALS. There are, however, some pathological evidence, such as the presence of ubiquitinated TDP-43 inclusions (Mackenzie, 2020), suggesting shared characteristics with ALS. Patients present with progressive spasticity and slowing of movements, without muscle atrophy or evident

fasciculations (Pringle et al., 1992). Distinguishing PLS from ALS, especially in the early stages, can be challenging because some individuals with ALS may initially exhibit only UMN signs. New criteria define that if there are no clinical or electromyographic LMN for 4 or more years after onset, a diagnosis of PLS is accepted as definitive (Turner et al., 2020). However, this distinction is clouded by the minor EMG changes commonly observed in patients with PLS (de Carvalho et al., 2020).

Cognitive impairment, in particular behavioral changes, can occur in individuals with PLS, mirroring the cognitive manifestations observed in ALS (Grace et al., 2011). Moreover, the same mutations can cause ALS and PLS phenotypes in the same family, highlighting the complex and heterogeneous nature this part of the MND spectrum (Corcia et al., 2021c).

Other variants

There are a wide range of ALS/MND variants.

The upper extremity regional variant, known as Flail-arm syndrome or Vulpian–Bernhart syndrome (Gamez et al., 1999), initially affects the proximal upper limb in a symmetrical pattern, without progression to another region for at least 12 months. Weakness and wasting gradually evolve leading to severe wasting of the shoulder gridle and arms.

The lower extremity regional variant, known as Flail leg syndrome or Pseudopolyneuritic form of ALS (Patrikios, 1918), usually involves both lower limbs in a symmetrical manner, with weakness and wasting beginning in the distal lower limbs.

Other variants are pseudobulbar palsy (PBP), and progressive bulbar atrophy (PBA), which primarily affects the muscles in the bulbar territory, including those of the tongue, pharynx, larynx, jaw, and face, with pure UMN (PBP) or LMN (PBA) signs

The Mill's syndrome (Mills, 1906), also known as hemiplegic ALS, is an uncommon UMN ALS variant phenotype, that resembles a form of PLS and is characterized by a progressive hemiplegic pattern of motor deficit with isolated UMN signs. Despite being considered a part of the MND spectrum, the classification as an ALS variant has been debated (Jaiser et al., 2019).

Table 1 - Phenotype classification based on clinically imputed anatomy of neuropathology

	CNS Anatomical Region Involved*			Innervated Peripheral Body Region Involved*		
	UMN	LMN	Fronto-temporal regions	Bulbar muscles	Limb muscles	Higher cortical function & behavior
Based on Level of involvement						
ALS	+ +	+ +		+ +	+ +	
PLS	+ + + +	+ / -	+ / -	+ +	+ +	+ / -
PMA	-	+ + + +		+ / -	+ + + +	
Based on Body Region of involvement						
Bulbar ALS	++	+ +		+ + + +	+ / -	
Pseudobulbar ALS	+ + + +	-		-	-	
Limb-onset ALS	+ +	+ +	+ / -	+ / -	+ +	+ / -
Limb-variants	-	+ + + +		+ / -	+ + + +	
Mill's variant	+ + + +	-		+ / -	+ + + +	
Associated cognitive changes						
FTD or behavioral/cognitive impairment	+ / -	+ / -	+ + + +	+ / -	+ / -	+ + + +

UMN – upper motor neuron; LMN – lower motor neuron; ALS – amyotrophic lateral sclerosis; PLS – primary lateral sclerosis; PMA – progressive muscular atrophy; FTD – frontotemporal dementia; ++ – typical and to variable degree; +/- – possible but not typical; ++++ – primary feature; - – not present. Note: Adapted from Ravits et al. (2013), with permission

2.2.2. Diagnosis

The clinical heterogeneity of ALS, further aggravated by its variants, makes a definitive diagnosis a challenging task. Over the past 30 years, several diagnostic criteria, using clinical and neurophysiological data, have been proposed and internationally established (Table 2). Through the years, these criteria have been revised to reflect the increasing knowledge of the disease and accumulated experience.

The original diagnostic criteria became known as the El Escorial criteria (Brooks, 1994). Some years later, the same research group from the World Federation

of Neurology, proposed a revised El Escorial criteria (Brooks et al., 2000). Several years later, a group of neurologists gathered in Awaji-shima, Japan, and proposed a new set of diagnostic criteria for ALS (de Carvalho et al., 2008). These criteria emphasize the importance of electromyographic findings, principally of the fasciculations potentials, which are considered equivalent to fibrillation or sharp waves when investigating strong muscles (in particular cranial-innervated muscles) from patients with ALS suspicion. These diagnostic criteria added a significant clinical impact in ALS diagnosis (Costa et al., 2012), and became widely used for many years. Recently some concern has been raised about the complexity and poor interrater variability (Johnsen et al., 2019) of both the revised El Escorial and the Awaji criteria, that may lead to poorer sensitivity. This is of particular significance in multicenter trials, where patients without criteria for “probable” or “definite” ALS may be excluded. Given these limitations, an international consensus group of experts from different fields gathered in Gold Coast, Australia, to rethink the current ALS diagnostic ALS criteria. This group proposed a simpler set of criteria, which improves the diagnostic process in earlier stages of ALS (Shefner et al., 2020), allowing possible future therapies the best chance of success in trial settings. In recent retrospective studies of large population of patients, the sensitivity of the Gold Coast criteria was compared with that of the Awaji and revised El Escorial criteria, showing higher sensitivity (Hannaford et al., 2021, Pugdahl et al., 2021), without loss of specificity (Pugdahl et al., 2021).

Table 2 - Diagnostic criteria for ALS

	Revised El Escorial criteria (2000)	Awaji criteria* (2008)	Gold Coast criteria⁺ (2019)
Presence of ALS	Different diagnostic categories (See below)	Different diagnostic categories (See below)	Progressive motor impairment documented by history or repeated clinical assessment, preceded by normal motor function, **AND** Presence of UMN and LMN dysfunction in at least one body region **OR** LMN dysfunction in at least two body regions, **AND** Investigations excluding other disease processes (EMG changes = to clinical signs)
Definite ALS	UMN and LMN signs in three spinal regions **OR** Bulbar region and two spinal regions	UMN and LMN signs in three spinal regions **OR** Bulbar region and two spinal regions	Abolished
Probable ALS	UMN and LMN signs in at least two regions with some UMN signs necessarily rostral to (above) the LMN signs	UMN and LMN signs in at least two regions with some UMN signs necessarily rostral to (above) the LMN signs (EMG changes = to clinical signs)	Abolished
Clinically probable ALS: laboratory-supported	UMN and LMN signs in one region, **OR** UMN signs alone present in one region, and LMN signs defined by EMG criteria present in at least two regions	Category abolished	
Possible ALS	UMN and LMN signs in one region, **OR** UMN signs in two or more regions; **OR** LMN signs are found rostral to UMN signs and the diagnosis of clinically probable ALS-laboratory-supported cannot be proven	UMN and LMN signs in one region, **OR** UMN signs in two or more regions; **OR** LMN signs are found rostral to UMN signs. Neuroimaging and clinical laboratory studies will have been performed and other diagnoses must have been excluded	Abolished

Abbreviations: ALS, amyotrophic lateral sclerosis; LMN, lower motor neuron; UMN, upper motor neuron.

* For Awaji criteria, LMN dysfunction was defined by clinical, electrophysiological, or neuropathological examination. Fasciculation potentials were regarded as equivalent to ongoing changes (fibrillation potentials and positive sharp waves) in the presence of chronic neurogenic changes.

⁺ For Gold Coast criteria, LMN dysfunction was defined clinically or by electrophysiological assessment. Diagnostic categories were excluded in the Gold Coast criteria. Note: Adapted from Vucic et al. (2021), with permission.

2.2.3. Prognosis

Death usually occurs due to respiratory failure. However, life expectancy in ALS is extremely variable, due to a significant variability in its prognostic factors (Chio et al., 2009). Median survival from symptom onset has been reported in the literature ranging from a mean of 3 to 5 years (Armon, 1994), to a span of a few months to more than 10 years (Chio et al., 2009). Patients with the classical form of ALS have worse

prognosis than those with incomplete forms of MND, such as PMA or PLS (Millul et al., 2005).

There is evidence, according to several published works, that several variables are linked to ALS patients' longer survival times. Younger age at symptom onset, longer interval between symptom onset and diagnosis (diagnostic delay), limb rather than bulbar onset, absence of cognitive impairment, absence of respiratory muscle weakness, high functional score at baseline and slow rate of its decay, and no weight loss are the most relevant favorable prognostic factors (Elamin et al., 2011, Pinto et al., 2012, Mousavi et al., 2014, Pupillo et al., 2014, Wolf et al., 2014).

Some studies have suggested that survival has increased in recent years, associated with a larger and earlier user of non-invasive ventilation and riluzole treatment (Alves et al., 2023).

2.2.4. Clinical management

The treatment of ALS requires a multidisciplinary approach. Given that a definitive cure has not yet been identified, the provision of comprehensive care, including respiratory and nutritional management, has been demonstrated to enhance the quality of life and extend survival for individuals with ALS.

Disease modifying treatments

Despite numerous clinical trials and advancements in our comprehension of ALS, the quest for agents capable of modifying the course of the disease or offering neuroprotection has yielded limited success. To date, riluzole is the only disease modifying treatment approved.

Riluzole, which principally acts as an anti-glutamatergic drug, was the first drug approved for ALS (Bensimon et al., 1994). It has been shown to have a modest effect on survival (Mitchell et al., 2006), with a probable increase by a few months, when taken for a 18 month period (Miller et al., 2007). The precise mechanism of action of riluzole is not fully understood, but it is believed to involve several processes. These include interference with N-methyl-D-aspartate (NMDA) receptor-mediated responses, stabilization of the inactivated state of voltage-dependent sodium

channels, inhibition of glutamate release from pre-synaptic terminals, and enhancement of extracellular glutamate uptake (Distad et al., 2008). It is generally well tolerated, without significant side effects other than a possible change in liver function tests, which should be regularly monitored (Bensimon and Doble, 2004).

Edaravone, which is a free radical scavenger, is believed to have an effect against oxidative stress, protecting neurons, glia, and vascular endothelial cells (Takei et al., 2017). It was first approved in Japan and South Korea in 2015, and in the USA in 2017. Currently it is approved only in a small number of countries worldwide. It has shown a very modest effect in delaying disease progression, as measured by the progression of the Amyotrophic Lateral Sclerosis Functional Rating Scale (ALSFRS) scale (ALS 19 STUDY GROUP, 2017), in a very selected population of patients and without any positive effect on respiratory function. Data on the impact of Edaravone in survival in ALS is scarce (Takei et al., 2017).

Very recently the antisense oligonucleotide Tofersen has been approved by the FDA for the treatment of ALS-associated SOD1 mutations. It has been shown to slow disease progression, in particular in fast progressors (Miller et al., 2022).

Numerous clinical trials are being conducted in ALS currently, with different types of drugs targeting different pathophysiological mechanisms (Figure 4). From old drugs with new indications, such as Tauroursodeoxycholic acid (TUDCA), TUDCA associated with sodium phenylbutyrate (AMX-0035), Tamoxifen, Xaliproden or Matisinib, among others, to use of stem cells, and new gene therapies, including antisense oligonucleotides, RNA interference, Clustered Regularly Interspaced Short Palindromic Repeats (CRISPR), adeno-associated virus (AAV)-mediated trophic support, and antibody-based methods, the next few years should bring exciting novelties regarding disease modifying therapeutics in ALS (Amado and Davidson, 2021, Corcia et al., 2021b). Of note, however, is the need to develop specific biomarkers that can adequately bridge the gap between preclinical studies and clinical efficacy of a given drug (Maragakis et al., 2023).

Symptomatic treatments

Respiratory insufficiency is a frequent occurrence in individuals with ALS and is the most relevant determinant of survival. The initial symptoms of respiratory muscle

weakness encompass difficulties in breathing during exertion or speaking, later followed by orthopnea, disrupted sleep, excessive daytime drowsiness, morning headaches, fatigue, loss of appetite, depression, reduced concentration, vivid nightmares, and nocturia (Heffernan et al., 2006). Clinical signs that become apparent during a physical examination may involve tachypnea, the use of accessory muscles for breathing, paradoxical movement of the abdomen, and a weak cough (Leigh et al., 2003). Measurements of the forced vital capacity (FVC) or slow vital capacity (SVC) are the most widely available measures for detecting respiratory insufficiency.

Figure 4 - The major ALS pathophysiological targets currently being pursued

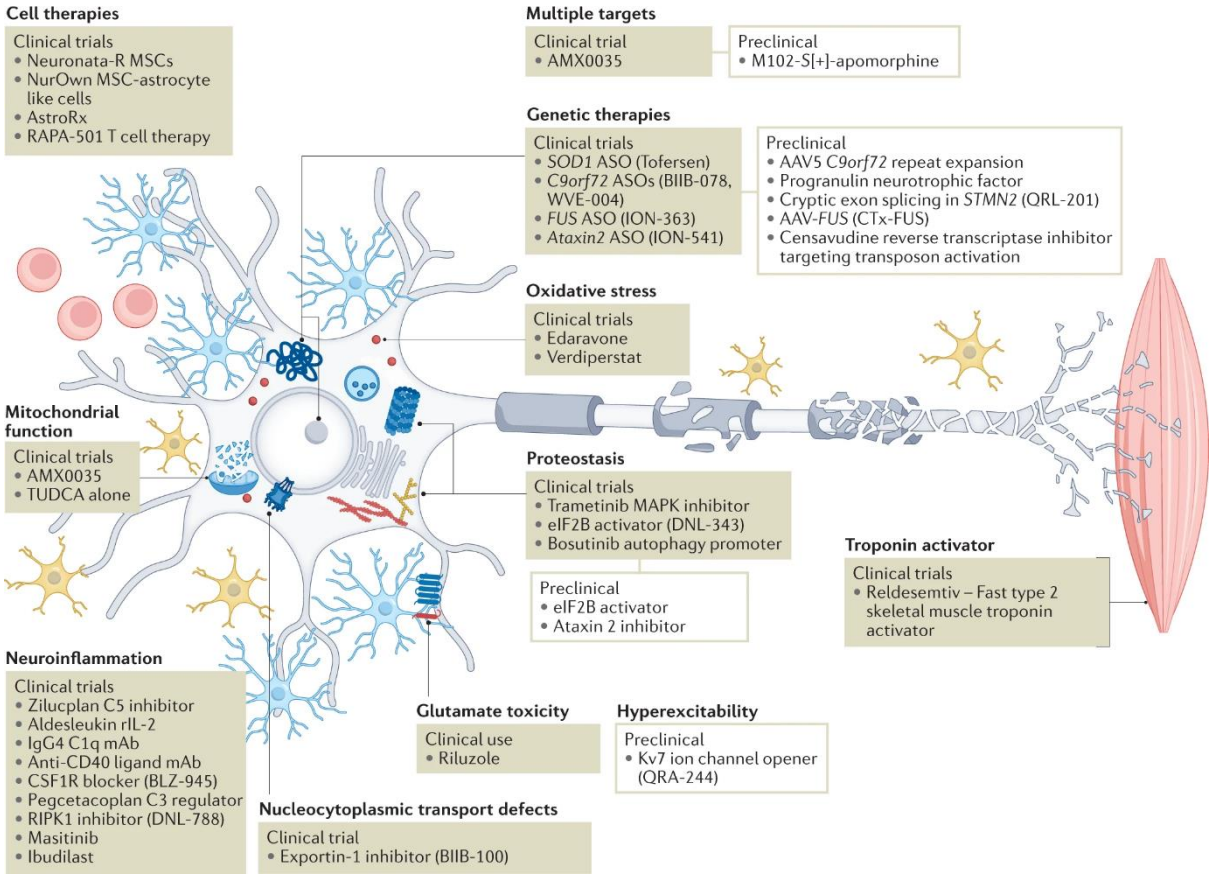

Note: Adapted from Mead et al. (2023), with permission.

Phrenic nerve responses may also be used to predict hypoventilation in ALS (Pinto et al., 2012). Taking proactive measures to address respiratory symptoms can have a beneficial effect on the quality of life and survival of individuals with ALS (Bourke et al., 2006). Respiratory support for ALS patients primarily relies on non-pharmacological interventions such as non-invasive ventilation (NIV) or, in selected cases, invasive ventilation through a tracheotomy. Among non-invasive ventilation

methods, bi-level positive pressure devices (BiPAP) are commonly employed, while continuous positive pressure (CPAP) ventilation is typically not as effective (The EFNS Task Force, 2012). NIV increases survival and quality of life of ALS patients, with a more positive impact on spinal-onset patients (Pinto et al., 1995).

Nutritional status is a significant prognostic risk factor in ALS. Major impediments to maintaining adequate nutrition in ALS patients include dysphagia and arm weakness. Additionally, factors such as anxiety, depression, and constipation further compound the challenges associated with ensuring proper nutrition for individuals with ALS. The initial management of dysphagia is based on dietary counselling, modification of food and fluid consistency (blending food, adding thickeners to liquids), prescription of high-protein and high-caloric supplements, and education of the patient and carers in feeding and swallowing techniques (The EFNS Task Force, 2012). When tube feeding is required, percutaneous endoscopic gastrostomy (PEG) is the standard procedure for enteral nutrition (The EFNS Task Force, 2012). Although it has been demonstrated to have a positive effect on nutrition, there does not seem to have a significant impact on quality of life or survival (Heffernan et al., 2004). In ALS, hypermetabolism and higher energy expenditure contributes to weight loss and poor prognosis (Funalot et al., 2009).

Further treatments usually employed in ALS are in the context of the symptoms that are typical of this disease like sialorrhea, spasticity, bronchial secretions, cramps, depression and anxiety, and pseudobulbar emotional liability, among others (The EFNS Task Force, 2012).

3. Neurophysiology in ALS – contributions to understanding spinal and supraspinal mechanisms of inhibition

Neurophysiology is a multifaceted field, with many different approaches and possibilities, allowing assessment of central, peripheral and even autonomic nervous system. In ALS, neurophysiology plays an irreplaceable role, from diagnostic, to understating pathophysiological mechanisms, monitoring disease progression, and, eventually, as a potential biomarker for assessing therapeutic efficacy.

Standard nerve conduction studies, motor and sensory neurography and F-wave studies, are usually unremarkable in ALS, and its role is mainly one of exclusion of other diseases (Eisen and Krieger, 2004, de Carvalho and Swash, 2006). On the other hand, conventional needle EMG has been an intrinsic part of the ALS diagnosis for many years and is still considered the standard tool to assess LMN involvement (Shefner et al., 2020). Fasciculation potentials are, usually, one of the earliest changes observed in affected muscles of ALS patients, while the presence of active denervation coupled with ongoing reinnervation is very characteristic of ALS, both of which are evident on needle EMG (de Carvalho and Swash, 2006, de Carvalho and Swash, 2013, 2016).

Other, less conventional techniques have also been used in ALS. Several different motor unit number estimation (MUNE) techniques have been studied, with the purpose of quantifying surviving motoneurons in ALS patients (Bromberg, 2013, Swash, 2017). Studies of the phrenic nerve have demonstrated its utility as a predictor of hypoventilation (Pinto et al., 2009) and survival (Pinto et al., 2012).

The aforementioned techniques, however, despite being invaluable in the study of the LMN, are not adequate for assessing the UMN or segmental spinal systems. In this chapter several techniques to assess spinal and supraspinal mechanisms, with an emphasis on inhibitory processes in ALS, will be discussed.

3.1. H Reflex

The Hoffmann reflex, commonly referred to as the H reflex (Magladery and McDougal, 1950), is one of the most studied reflexes in humans. This reflex, initially described by Hoffmann in the early 20th century (Hoffmann, 1918), provides valuable insights into the functioning of the human nervous system. Magladery et al. (1951) demonstrated that the latency of the motoneurons discharge in the H reflex is consistent with a monosynaptic pathway, which is equivalent to the monosynaptic reflex in animal studies (Paillard, 1955). The H reflex is, mainly, a monosynaptic spinal reflex that involves the excitation of alpha-motoneurons in response to electrical stimulation of peripheral nerves. It bypasses the muscle spindle, and is theoretically less affected by the fusimotor drive, directly activating the alpha motor neurons (Pierrot-Deseilligny and Mazevet, 2000, Burke, 2016). Its unique characteristics have made the H reflex an invaluable tool in the study of neuromuscular physiology, offering a window into the complex interplay of neural pathways that govern motor control and sensory feedback, allowing the examination of spinal cord excitability and motor neuron activity (Pierrot-Deseilligny and Burke, 2012).

When a mixed peripheral nerve is electrically stimulated above the motor threshold (MT), it elicits two distinct responses in the corresponding muscle: an M-wave and an H reflex (Figure 5). The M-wave is a short-latency direct motor response due to the stimulation of motor axons. It is generated by the orthodromic activation of alpha-motoneurons, which in turn activate their corresponding muscle fibers. The H reflex is a longer-latency reflex response due to the activation of Ia afferents. Ia afferents are sensory neurons that originate in the muscle spindles and project to the spinal cord where they have a monosynaptic projection onto alpha-motoneurons, which in turn activate their muscle fibers. At supramaximal stimulation, the H reflex is absent due to collision of the descending motor volley with the orthodromic afferent volley. The descending motor volley is the motor signal that travels back down the motor axons to the muscle. The orthodromic afferent volley is the sensory signal that travels up the Ia afferents to the spinal cord. When these two volleys collide, they cancel each other out, and the H reflex is not produced (Figure 5 d,h).

Figure 5 – Recruitment curve of the H and M waves in the soleus

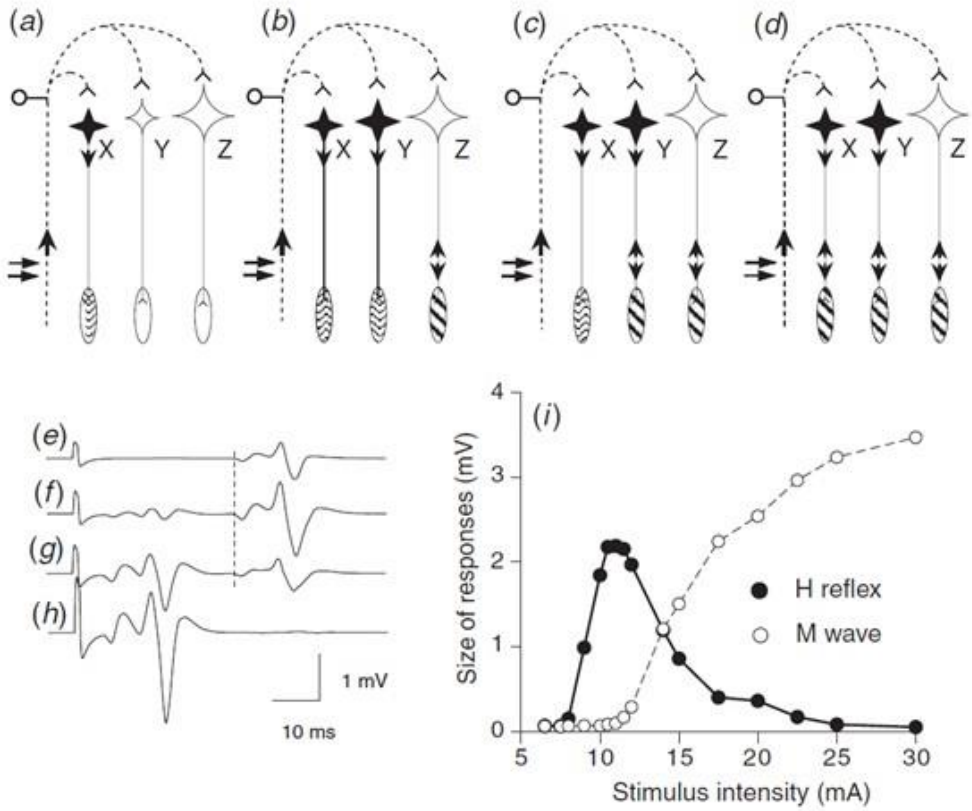

Sample electromyographic (EMG) responses are shown in (e)–(h) and sketches of the corresponding volleys in Ia afferents (dotted lines) and motor axons (continuous lines) in (a)–(d) when the stimulus intensity is progressively increased. Motoneurons discharged by the Ia volley are black, muscle fibres activated by the H reflex are speckled and those activated by the M wave are hatched. (a) and (e) Stimulation (at 9 mA) activates only Ia afferents and causes motoneuron 'X' to fire in the H reflex. (b) and (f) Stronger stimulation (12 mA) activates more Ia afferents and this causes motoneurons 'X' and 'Y' to fire in the H reflex, which increases in size. It also elicits a motor volley in the axon of motoneuron 'Z' and an M wave appears in the EMG. The antidromic motor volley in motoneuron 'Z' does not collide with the reflex response, because this MN does not contribute to the reflex. (c) and (g) Even stronger stimulation (15 mA) causes motoneurons 'X' and 'Y' to fire in the H reflex and elicits a motor volley in the axon of motoneurons 'Z' and 'Y'. As a result, an M wave appears in the muscle fibres innervated by motoneuron 'Y'. The antidromic motor volley collides with and eliminates the reflex volley in the axon of motoneuron 'Y', and the H reflex decreases. (d) and (h) Yet stronger stimulation (30 mA) produces Mmax, and the H reflex is eliminated by collision with the antidromic motor volley. Note that collision between the antidromic volley and the reflex discharge will also prevent antidromic invasion of those reflexly activated motoneurons, so that F waves cannot occur in them. The vertical dashed line in (e)–(g) indicates the latency of the H reflex. (i) The amplitude of the H reflex (●) and of the Mwave (○) are plotted against stimulus intensity. Note: adapted from Pierrot-Deseilligny and Burke (2012), with permission

It is important to note that the H reflex and M wave activate different sets of alpha-motoneurons. The recruitment of alpha-motoneurons follows an organized pattern (Figure 6), starting from the smallest (which are more excitable and associated with larger Ia EPSPs) and progressing to the largest (less excitable with smaller Ia EPSPs), as described by Henneman et al. (1965). Consequently, during the H reflex,

smaller motoneurons, which innervate slow motor units, are recruited first. In contrast, electrical motor stimulation preferentially stimulates larger diameter axons innervating fast motor units, and motor axons closer to skin surface.

Figure 6 - Classification of motor unit types from muscle fibers based on histochemical profile, size, and twitch (contractile) characteristics

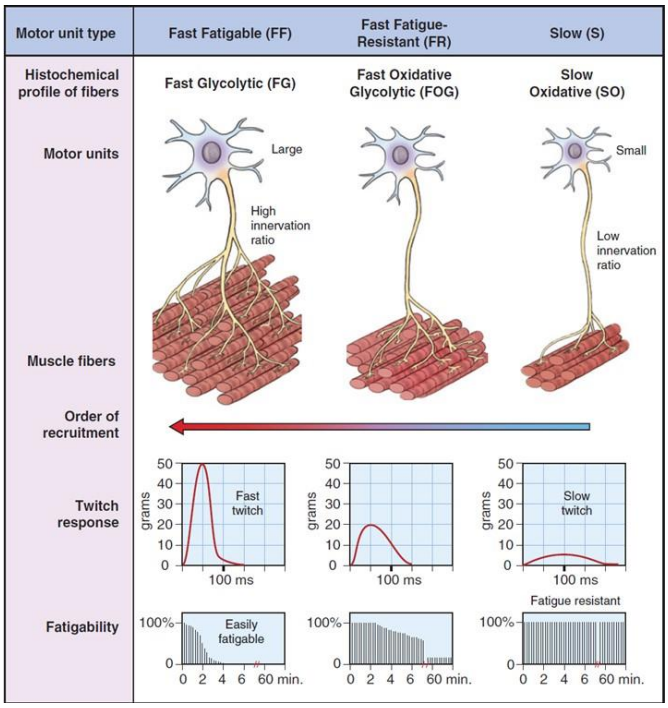

A theoretical continuum of differing contractile and morphologic characteristics is shown for each of the three motor unit types. It is important to note that the range of any single characteristic may vary considerably within any given motor unit (either within or between whole muscles). Note: Adapted from Neumann et al. (2017), with permission.

There are, however, some misconceptions regarding this reflex response that are important to address. The H reflex is often regarded as the electrical equivalent of the tendon jerk or stretch reflex, with the primary distinction being that the H reflex operates independently of the muscle spindle mechanisms that are typically involved in the tendon jerk reflex. However, there are ample evidence on the literature that this view is too narrow and ignores other well-established differences (Pierrot-Deseilligny and Burke, 2012). Despite depending on monosynaptic excitation, the H reflex is not exclusively a monosynaptic reflex (Burke, 2016). Ia afferents establish robust monosynaptic excitatory connections with motoneurons within the homonymous motor neuron pool. They also form, however, relatively weaker monosynaptic projections to motoneurons in heteronymous (synergistic) motor neuron pools. Additionally, there is evidence to suggest the presence of oligosynaptic projections connecting Ia afferents

to both homonymous and synergistic motoneurons (Knikou, 2008, Pierrot-Deseilligny and Burke, 2012). Technically it is not possible to stimulate the Ia afferents, without also stimulating other neural structures. This is of particular importance if we consider the group Ib afferents from the Golgi tendon organs that exert an inhibitory effect on the motoneuron pool (Pierrot-Deseilligny et al., 1981). Based on probable conduction velocities of afferent neurons (Pierrot-Deseilligny and Burke, 2012), the excitatory and inhibitory influences will arrive in the same time frame to the motoneuron pool. As a result, although the excitation driving the H reflex is predominantly monosynaptic, the actual reflex response is influenced by a delicate interplay between the excitation from Ia afferents and the inhibitory input from Ib interneurons. This balance dictates the discharge of the reflex, which is also contingent on the level of excitability exhibited by the Ib inhibitory interneuron (Burke, 2016).

There are a few studies of the standard H reflex in ALS, albeit with somewhat surprising findings. Typically, the H_{max}/M_{max} ratio is increased in diseases characterized by spasticity and hyperreflexia (Misiaszek, 2003), however, in ALS this is not the case (Raynor and Shefner, 1994, Mazzini et al., 1997), even in patients with clinical UMN signs. This finding has been attributed to changes in the recruitment curve of the H reflex relatively to the M wave recruitment curve, probably due to a preferential loss in large, faster conducting peripheral axons, altering the dynamic of H reflex recruitment and decreasing the H_{max} amplitude. This loss also increases H reflex latency (Simon et al., 2015). An alternative measure has been recently proposed, the H_θ/M_θ ratio (Simon et al., 2015). H_θ and M_θ are calculated from the slope angle of the earliest rising phase of the H- and M-wave recruitment curves, respectively. This ratio is not influenced by the collision phenomenon of antidromic and orthodromic impulses, given that the recruitment of the H reflex follows the size principle (Buchthal and Schmalbruch, 1970), whereas the earliest phase of the M wave recruitment curve is formed by large caliber motor axons (Feiereisen et al., 1997). The H_θ/M_θ ratio is increased in ALS/MND relatively to healthy controls, while the H_{max}/M_{max} ratio was not significantly different (Simon et al., 2015). Another frequent finding in ALS patients is the easiness with which this reflex can be recorded in muscles typically difficult to obtain a response in healthy subjects, like in the intrinsic hand muscles, as well as the presence of an H reflex in weak or wasted muscles (Bae et al., 2013).

The H reflex can also be used in conditioning paradigms to assess post-synaptic events or changes in the amount of the presynaptic inhibition acting on Ia afferent terminals. This is possible because the amplitude of the H reflex is influenced by the excitability of motoneurons, and the ongoing presynaptic inhibition exerted on the Ia afferents responsible for conveying the test afferent volley. Consequently, the H reflex provides an effective means to investigate spinal neuronal pathways and mechanisms, both in a resting state and during various movements in human subjects. There are several of these condition paradigms described in human subjects (Pierrot-Deseilligny and Burke, 2012). In the next pages, some of these paradigms (the ones relevant to the present work) will be described.

Recurrent inhibition

The first spinal pathway to be identified was recurrent inhibition, which was extensively studied in terms of its structure, function, and response to drugs in animal experiments long before other spinal pathways could be explored (Renshaw, 1946). Additionally, it was among the earliest pathways for which a dependable, selective investigative technique was developed for use in human subjects (Pierrot-Deseilligny and Bussel, 1975). This capability stemmed from its distinctive characteristic of being triggered by the final motor output rather than relying on a specific afferent input (Eccles et al., 1954). While human experiments have contributed to our understanding of the practical significance of this form of negative feedback, the precise role, or roles it serves remains a subject of ongoing debate.

Recurrent inhibition is mediated by a specific inhibitory neuron located medially to the motor nuclei in the ventral horn, called the Renshaw cell (Renshaw, 1946). These cells are stimulated by axon branches originating from motoneurons and exert inhibition to alpha-motoneurons that innervate either the same or synergistic muscles (Figure 7). Renshaw cells are influenced by dorsal roots, group II and III muscle afferents, cutaneous afferents and ipsilateral and contralateral segmental afferents (Knikou, 2008).

Figure 7 – Recurrent inhibition pathway diagram

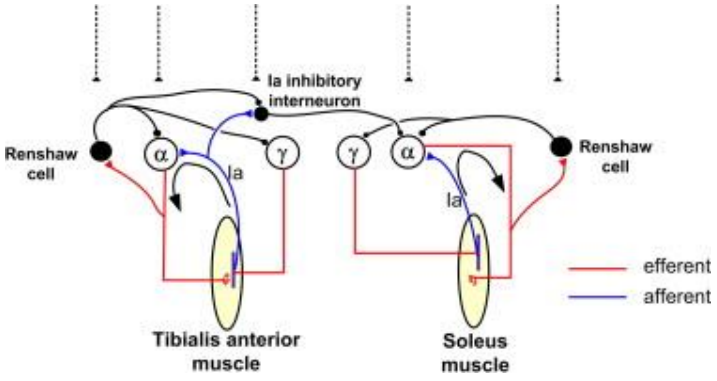

Spinal circuit denotes the neuronal pathway of Renshaw cells and their connections to alpha (α)- and gamma (γ)-motoneurons, and Ia inhibitory interneurons between ankle flexors and extensors. Renshaw cells depress the activity of α–γ motoneurons, and Ia inhibitory interneurons. Broken lines indicate parallel control of α-motoneurons, Ia inhibitory interneurons, and Renshaw cells by the brain; closed circles: inhibition, closed triangles: facilitation. Note: Adapted from Knikou (2008), with permission.

This extensive merging of input from various reflex pathways implies that the local feedback control offered by recurrent inhibition is adaptable and not fixed in a rigid, predetermined manner. Recurrent inhibition plays a significant role not only as a feedback tool of motoneurons, but also as a relevant mechanism in the neural control of movement.

Figure 8 – Presynaptic inhibition of Ia afferents reflected by changes of heteronymous Ia facilitation - heteronymous recurrent inhibition

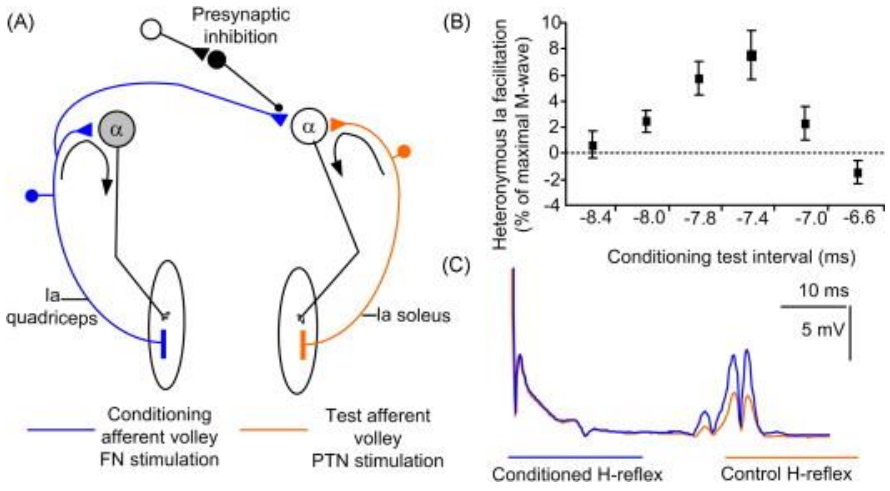

(A) Sketch illustrates the spinal circuit during which femoral nerve (FN) stimulation at low intensities delivered after posterior tibial nerve stimulation induces monosynaptic excitation of soleus α-motoneurons. Changes in the amount of heteronymous Ia facilitation reflect modulation of the on-going presynaptic inhibition acting on the Ia afferents of the conditioning afferent volley (quadriceps Ia afferents), (B) time course of soleus H-reflex facilitation by FN stimulation in one seated subject and (C) full-wave waveform rectified averages (n = 20) of the control and conditioned H-reflex following FN stimulation at −7.8 ms

are shown. Note that the heteronymous Ia reflex facilitation occurred without a significant change in the size of the M-wave. Note: Adapted from Knikou (2008), with permission.

Recurrent inhibition may be estimated in humans by assessing heteronymous recurrent inhibition (Figure 8) through stimulation of a nerve supplying an heteronymous muscle to the one being assessed, or by assessing homonymous recurrent inhibition (Figure 9) using the paired H reflex technique (Pierrot-Deseilligny and Burke, 2012).

Figure 9 – Assessment of homonymous recurrent inhibition, with the paired H reflex technique

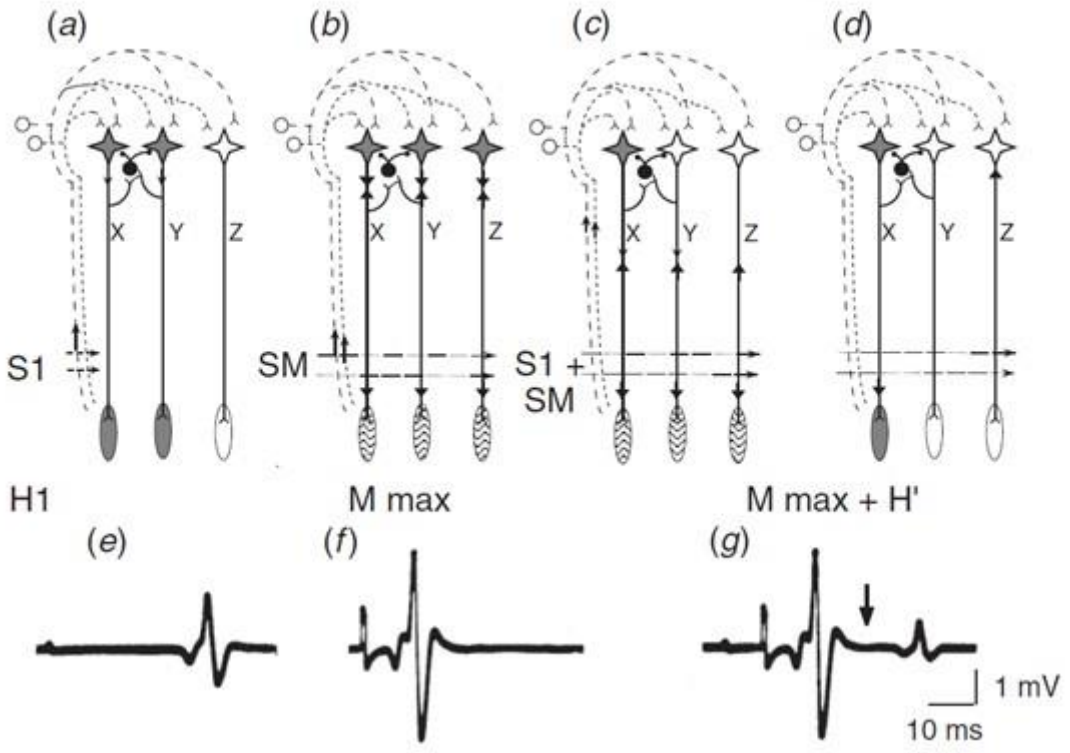

(a)–(g) Volleys in Ia afferents and motor axons ((a)–(d)), and corresponding EMG responses ((e)–(g)). Motoneurones (MNs) and muscle fibres activated in the H reflex are grey; muscle fibres activated in the M wave are speckled; orthodromic and antidromic volleys are indicated by vertical arrows. (a) Conditioning stimulation (S1) activates some Ia afferents (dashed line) and discharges MNs 'X' and 'Y', and the resulting H1 response is shown in (e). (b) Supramaximal (SM) stimulation recruits all Ia afferents (dashed and dotted lines) and all motor axons, producing the maximal M wave in (f), which is not followed by a reflex response, because the antidromic motor volley collides with and eliminates any reflex volley in motor axons. (c) When S1 precedes SM by 10 ms, the EMG contains the Mmax response (g). The antidromic volley evoked by SM collides with the conditioning H1 reflex discharge elicited by S1 in MNs 'X' and 'Y', and eliminates it in the corresponding axons, so that the H1 discharge does not appear in the EMG (the arrow in (g) indicates its predicted site). (d) Because of the collision between the SM antidromic volley and the H1 reflex discharge, the axons of MNs 'X and 'Y' are freed from antidromic impulses, and the reflex response due to SM (H') can appear in the EMG in (g). However, due to recurrent inhibition brought about by the H1 reflex discharge, the strong Ia volley due to SM cannot fire MN 'Y' ((c)–(d)) and H' is smaller than H1. Because MN 'Z' is not involved in the conditioning reflex, it cannot be assessed by the test reflex. Note: Adapted from Pierrot-Deseilligny and Burke (2012), with permission.

There are very few studies assessing this paradigm in ALS. Raynor and Shefner (1994) have reported a decrease in homonymous recurrent inhibition in a cohort of 12 ALS patients with lower limb spasticity. A reduced duration of recurrent inhibition was reported by Özyurt et al. (2020), using single motor unit recordings. A recent study by Sangari et al. (2022), has reported interesting findings by assessing heteronymous recurrent inhibition in ALS patients. This study showed that heteronymous recurrent inhibition was increased proximally (quadriceps) but reduced distally (soleus) as compared with healthy controls. Interestingly, higher amounts of inhibition were reported in early affected patients, while lower inhibition in patients with more severe involvement of the lower limbs was seen.

Presynaptic inhibition of Ia terminals

A continuous stream of afferent input is directed towards the spinal cord from multiple sources, encompassing the skin, muscles, tendons, and joints. The regulation of this sensory feedback, either through inhibition or facilitation, is essential for the successful execution of motor tasks. One critical juncture where the control of sensory feedback from the periphery can be efficiently managed is at the presynaptic inhibitory synapses situated on the afferent terminals that connect with alpha-motoneurons (Knikou, 2008).

These inhibitory synapses are GABAergic (Rudomin and Schmidt, 1999) and mediated by spinal interneurons activated by group I afferents and controlled by descending tracts (Jankowska, 1992). The inhibitory effect of this pathway has a long-lasting duration (several hundreds of milliseconds), probably reflecting the slow dynamics of GABA (Rudomin and Schmidt, 1999). Presynaptic inhibition is a phenomenon that can originate from various sources and serves as an inhibitory mechanism involved in the modulation of monosynaptic reflexes across a wide range of conditions. There are several control mechanisms of interneurons mediating presynaptic inhibition (Figure 10). Regarding descending control from higher centers, most of the modulation is inhibitory, i.e., it decreases the presynaptic depolarization and thereby the presynaptic inhibition.

This mechanism of inhibition of Ia afferents holds a pivotal role in the neural control of movement as it acts as a gatekeeper for sensory afferent feedback entering the spinal cord, facilitating the seamless execution of movements and motor tasks.

The fine-tuning of presynaptic inhibition by Ia afferents to motoneurons, depending on whether they are engaged in contraction or not, can significantly contribute to the creation of muscle synergies and movement patterns tailored to the specific motor task being performed (Rudomin and Schmidt, 1999, Knikou, 2008).

Figure 10 – Wiring diagram of pathways of presynaptic inhibition with primary afferent depolarization on Ia terminals in the cat

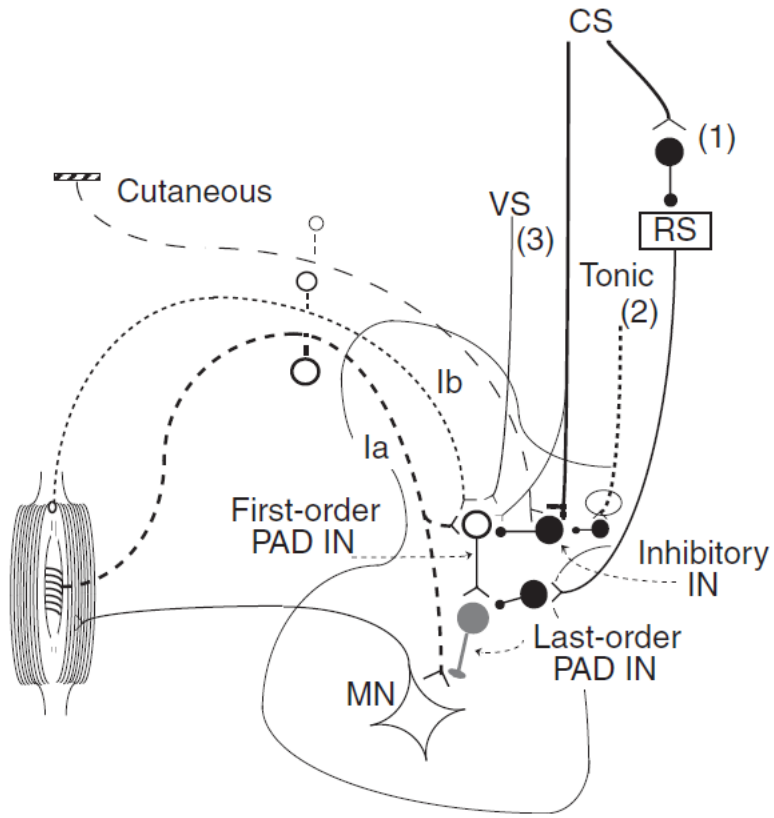

Excitatory synapses are represented by Y-shape bars and inhibitory synapses by small filled circles, first-order excitatory primary afferent depolarization (PAD) interneurons (IN) by open circles, last-order GABAA-ergic PAD INs by filled grey circles and inhibitory INs by large filled circles. First-order PAD INs receive excitation from Ia and Ib afferents and the vestibulospinal (VS) tract, and inhibition through the same inhibitory INs from cutaneous afferents and the corticospinal (CS) tract (though there is an alternative corticospinal pathway facilitating first order PAD INs, indicated by the thin continuous line). Inhibitory INs inhibiting first-order PAD INs receive descending tonic inhibition (dotted line). Last-order PAD INs receive inhibition from reticulospinal (RS) pathways, themselves inhibited from higher centres. Three mechanisms could contribute to a tonic level of presynaptic inhibition at rest in human subjects: (i) tonic inhibition from higher centres of the brainstem structures through which RS pathways maintain tonic inhibition on last-order PAD INs (i.e., disinhibition of PAD INs through control of RS suppression: pathway [1]); (ii) tonic inhibitory control of the inhibitory INs transmitting cutaneous inhibition of first-order PAD INs (i.e., disinhibition of PAD INs through control of afferent suppression: pathway [2]); (iii) tonic VS excitation of first-order PAD INs (i.e., descending excitation: pathway [3]). Note: Adapted from Pierrot-Deseilligny and Burke (2012), with permission.

There are several methodologies to assess presynaptic inhibition in man (Pierrot-Deseilligny and Burke, 2012): applying a brief vibration on a heteronymous

muscle; electrical stimulation of nerves supplying muscles antagonistic to the motoneuron pool tested; and assessing the amount of heteronymous Ia monosynaptic facilitation and thus infer background presynaptic inhibition. Figure 11 illustrates one of the possible pathways for assessing presynaptic inhibition, by stimulating a nerve supplying an antagonist of the target muscle.

Figure 11 – Presynaptic inhibition of Ia afferents induced by a conditioning afferent volley

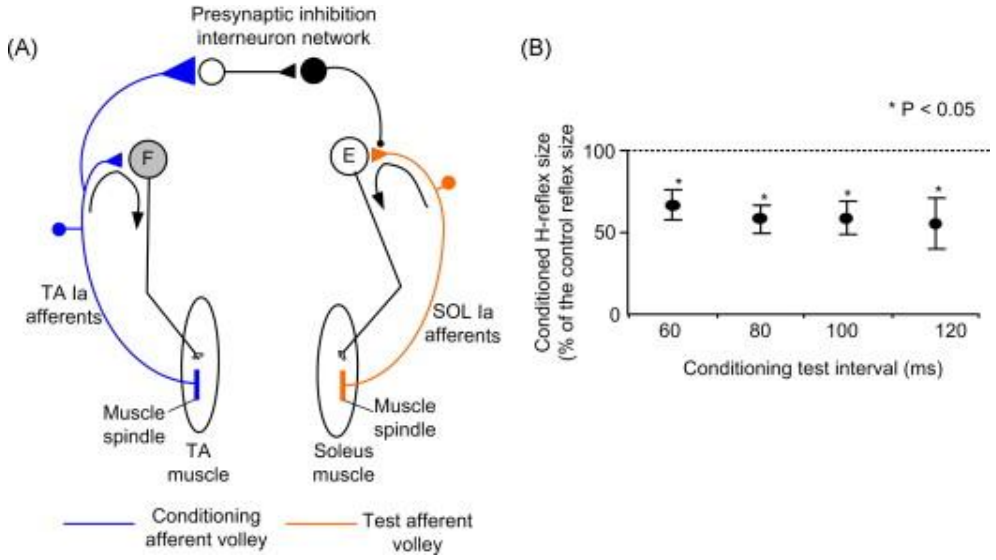

Common peroneal (CP) nerve stimulation at low intensities is delivered before posterior tibial nerve stimulation to establish based on the amplitude of the conditioned soleus H-reflex the amount of presynaptic inhibition acting on soleus Ia afferent terminals (A) and average size of the soleus H-reflex conditioned by CP nerve stimulation at C–T intervals ranged from 60 to 120ms for 10 seated subjects (B). Note: Adapted from Knikou (2008), with permission.

There is little information on presynaptic inhibition in ALS. (Schieppati et al., 1985) described less inhibition of the soleus H reflex after relaxation of a voluntary soleus contraction in ALS patients, which was interpreted as a failure to activate presynaptic inhibitory processes. Presynaptic inhibition was also described as decreased after a conditioning vibration stimulus (Morin and Pierrot-Deseilligny, 1988, Pierrot-Deseilligny, 1990). More recently, Howells et al. (2020) elegantly described a decrease in presynaptic inhibition of Ia afferents by using a conditioning stimuli in the deep peroneal nerve 11-50 ms prior to the test H reflex stimulus (D1 inhibition see Mizuno et al. (1971)). A novel threshold tracking technique, instead of the conventional constant-stimulus technique, was used. The findings of this work led the authors to suggest that dysfunction of spinal interneurons could play a major role in ALS pathophysiology.

Inhibition after cutaneous stimulation

Cutaneous receptors play a vital role in generating a wide range of sensations, including touch, pain, and temperature. However, it is important to note that all cutaneous mechanoreceptors can become active during movement, even in the absence of contact with an external object. Additionally, cutaneous axons of varying sizes can influence motor behavior. Like muscle afferents, cutaneous afferents are not uniform; they vary in terms of receptor type, fiber type, spinal pathway connectivity, central projections, and functional role.

Cutaneous afferents can impact motor behavior through shared pathways due to their extensive convergence onto interneurons located within pathways fed by muscle afferents and descending nerve tracts. They also influence primary afferent depolarization interneurons. Additionally, they have the capacity to independently modulate motor behavior through various routes (Pierrot-Deseilligny and Burke, 2012) (Figure 12).

Figure 12 – Wiring diagram of one of the presumed pathways, postsynaptic, of cutaneous influence over alpha motoneurons

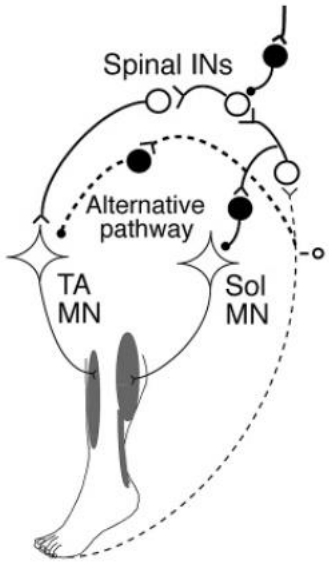

Excitatory synapses are represented by Y-shape bars and inhibitory synapses by small filled circles. Cutaneous fibers activate a chain of interneurons (Ins) that produce postsynaptic inhibition of Soleus motoneurons and excitation of the antagonist Tibialis anterior motoneurons. Note: Adapted from Pierrot-Deseilligny and Burke (2012), with permission.

In humans, changes in excitability of the soleus motoneuron pool after stimulation of the sural nerve have been described (Bathien and Hugon, 1964, Hugon, 1973, Pierrot-Deseilligny et al., 1973, Delwaide et al., 1981, Klomjai et al., 2014). These changes are dependent on the intensity of the stimulus (painful vs non-painful), the number of stimulus (one stimulus vs a train of stimuli) and the time course between the conditioning and the test stimulus. Delwaide et al. (1981) elegantly demonstrated that a train of 7 stimuli of 1 ms duration applied to lateral malleolus, provoked inhibition and facilitation of the soleus H reflex at different time points and depending on the stimulus intensity (Figure 13). Of interest, at the same timepoints, the H reflex of the TA was greatly facilitated.

There are no studies reported in the literature assessing this specific pathway in ALS.

Figure 13 – Recovery curves of the soleus H reflex after stimulation of the ipsilateral sural nerve at different intensities

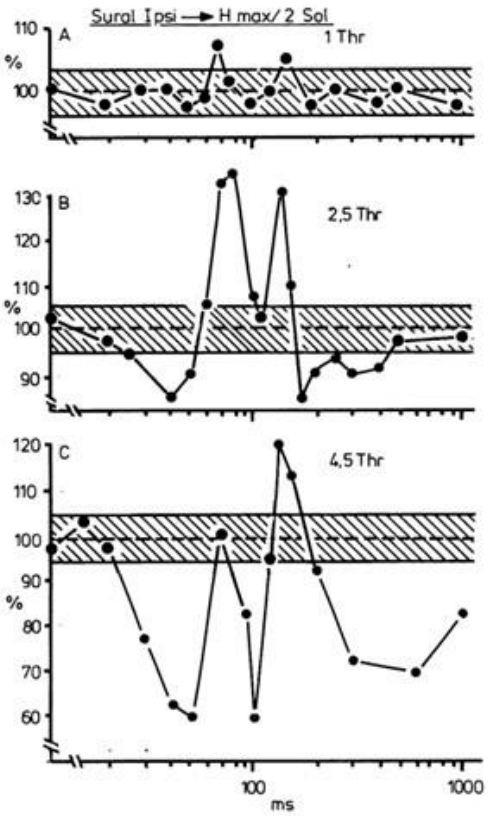

A: at threshold; B: at 2-5X threshold intensity and C: at 4*5X the threshold intensity. In abcissa (semi log): delays in ms between the stimulation of the sural nerve and that of the posterior tibial nerve. In ordinate, the amplitude of the conditioned responses expressed as a percentage of reference values. The limits of standard deviations appear on both sides of the control values. Note: Adapted from Delwaide et al. (1981), with permission.

A detailed revision of the H reflex physiology, mechanisms and conditioning paradigms is beyond the scope of this thesis. There are several detailed and comprehensive reviews of the H reflex in humans the reader can refer to (Burke et al., 1999, Pierrot-Deseilligny and Mazevet, 2000, Fisher, 2002, Misiaszek, 2003, Knikou, 2008, Pierrot-Deseilligny and Burke, 2012).

3.2. Cutaneous Silent Period

The temporary interruption of voluntary skeletal muscle contraction following strong stimulation of a cutaneous nerve is referred to as the cutaneous silent period (CutSP) (Shahani and Young, 1973). Thus, a CutSP is characterized by a temporary reduction, either relative or absolute, in the voluntary EMG activity that occurs after the application of noxious stimulation to a nearby cutaneous nerve. As represented in Figure 14, based on its characteristics, it is considered that this reflex is mediated at the spinal level, with the afferent arc depending on A-delta fibers, while the efferent arc is supplied by alpha-motoneurons (Leis et al., 1991, Floeter, 2003, Kofler et al., 2019a).

Upper limb CutSPs are integral components of a multifaceted pre-attentional protective reflex mechanism (Inghilleri et al., 1997, Leis et al., 2000, Kofler, 2003). They function in concert with excitatory cutaneous withdrawal reflexes, which serve the purpose of rapidly retracting the hand or limb away from a potentially harmful or noxious stimulus (Rossi et al., 2003). It is worth noting that both the inhibitory and excitatory reflex components appear to engage common spinal neural circuitry, which is activated by high-threshold, small-diameter nerve fibres (Rossi et al., 2003). At its core, the physiological underpinning of CutSPs seems to be the simplification of complex motor behaviour. This is achieved by essentially "turning off" specific muscle synergies, providing a means to momentarily inhibit voluntary muscle contractions (Leis et al., 2000). The coordinated interplay between inhibitory CutSPs and excitatory withdrawal reflexes helps safeguard the body from harm by allowing for swift and automatic responses to potentially dangerous stimuli. This reasoning is based on several features of the CutSP. The magnitude of muscle activity suppression is higher in muscle groups involved in reaching, pinching and grasping, than it is muscle groups involved in limb withdrawal (Kofler et al., 2019a). One convincing evidence of the classification as a possible protective mechanism is the fact that CutSPs can be produced by stimulation of the palm of the hand, but not the dorsum (Romaniello et al., 2004). Comparison of onset latencies of inhibition of distal hand muscles with facilitation of proximal flexor muscles also suggests a protective nature of this reflex (Kofler, 2003, Urban et al., 2004).

There is ample evidence supporting the role of A-delta fibers as the afferent arc of the CutSP. First, and foremost, the stimulus intensity necessary to obtain a reproducible CutSP needs to be painful or, at least, unpleasant (Uncini et al., 1991, Kofler, 2003). The estimated conduction velocities of the afferent volley are, on average, 12 to 13 m/s, which are in range of A-delta conduction (Inghilleri et al., 1997). Additionally, ischemia induced nerve block (Serrao et al., 2001) and severe neuropathies of large diameter fibres (Uncini et al., 1991), did not eliminate the CutSP.

Regarding the spinal mechanisms, the precise origin of the CutSP remains a subject of ongoing debate within the scientific community (Floeter, 2003, Kofler et al., 2019a). Based on existing knowledge, Kofler et al. (2019a) put forth three potential pathways to explain the CutSP. A presynaptic inhibitory pathway (Figure 15 A), in which the CutSP is attributed to presynaptic inhibition of sensory nerve terminals. This, in turn, leads to decreased excitability of motor neurons. In Figure 15 B, presynaptic and postsynaptic inhibition are combined. It posits that a combination of presynaptic, onto Ia afferents, and postsynaptic, directly to alpha motoneurons, mechanisms contribute to the CutSP's inhibitory effects. In Figure 15 C is represented a postsynaptic inhibition model suggesting that the CutSP is a result of inhibitory signals acting directly on the motoneurons themselves, making them less responsive to excitatory inputs. All these proposed models emphasize the potential involvement of spinal interneurons. These interneurons play a critical role in mediating signals between sensory and motor neurons and are believed to be key players in the origin of CutSP. While research continues to investigate and refine our understanding of CutSP, these models provide valuable insights into the complex neural mechanisms that underlie this phenomenon.

CutSP can be elicited in both upper and lower limbs, after noxious stimulation of a distal cutaneous afferent nerve. Typically, in upper limbs stimulation is applied to the fingers, while in lower limbs the sural nerve is stimulated in the ankle. The maximal duration of the EMG inhibition follows a stimulus intensity 8-15 times the sensory threshold (Floeter, 2003, Kofler et al., 2019a). Recordings should be performed with surface electrodes, using standard EMG equipment and filter settings (Kofler et al., 2019a). Onset and offset latencies should be defined by quantitative criteria, such as

a drop of the EMG trace below 50–100% of the baseline preceding the stimulus, in order to assure consistency of markings.

Figure 14 - Diagram of the proposed pathways mediating the cutaneous silent period following noxious digital nerve stimulation

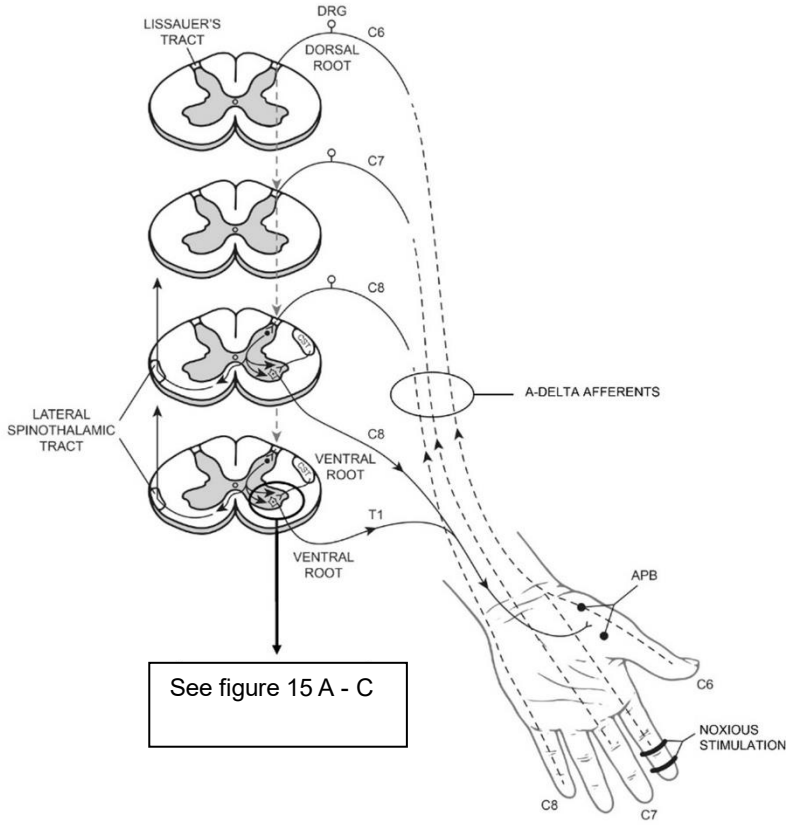

Afferent impulses in thinly myelinated A-delta fibers enter the spinal cord via the lateral portion of the dorsal root, where they descend several segments in Lissauer's tract. Collaterals and terminal branches synapse on dorsal horn cells in laminae I and V of Rexed, where they give rise to propriospinal projections that suppress activity in alpha-motoneurons of limb muscles. APB = abductor pollicis brevis muscle (as one exemplary muscle); DRG = dorsal root ganglion. Note: Adapted from Kofler et al. (2019a), with permission.

Due to its physiological properties, CutSP has been studied in several different pathological processes. In the last three decades, more than 80 papers have been published assessing CutSP in pathology (Kofler et al., 2019b), from peripheral to central nervous system diseases. For a comprehensive review of the physiological properties, technical aspects and uses in pathophysiological processes of the CutSP, please refer to Kofler et al. (2019a, 2019b).

In ALS, there are a few studies analyzing this reflex (Gilio et al., 2008, Kim and Kwak, 2010, Cengiz et al., 2018, Castro and de Carvalho, 2019, Gutierrez et al., 2020,

Castro et al., 2021, 2023b). There is a significant consistency in the results published, showing increased onset latencies, without changes in duration, both in upper and lower limbs.

Figure 15 - Three possible models for the effects of A-delta afferent input to account for the cutaneous silent period

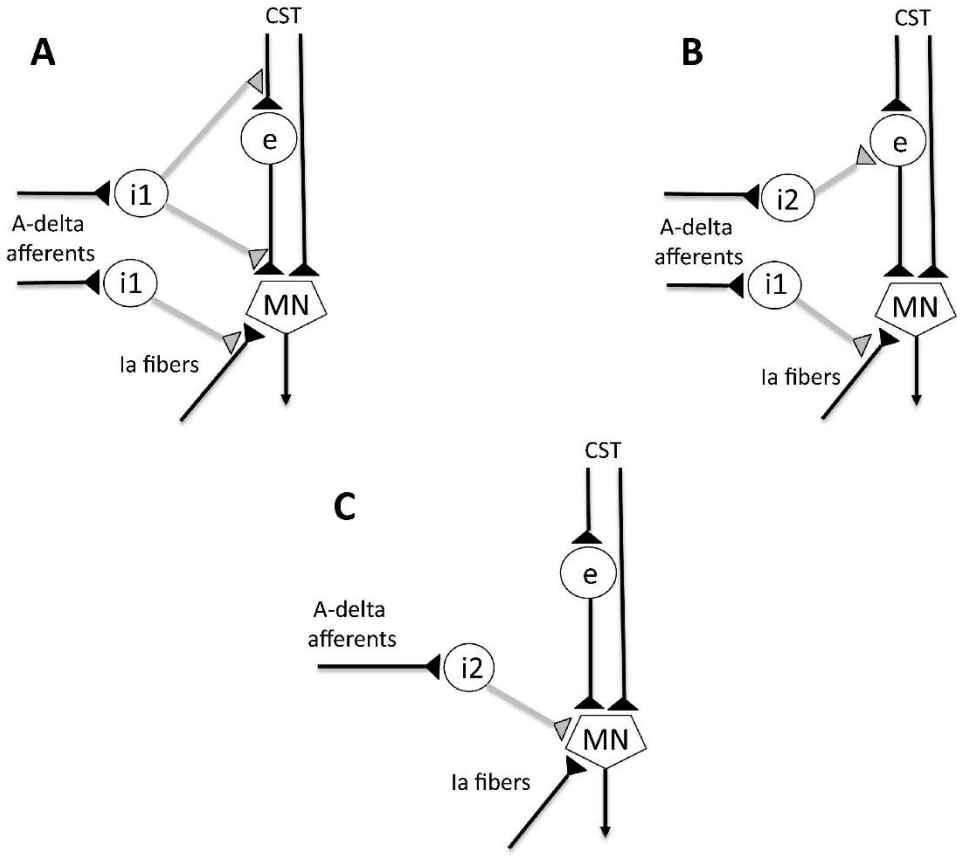

A. Classic presynaptic inhibition: in this model, cutaneous A-delta afferent impulses from digital nerve stimulation activate interneurons (i1) that presynaptically control the synaptic effectiveness of the corticospinal tract (CST), of excitatory premotor interneurons (e), and of Ia afferent connections (Ia fiber) to the alpha-motoneuron. B. Inputs to specific interneurons with different roles: In this model, cutaneous A-delta afferent impulses from digital nerve stimulation activate an inhibitory interneuron (i2), which exerts postsynaptic inhibition onto the excitatory premotor interneuron (e), thereby reducing descending corticospinal drive to the alpha-motoneuron, while Ia-afferent input (Ia fiber, similarly depicted as in A) to the same alpha-motoneuron is presynaptically inhibited by a different inhibitory interneuron (i1). C. Classic postsynaptic inhibition: In this model, cutaneous A-delta afferent impulses from digital nerve stimulation activate an inhibitory interneuron (i2), that directly inhibits the alpha- MN postsynaptically. In all three models, a small proportion of CST neurons, which connect directly with alpha-motoneurons remain uninhibited, explaining that residual motor evoked potentials can be detected even during maximum exteroceptive EMG suppression during the cutaneous silent period. In models A and B only, however, a different proportion of inhibition of Ia fiber input versus CST input would also explain disparate suppression of H reflexes versus motor evoked potentials during the cutaneous silent period. Connections depicted in grey indicate inhibitory interneurons, exerting either presynaptic (i1) or postsynaptic (i2) inhibition. Note: Adapted from Kofler et al. (2019a), with permission.

3.3. Transcranial Magnetic Stimulation

For many years, noninvasive brain stimulation was possible with the use of transcranial electrical stimulation (TES) (Merton and Morton, 1980). However, due to the high resistance of the skull to the passage of electrical current, high voltages are required to produce efficient currents to depolarize neurons in the cortex. The voltages required are thus very painful and inadequate to use in the awake human subject. Some years later, Barker et al. (1985), based on Faraday's law of induction, introduced TMS as a non-invasive, safe and well tolerated technique to study the human motor cortex (Figure 16). Currently, the use of TES is limited to monitoring motor pathways under general anesthesia (Deletis and Sala, 2008), while in all other applications, TMS is the standard technique used.

TMS employs electromagnetic induction as an effective and painless method to generate supra-threshold currents within the brain. A basic TMS apparatus consists of several circular loops of copper wire connected to a large electrical capacitance through a switch. These circular copper wire loops form the coil, which can take various configurations. The current pulse passing through the coil can be either monophasic or biphasic, creating a rapidly changing and brief magnetic field perpendicular to the coil plane. The peak strength of this magnetic field is comparable to that of the static field in a magnetic resonance imaging scanner (approximately 1-2 Tesla) (Rossini et al., 2015). Magnetic fields easily penetrate the brain without being significantly attenuated by the scalp or skull, inducing currents in accordance with Faraday's law of electromagnetic induction (Miranda, 2013).

Given the progressive loss of magnetic field strength with increasing distances, TMS is only able to stimulate relative superficial structures, about 3 to 4 centimeters away from the coil (Miranda, 2013). Given the intrinsic electrical characteristics of neurons, TMS preferentially activates axons instead of cell bodies and the threshold for this stimulation strongly depends on the relative current direction. Thus, axons are easier stimulated by the current that flows nearly in parallel with their main orientation (Miranda, 2013). These characteristics imply that TMS, at lower intensities, activate indirect waves (I-waves), reflecting indirect activation of corticospinal neurons through cortical interneurons. At higher intensities, TMS is able to recruit direct waves (D-waves), by direct stimulating corticospinal axons, although this depends also on coil

orientation (Di Lazzaro et al., 2004a, Di Lazzaro et al., 2004b). A single action potential, as the one elicited by the D-wave is insufficient to depolarize the spinal motoneuron at rest, and summation of D and I-waves are necessary to generate a motor evoked potential (MEP).

Over the years, and with the increase in electronic capabilities, other applications of TMS have been developed, from paired pulse techniques, to repetitive TMS (rTMS), theta burst stimulation or the real-time integration of TMS with electroencephalography (EEG), positron emission tomography (PET) and functional magnetic resonance imaging (fMRI) (Rossi et al., 2009, Lefaucheur, 2019). Given all the developments of the last four decades, nowadays the field of TMS is a diverse and complex world. The next pages will focus on TMS techniques particularly relevant in ALS and in the context of this dissertation. For comprehensive and detailed reviews of TMS, the reader should refer to (Rossi et al., 2009, Klomjai et al., 2015, Rossini et al., 2015, Valero-Cabré et al., 2017, Lefaucheur, 2019).

Figure 16 – Diagram illustration of transcranial magnetic stimulation over the motor cortex

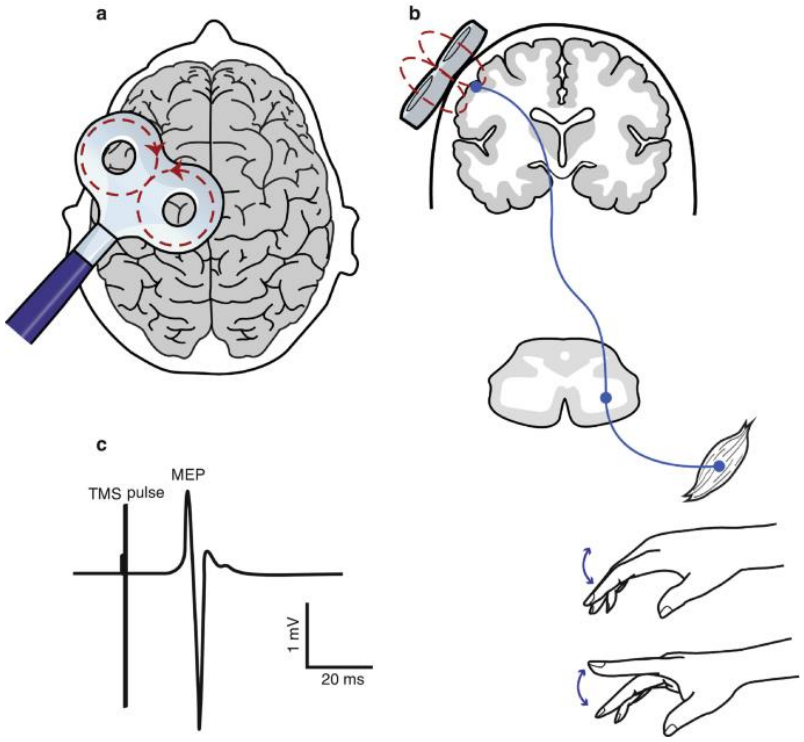

TMS – Transcranial magnetic stimulation: MEP – motor evoked potential; Note: Adapted from Hui et al. (2020), with permission.

3.3.1. Conventional TMS

The main use of the conventional single pulse TMS technique is the study of the motor cortex, given the easily accessible way of recording a direct response to the stimulus applied. A simple surface EMG recording over a given muscle during the stimulus, an MEP, quickly allows for the evaluation of several parameters that depend on specific circuits of the motor cortex. A number of neurophysiological measures can offer insights into changes in motor cortical control or corticospinal output associated with diseases affecting the central nervous system.

Motor threshold

Motor Threshold (MT) has been objectively defined by the International Federation of Clinical Neurophysiology as the minimum intensity required to evoke a small MEP in the target muscle (Rossini et al., 2015). MT can be defined at rest (MEP > 50 μV in at least 5 of 10 trials; resting motor threshold - RMT), in this manner, MT represents the ease with which cortical motoneurons are excited. Lower MTs have been observed for muscles controlling fine hand movements (Brouwer and Ashby, 1990, Macdonell et al., 1991). Additionally, MTs tend to be lower for the dominant hand (Macdonell et al., 1991) and correlate with fine finger task performance (Triggs et al., 1997). These findings suggest that MT reflects the density of corticomotoneuronal connections to the anterior horn cell (Rossini et al., 1999) and can potentially act as a neurophysiological biomarker of corticomotoneuronal representation and function. Furthermore, MT may reflect cortical neuronal membrane excitability (Amassian et al., 1987, Epstein et al., 1990). It has been demonstrated that inhibition of voltage-gated sodium channels leads to increased motor thresholds (Boroojerdi et al., 2001). Glutamatergic neurotransmission, through AMPA receptors, also appears to influence motor thresholds, with excessive glutamate activity reducing them (Di Lazzaro et al., 2003) as well as being modulated by sodium channel blockers (Vucic et al., 2013).

In the context of ALS, changes in motor thresholds have been observed but reports in the literature seem somewhat conflicting. Some studies report increased thresholds or even an inexcitable motor cortex in ALS patients (Eisen et al., 1990, Triggs et al., 1999, de Carvalho et al., 2003), while others document normal or reduced motor thresholds (Caramia et al., 1991, Vucic and Kiernan, 2006, Vucic et al., 2008). These discrepancies likely stem from the heterogeneity of ALS presentations and the

disease stage at the time of testing. Longitudinal studies have shown a reduction in motor threshold early in the course of ALS, which gradually increases to the point of cortical inexcitability as the disease progresses. This early reduction in motor threshold appears most pronounced in ALS patients with profuse fasciculations and hyperreflexia (Eisen and Weber, 2001). Given that motor threshold can be influenced by glutamate activity, this early reduction suggests that cortical hyperexcitability contributes to progressive neurodegeneration through glutamate toxicity (Vucic and Kiernan, 2013).

MEP amplitude

MEP amplitude is a reflection of complex corticospinal volleys, including D and I-waves. Increasing the stimulus intensity leads to an increase in MEP amplitude. This relationship may be used to generate a stimulus–response curve, which follows a sigmoid function (Devanne et al., 1997). Like MT, MEP amplitude, and the stimulus–response curve gradient, provides insight into the density of corticomotoneuronal connections to motor neurons. However, MEPs likely assess neurons that are less excitable or farther from the center of the TMS-induced electrical field compared to MT (Vucic et al., 2023).

MEP amplitude is typically expressed as a percentage of the maximum CMAP evoked by peripheral nerve stimulation (Rossini et al., 2015). This normalization accounts for any LMN pathology and offers information about the proportion of the motor neuron pool activated during the MEP. However, normative values for the MEP-to-CMAP ratio show substantial inter-subject variability, limiting its sensitivity and diagnostic value in detecting corticomotoneuronal abnormalities (Vucic et al., 2023). The modulation of MEP responses involves various neurotransmitter systems within the central nervous system. GABAergic neurotransmission via $GABA_A$ receptors suppresses MEP amplitude, while glutamatergic and noradrenergic neurotransmission enhances it. Remarkably, these changes in MEP amplitude occur independently of changes in MT, suggesting diverse physiological mechanisms underlying their generation (Ziemann, 2003).

Abnormalities in MEPs are well-documented in ALS (Vucic et al., 2023). Increases in MEP amplitude have been observed in both sporadic and familial forms of ALS, particularly in the early stages of the disease (Vucic et al., 2008). MEP

amplitude correlates with surrogate markers of axonal degeneration, such as the strength-duration time constant, establishing a link between cortical hyperexcitability and motor neuron degeneration (Vucic and Kiernan, 2006). Importantly, this increase in MEP amplitude is not observed in mimic disorders with similar LMN dysfunction (Vucic and Kiernan, 2008), implying that the changes in MEP amplitude in ALS may be excitotoxic in nature.

Central motor conduction time

The central motor conduction time is the interval between the stimulation of the motor cortex and the beginning of the ensuing MEP (Rossini et al., 2015). The time it takes for pyramidal cells to activate, the time it takes for the descending signal to travel along the corticospinal tract, synaptic transmission, the activation of spinal motor neurons, motor axon conduction, and neuromuscular transmission are all factors that influence the generation of central motor conduction time (Mills, 2004). The F-wave or cervical nerve root stimulation are two approaches that can be used to measure central motor conduction time (Rossini et al., 2015). It is important to note that each of these methods produces an estimate of central motor conduction time, and a large range of normative data exists due to different technical, physiological, and pathological factors influencing this measurement.

In ALS, central motor conduction time is typically prolonged (Eisen et al., 1990, Mills, 2003, Civardi et al., 2020). Assessing central motor conduction time can be particularly valuable for documenting subclinical UMN dysfunction, assisting in the diagnosis of ALS. However, it does not seem a sensitive measure of disease progression (de Carvalho and Swash, 2023). Although the precise mechanisms responsible for the prolongation of central motor conduction time in ALS are not fully understood, it is proposed that increased desynchronization of corticomotoneuronal volleys due to axonal loss may be the underlying mechanism (Eisen et al., 1996, Komissarow et al., 2004).

3.3.2. Cortical Silent Period

The cortical silent period (CSP) refers to a period of electrical silence in the background EMG activity of a contracting muscle following suprathreshold TMS of the

primary motor cortex (M1) (Figure 17A). It typically lasts from 50 to 300 milliseconds (Cantello et al., 1992). The duration of CSP increases stimulation intensity but is not correlated with the size of the preceding MEP response (Triggs et al., 1992) or the strength of contraction of the muscle being targeted (Inghilleri et al., 1993). Interestingly, the threshold for the CSP is typically below the threshold for MT strongly suggesting that the CSP is not dependent on the activation of the corticomotoneuronal system (Ziemann, 2004). CSP can thus be explained by suppression of voluntary motor drive (Tergau et al., 1999), with its duration being a possible surrogate marker of motor cortical inhibition (Hallett, 1995).

The CSP primarily arises from the activation of cortical inhibitory neurons. However, it's worth noting that spinal mechanisms may also play a role, particularly in the early segments of the CSP (Cantello et al., 1992, Inghilleri et al., 1993). Specifically, long-lasting inhibitory postsynaptic potentials mediated by GABAB receptors appear to have a significant role in generating the CSP (Inghilleri et al., 1993, Ziemann et al., 1993). This is supported by pharmacological studies indicating that GABAB receptor agonists and GABA reuptake inhibitors can prolong the duration of the CSP (Werhahn et al., 1999). Furthermore, the duration of the CSP seems to be influenced by the density of corticomotoneuronal projections to anterior horn cells, with upper limb muscles exhibiting the longest CSP duration (Vucic et al., 2023). Studies have shown that CSP duration is generally reduced in older adults (Sale and Semmler, 2005, Davidson and Tremblay, 2013). However, there are some reports of comparable CSP durations between young and older adults (Fujiyama et al., 2012), and CSP duration does not appear to be influenced by gender (Shibuya et al., 2016a).

In addition to CSP, there is the concept of ipsilateral inhibition (ipsilateral silent period, iSP), which is induced by stimulating the motor cortex and results in the interruption of ongoing voluntary EMG activity in muscles on the same side as the stimulus (Figure 17 B). The iSP primarily reflects transcallosal inhibition (Meyer et al., 1995), although non-callosal pathways below the corpus callosum may also contribute to this phenomenon (Compta et al., 2006). The iSP typically begins around 30 to 40 milliseconds after TMS and lasts for 20 to 25 milliseconds (Meyer et al., 1995). In older adults, the onset latency and transcallosal conduction time is increased, whereas the area of the iSP is decreased, suggesting a decline in transcallosal inhibition with age

(Davidson and Tremblay, 2013). Factors such as muscle contraction level, direction of TMS-induced current, or limb dominance do not seem to significantly affect the iSP (Davidson and Tremblay, 2013, Kuo et al., 2017).

Figure 17 – Illustrative examples of cortical silent period and ipsilateral silent period

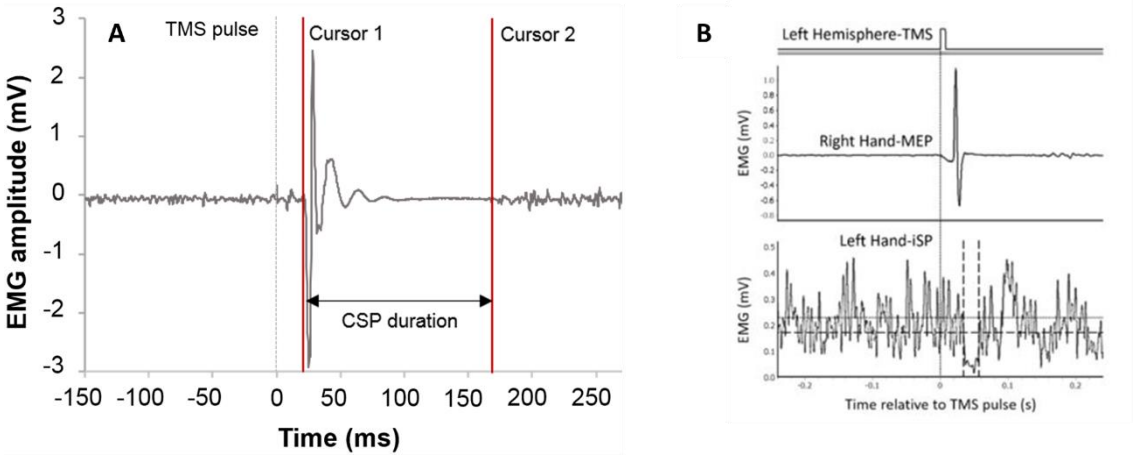

CSP – cortical silent period; iSP – ipsilateral silent period; Note: Adapted from Wilke et al. (2016) (A) and Tian et al. (2021) (B), under CC-BY attribution license

Studies conducted in individuals with ALS consistently reveal abnormalities in the CSP. There is a notable absence or reduction in the duration of the CSP, and these abnormalities have been observed in both sporadic and familial forms of ALS. The most significant reductions in CSP duration tend to occur early in the course of the disease and (Prout and Eisen, 1994, Siciliano et al., 1999, Mills, 2003, Vucic and Kiernan, 2006, Wittstock et al., 2007, Vucic et al., 2008) are more prominent in patients with UMN signs (Civardi et al., 2020). With disease progression, CSP duration tends to increase (de Carvalho and Swash, 2023). Importantly, these reductions in CSP duration appear to be specific to ALS and are not observed in mimic disorders (Vucic and Kiernan, 2008). While the precise mechanisms responsible for the reduction in CSP duration in ALS are still being investigated, it is believed that intrinsic factors, such as decreased motor drive and impaired GABAergic inhibition, play a role. This impairment may be due to the degeneration of inhibitory interneurons or dysfunction of GABAB-mediated receptor inhibition (Vucic et al., 2013).

Abnormalities in the iSP have also been reported in ALS. The iSP reflects the functioning of transcallosal inhibitory fibers, as supported by the fact that iSP abnormalities are observed in patients with lesions in the corpus callosum (Meyer et

al., 1995). In ALS, the iSP is either absent or delayed, and these abnormalities tend to appear early, often preceding the clinical onset of ALS (Karandreas et al., 2007, Wittstock et al., 2007, Wittstock et al., 2020, Hübers et al., 2021b). These findings suggest that degeneration of callosal neurons, which regulate the activity of inhibitory GABAergic neurons responsible for generating the iSP, may contribute to these abnormalities in ALS. Additionally, studies have also shown atrophy of the corpus callosum in ALS patients, regardless of clinical signs of UMN involvement (Yamauchi et al., 1995, Filippini et al., 2010, Hübers et al., 2021a, Hübers et al., 2021b).

3.3.3. Paired pulse techniques

The preceding sections have focused on TMS parameters that are evaluated by stimulating the motor cortex with single impulses. Motor cortical excitability can also be evaluated using paired-pulse techniques, where a conditioning stimulus influences the response to a subsequent test stimulus. Various paired-pulse paradigms have been developed, but three commonly used ones in ALS clinical research to assess cortical excitability are: short interval intracortical inhibition (SICI), intracortical facilitation (ICF), long interval intracortical inhibition (LICI) and intrahemispheric inhibition (IHI). These paradigms provide valuable insights into the excitability of the motor cortex and are frequently employed in ALS studies.

Short interval intracortical inhibition and Intracortical facilitation

SICI and ICF are both assessed at short inter-stimulus intervals (ranging from 1 to 30 milliseconds) and involve the modulation of the amplitude of a test MEP by a sub-threshold conditioning pulse applied using the same stimulating coil (Kujirai et al., 1993, Ziemann et al., 1996).

SICI occurs at inter-stimulus intervals of 1 to 5 ms, while ICF occurs at intervals of 7 to 20 ms (Kujirai et al., 1993, Ziemann et al., 1996). Typically, the intensity of the conditioning pulse is set to 80% of resting MT and the intensity of the test pulse is adjusted to produce a test MEP of 1 millivolt or less in peak-to-peak amplitude (Kujirai et al., 1993, Ziemann et al., 1996). Given the intrinsic variability of MEP (Hanajima et al., 1998), threshold tracking techniques have been posteriorly developed, using a

constant target MEP response and measuring the changes in the stimulus needed to achieve the target MEP amplitude (Fisher et al., 2002, Vucic and Kiernan, 2006).

Through epidural recordings of the descending corticomotoneuronal volley, data has suggested that both SICI and ICF originate from mechanisms within the motor cortex itself (Nakamura et al., 1997, Di Lazzaro et al., 1998). A decrease in the number and amplitude of late I-waves is associated with SICI, while ICF is associated with an increase in these parameters. The orientation of stimulation coil has different influences in both SICI and ICF (Pavey et al., 2023). These observations suggest that ICF is not merely a rebound facilitation but represents a distinct physiological process separate from SICI (Ziemann, 2004, Van den Bos et al., 2018).

Neuropharmacological studies have provided additional evidence that SICI and ICF are physiologically different mechanisms. GABA agonists, like benzodiazepines, enhance GABAergic transmission via GABAA receptors increasing SICI (Di Lazzaro et al., 2000). This suggests that SICI is mediated by cortical synaptic mechanisms involving inhibitory interneurons. On the contrary, ICF is reduced by GABAA agonists (Ziemann, 2004). Additionally, tiagabine, a GABA reuptake inhibitor, decreases SICI, possibly by activating presynaptic GABAB receptors, leading to autoinhibition of postsynaptic GABAA receptor-mediated inhibition (Werhahn et al., 1999). Interestingly, ICF seems to be unaffected by this autoinhibition (Werhahn et al., 1999).

Apart from GABAergic modulation, SICI and ICF are influenced by various other cortical neurotransmitter systems in distinct ways. For instance, glutamate antagonists like riluzole, dopamine receptor agonists, and norepinephrine antagonists increase SICI, while dopamine antagonists and norepinephrine agonists reduce it. Conversely, glutamate antagonists that inhibit NMDA receptors, selective serotonin reuptake inhibitors, and norepinephrine antagonists decrease ICF, whereas norepinephrine agonists increase it (Vucic and Kiernan, 2013).

Measurements of SICI and ICF are thus particularly valuable when investigating disorders involving GABA or glutamate-dependent neuronal circuits within the motor cortex.

Both sporadic and familial ALS have a consistent pattern of diminished or absent SICI, frequently associated withincreased ICF, suggesting cortical

hyperexcitability (Hanajima et al., 1996, Yokota et al., 1996, Ziemann et al., 1997, Sommer et al., 1999, Stefan et al., 2001, Zanette et al., 2002b, Vucic and Kiernan, 2006, 2008, Vucic et al., 2008, Geevasinga et al., 2014, Menon et al., 2019, Cengiz and Kuruoğlu, 2020, Dharmadasa et al., 2020, Tankisi et al., 2021, van den Bos et al., 2021, de Carvalho and Swash, 2023, Tankisi et al., 2023). Notably, this reduced SICI appears to be an early sign of sporadic ALS (Vucic and Kiernan, 2006) and correlates with peripheral neurodegenerative measurements (Vucic and Kiernan, 2008, Vucic et al., 2010, Vucic et al., 2011). At least in familial ALS, it appears before the onset of clinical symptoms (Vucic et al., 2008). Additionally to the early changes detected, SICI seems to decrease over time with disease progression (Shibuya et al., 2017, de Carvalho and Swash, 2023), and correlates with worst prognosis (Shibuya et al., 2016b).

The underlying mechanism for these changes in SICI may involve the degeneration of inhibitory cortical interneurons. This hypothesis is supported by neuropathological studies revealing a loss of parvalbumin-positive inhibitory interneurons in ALS (Nihei et al., 1993). Furthermore, a potential role for a glutamate-mediated excitotoxic process is suggested by the partial restoration of SICI in ALS patients treated with the glutamate antagonist riluzole (Stefan et al., 2001, Geevasinga et al., 2016). Reduced SICI at inter-stimulus intervals of 1 and 3 ms at various conditioning stimulus intensities (low, medium, and high) in ALS patients, provided additional support for the idea that SICI is likely influenced by a combination of glutamate excitotoxicity and the degeneration of inhibitory cortical circuits (Vucic et al., 2009). Recently, Ezogabine, a potassium channel activator antiepileptic approved drug, demonstrated a dose-dependent effect in decreasing hyperexcitability in ALS, by increasing SICI after a 10-week treatment (Wainger et al., 2021).

Long interval intracortical inhibition

Paired-pulse paradigms with longer intervals (20–200 ms) are used to evaluate how a suprathreshold conditioning pulse modulates the amplitude of the subsequent suprathreshold test MEP, both delivered through the same stimulating coil. Typically, both pulses are administered at a stimulus intensity ranging from 110% to 150% of MT. At inter-stimulus intervals longer than 50 ms, the conditioning pulse typically exerts an inhibitory effect (Claus et al., 1992, Valls-Solé et al., 1992).

Epidural recordings of the descending corticomotoneuronal volley from the spinal cord have shown that LICI is associated with a decrease in late I-waves (Nakamura et al., 1997), indicating that LICI is primarily a process occurring within the motor cortex. It's important to note that the inhibitory mechanisms responsible for LICI are different from those underlying the CSP. This distinction is supported by findings in patients with idiopathic Parkinson's disease who exhibited a decreased CSP duration but an increased LICI (Berardelli et al., 1996).

LICI can be understood as a measure of how responsive the motor cortex is to synchronized excitatory input from TMS during cortical inhibition induced by the conditioning pulse. In contrast, the CSP reflects how this inhibition interacts with the ongoing voluntary motor drive to the motor cortex. Both CSP and LICI are modulated by tiagabine, a GABA reuptake inhibitor, suggesting an influence of GABAB receptors on these inhibitory mechanisms (Werhahn et al., 1999).

In ALS, LICI at an interval of 155 ms was found decreased in patients, when compared to controls, independently of site of onset (spinal vs bulbar) (Salerno and Georgesco, 1998). At intervals of 100-150 ms, Zanette et al. (2002b) showed a significant decrease of LICI in ALS patients, more prominent in subjects with UMN signs. These findings suggest a significant impairment of long-lasting GABA mediated inhibitory mechanisms in ALS.

Interhemispheric inhibition (IHI)

Sparce connections between motor cortices on both hemispheres have been demonstrated by fibers that traverse the corpus callosum, in the hand area of the monkey (Rouiller et al., 1994). In humans, imaging studies have shown that the patterns of connectivity closely resemble those derived from anatomical tracing in primates (Ruddy et al., 2017). This pathway represents a homotopic connection between corresponding motor cortical regions, and can be confirmed by single (Amassian and Cracco, 1987) and paired-pulse protocols (Ugawa et al., 1993) in humans. There is debate over the excitatory or inhibitory profile of the transcallosal pathway (Bloom and Hynd, 2005), however, in this paradigm, the predominant effect is clearly inhibitory. IHI is elicited by a supra-threshold conditioning stimulus applied to one motor cortex and refers to an inhibition of the test MEP, produced by the stimulus over the contralateral motor cortex (Ferbert et al., 1992, Hanajima et al., 2001,

Daskalakis et al., 2002). The stimuli are delivered through two different focal stimulating coils over the hand area of either motor cortex. The IHI is usually stronger at ISI of 10 ms. The magnitude and duration of IHI are higher with increasing intensities of the conditioning stimulus and can reach up to 50% and 30 ms, respectively (Ferbert et al., 1992, Hanajima et al., 2001).

Epidural recordings, from the cervical spinal cord, of the descending corticospinal volley showed a reduction of the amplitude of late I-waves, more specifically the I3-wave, with an ISI of 6 ms (Di Lazzaro et al., 1999). It is thus very likely that the IHI occurs at the level of the test motor cortex. It estimated that 9-12 ms is the minimum conduction time between motor cortices through the corpus callosum (Cracco et al., 1989). Adding the time of the shortest effective ISI (6-7 ms) with the delay of about 3 ms between I1 and I3 gives a similar time to the estimation of callosal conduction, suggesting the IHI is effectively mediated through the corpus callosum. Additionally to this empiric reasoning, IHI was absent in a patient with callosal agenesis (Rothwell et al., 1991). An inverse correlation between IHI and mirror activity has also been demonstrated (Hübers et al., 2008). Pathological mirror movements are common in diseases of the corpus callosum (Cincotta and Ziemann, 2008). Despite the fact that callosal pathways are primarily excitatory, the predominantly inhibitory interhemispheric interaction is most likely explained by strong surround inhibition in the test motor cortex (Hanajima et al., 2001).

In ALS, a significant decrease of IHI has been reported (Karandreas et al., 2007, Hübers et al., 2021a, van den Bos et al., 2021). The decrease in IHI correlated with greater disability and faster disease progression (van den Bos et al., 2021), as well as with structural impairment of the corpus callosum (Hübers et al., 2021a), suggesting that impairment of transcallosal inhibitory mechanisms may play a significant role in ALS pathophysiology.

3.4. Mirror Movements

Performing tasks that involve only one side of the body requires a decrease in the neural activity originating from the ipsilateral primary motor cortex (M1) (Carson, 2005). When the neural pathways responsible for controlling unilateral voluntary movements and the associated inhibitory circuits are impaired or dysfunctional, it can result in unintended neural signals crossing the midline (Cincotta and Ziemann, 2008). This phenomenon is referred to by various names in the literature, such as motor overflow, mirror activity (MA), or mirror movements (MM).

There are three proposed pathophysiological mechanisms (Figure 18) to explain this phenomenon (Cincotta and Ziemann, 2008, Sehm et al., 2010). The first explanation involves the activation of the uncrossed corticospinal projection, which directly connects to the LMN on the same side of the body (Farmer et al., 1990, Mayston et al., 1997). The second possibility suggests that a decrease in IHI allows for the activation of the motor cortex on the opposite side of the body through transcallosal pathways (Cernacek, 1961, Hübers et al., 2008). A third possibility is an abnormal motor planning and/or abnormal transmission of the motor plan from the supplementary motor areas (SMA) to the primary motor areas might also be involved in MM generation (Welniarz et al., 2015). It is important to note that these explanations are not mutually exclusive and may interact in complex ways to produce the observed motor overflow or mirror activity phenomenon.

Efficient lateralization of voluntary movements is typically seen in individuals with a mature motor system. This is evident from the presence of MM during intended unimanual tasks in healthy children (Cohen et al., 1967, Lazarus and Todor, 1987, Mayston et al., 1999). In contrast, normal adults generally demonstrate the ability to perform unilateral movements in their daily activities (Schott and Wyke, 1981). However, slight, involuntary mirroring or unintended mirror activity can sometimes be observed (Cernacek, 1961, Armatas et al., 1994, Castro et al., 2023a). Assessment of this mirror activity has been reported either by clinical observation (Woods and Teuber, 1978, Krampfl et al., 2004, Magne et al., 2021), by force transduction measurements (Armatas et al., 1994, Uttner et al., 2005), or by recording surface EMG signal (Cernacek, 1961, Krampfl et al., 2004, Cincotta et al., 2006, Vardy et al., 2007, Hübers et al., 2008). In patients, MM have been described mainly in the hands (Schott

and Wyke, 1981, Farmer et al., 1990), although there have been reports of the presence of this activity in the lower limbs (Espay et al., 2005, Maudrich et al., 2017).

Figure 18 – Hypothetical mechanisms of mirror movements generation

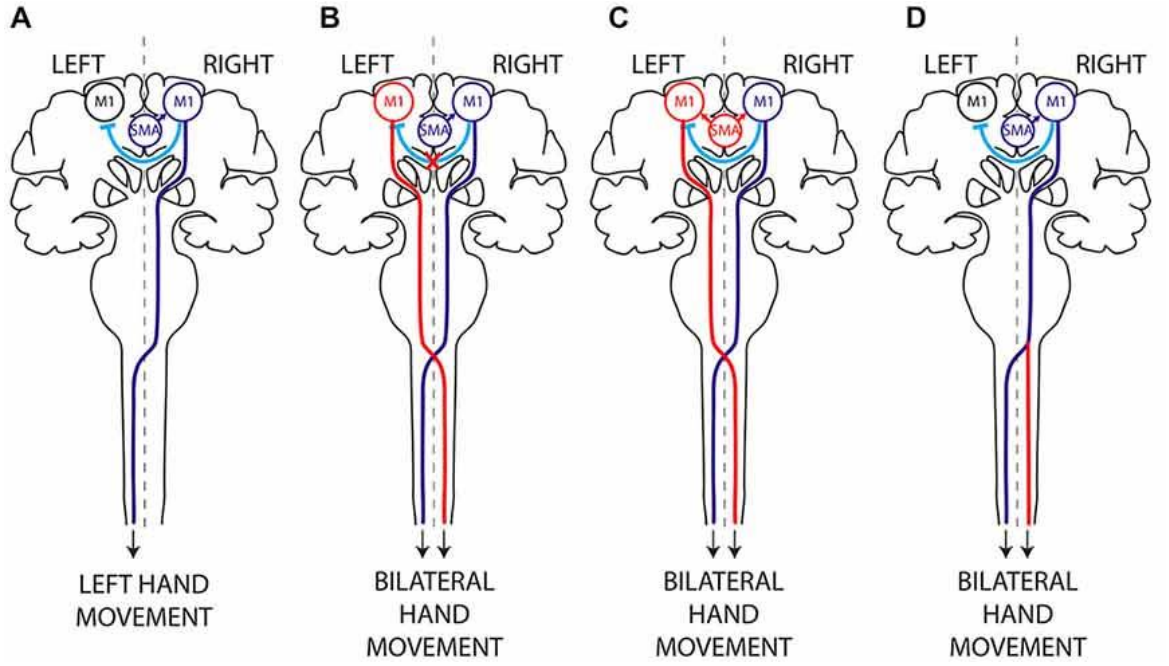

(A) In humans, execution of a unilateral left-hand movement requires both lateralized activation of the right primary motor cortex (M1) by interhemispheric inhibition (IHI) and proper motor planning and then transmission of the motor command to the contralateral (left) hand alone, through a crossed corticospinal tract. There are three hypothesis underlying MM: abnormal IHI (B), abnormal delivery of the motor plan from the supplementary motor area (SMA) to M1 (C), resulting in bilateral activation of the primary motor cortices; activation of the uncrossed corticospinal projection, which directly connects to the lower motor neurons on the same side of the body (D). Note: Adapted from Welniarz et al. (2015), under CC-BY attribution license.

In healthy adults, the level of mirror EMG activity tends to increase during more demanding motor tasks, when experiencing fatigue, cognitive distraction, reduced attentional capacity, and with aging (Cincotta and Ziemann, 2008). It's worth noting, however, that even in a large unselected group of elderly healthy volunteers, slight mirror movements have been frequently observed during relatively simple unimanual tasks, particularly if the subjects were not explicitly instructed to suppress unintended motor activity (Ottaviani et al., 2008). For a comprehensive review of physiological aspects and pathophysiology of MM in humans, please refer to Cincotta and Ziemann (2008).

MM have been documented in ALS (Krampfl et al., 2003, Krampfl et al., 2004, Wittstock et al., 2007, Meister et al., 2011, Wittstock et al., 2011, Wittstock et al., 2020, Hübers et al., 2021a, Hübers et al., 2021b) albeit with variable frequency. These

studies have, however, relied principally on clinical observation of the MM, which can be a major limitation. Generally, it has been proposed that MM in ALS patients are due to callosal dysfunction.

4. Research aims

The overall aim of this thesis was to obtain a better understanding of the physiology and pathophysiology of spinal and supraspinal inhibitory pathways in ALS. For that purpose, several experiments using original neurophysiological approaches were explored.

Specifically for each study, the aims were:

Study I: To investigate CutSP latencies and duration in different phenotypes of MND categorized by the severity of the UMN signs. To test the effect of simultaneous contralateral hand contraction on the CutSP.

Study II: To explore the statistical relation between features of UMN lesion as detected by clinical examination and by TMS of the brain, and CutSP changes in upper and lower limbs of patients with ALS.

Study III: Development of a simple mathematical algorithm to quantify EMG mirror activity during short isometric maximum voluntary contractions of the abductor digiti minimi (ADM) and the tibialis anterior (TA) muscles. To calculate normative values for these measurements.

Study IV: To analyse the amount of mirror activity in a group of ALS subjects, using our previous developed algorithm, and assess possible correlations with measures of cortical and cognitive function.

Study V: To systematically assess different spinal inhibitory networks in ALS patients, by using several conditioning paradigms of the H Reflex.

5. Materials and Methods

5.1. Participants

ALS patients

For all studies, patients with ALS were recruited from the ALS clinic in Lisbon, Portugal. It was required that criteria for probable or definite ALS, according to the Awaji criteria (de Carvalho et al., 2008), were met. These diagnostic criteria require evidence of gradual disease progression through clinical and/or EMG analysis, and the exclusion of alternative potential diagnoses. Additionally, for study I, patients with a PMA diagnosis, with at least two regions with clinical signs of LMN dysfunction, with absent UMN signs (de Carvalho et al., 2007), and patients with a PLS diagnosis, with a follow-up greater than 4 years without clinical or neurophysiological signs of LMN dysfunction (Gordon et al., 2006, Turner et al., 2020), were also included.

Different requirements for inclusion of ALS patients were established for each study, according to the purposed aim:

Study I: ADM ≥ 4 on the Medical Research Council (MRC) scale in both hands, and normal ulnar nerve conduction studies (motor and sensory nerve responses) without signs of nerve entrapment.

Study II: ADM and TA strength ≥ 4 on the MRC scale on at least one side of the body, normal nerve conduction studies in ulnar and peroneal nerves (motor conduction studies and sensory nerve action potentials) and normal sural nerve sensory nerve action potentials.

Study IV: ADM and TA strength ≥ 4 on the MRC scale, bilaterally, normal nerve conduction studies in ulnar and peroneal nerves (motor conduction studies and sensory nerve action potentials).

Study V: Soleus and TA strength ≥ 4+ on the MRC scale on at least one side of the body.

Individuals who were unable to give informed consent, not tolerating the recumbent position or the electrical stimulation, with other neurological diseases (like as peripheral neuropathy and epilepsy), with metallic brain implants or pacemakers,

or taking drugs that could affect central nervous system excitability were not included in any of the studies.

All patients were stabilized on Riluzole for more than one month prior to the inclusion in any of the studies.

Healthy controls

For studies I, III and V, healthy subjects, matched for gender and age to the ALS patients' group in studies I and V, were recruited.

Subjects with a history of neurological disease or who were taking drugs that could alter central nervous system excitability were excluded.

5.2. Methods

5.2.1. Study I

Participants

Given the variable UMN involvement in MND patients, subjects were divided into three groups: ALS without spasticity (ALS group); PMA; and a group merging patients with PLS and predominant UMN-ALS (spasticity in lower limbs and/or upper limbs).

Cutaneous Silent Period

Studies were conducted in a quiet room, with the subjects sitting in a comfortable position, with a Dantec Keypoint G4, with Keypoint.Net software (Natus Medical Inc., Pleasanton, California). The stronger hand was investigated; if hands had similar strength the right side was selected. Surface recording electrodes were used, with the active electrode over the belly of the ADM muscle and the reference electrode on the dorsum of the hand. The ground electrode was placed at the wrist. Recordings were made in a 1 second window, with a period of 100 ms pre-stimulus signal, digitized at a sampling frequency of 30 kHz and bandpass-filtered between 30 Hz and 10 kHz.

Sensory orthodromic stimulation, with a constant current square wave of 0.2 ms duration, was applied by ring electrodes around the V finger (cathode and anode at the first and second inter-phalangeal joints, respectively). Sensory threshold was defined as the lowest intensity required for the subject to identify 3 out of 6 random stimuli. Stimulation was then performed with an intensity 15x the sensory threshold, with all subjects reporting a significant discomfort with each stimulus. Skin temperature was kept >30ºC.

For each subject, the initial electrical signal from maximum ADM contraction was recorded to estimate the electrical signal amplitude at full contraction and at about 50% maximum force. Thereafter, two experiments were performed. In the first experiment (baseline condition), subjects were asked to maintain a stable contraction of the ADM muscle of around 50% of maximum force. In the second experiment (test condition), patients were asked to maintain a stable contraction of the ADM muscle of

around 50% of maximum force, while doing a maximum contraction of the contralateral ADM. In order to help subjects to maintain a stable contraction of the target muscle, auditory and visual feedback was provided. The CutSP was then obtained by electrical stimulation of the V finger at irregular intervals (10 to 15 consecutive traces were recorded for each condition to ensure reliability). Typically in contractions between 20-80% of maximal strength CutSP measurements are stable (Floeter, 2003).

Signals were rectified, averaged, and analyzed offline, using custom MatLab functions (MatLab R2018a, The Mathworks, Inc., Natick, Massachusetts). The CutSP onset latencies was defined at the drop of the EMG trace below 80% of the baseline preceding the stimulus and duration of CutSP was calculated from the onset latency to the return of the EMG signal above 80% of baseline (Floeter, 2003, Kofler et al., 2019a). The degree of contraction during the CutSP measurement, $\left(\frac{Average\ EMG\ amplitude\ pre-stimulus\ signal\ during\ CSP}{Average\ EMG\ amplitude\ in\ full\ contraction} \times 100\right)$, and the magnitude of EMG suppression $\left(\frac{Average\ EMG\ amplitude\ during\ CSP}{Average\ EMG\ amplitude\ pre-stimulus\ signal} \times 100\right)$ during the CutSP were also evaluated (Figure 19) (Uncini et al., 1991). CutSP was considered absent if EMG suppression was <15 ms (Floeter, 2003, Kofler et al., 2019a).

Figure 19 – Cutaneous silent period illustrative example with the measurements included

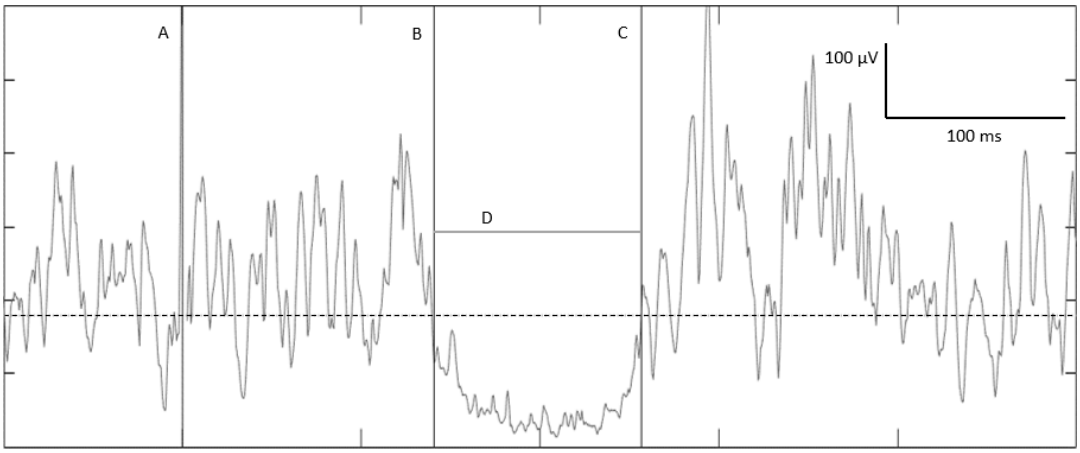

A – Electrical stimulus; B – Cutaneous silent period (CutSP) onset; C – CutSP end; D – CutSP duration; Horizontal dashed line – 80% of pre-stimulus average EMG signal. Note: Adapted from Castro et al. (2021), with permission.

Statistical Analysis

Means and standard deviations were calculated for each variable. Gender differences were analyzed with χ2 test. Normality of distribution was checked with the

Shapiro-Wilk test. Comparison of CutSP parameters between groups was performed with a one-way ANOVA, with the Tukey test for post-hoc analysis. In each group comparison between baseline and tested condition was assessed by paired-t test; $p < 0.05$ was considered statistically significant. The comparisons were corrected using the Bonferroni method. All analyses were performed in SPSS for Windows Version 21.0 (IBM. Armonk, NY).

5.2.2. Study II

Clinical Assessment

Full clinical and EMG assessment (MdeC) was completed before neurophysiological investigation, which was always arranged within one month following the first clinical evaluation. An UMN score, as described by Geraldo et al. (2018), was calculated. In each limb this score rated, tendon reflexes as 0 (absent or very weak) to 3 (very brisk), spasticity as 0 (no spasticity) to 3 (corresponding to a 3 or 4 on modified Ashworth scale), plus Hoffmann sign for upper limbs (0 or 1 if present), and plantar response as 0 or 1 (if present) - (maximum score 7 per limb). The bulbar region was scored from 0 to 3 (tongue spasticity, absent 0, present 1; jaw jerk, absent 0, brisk 1, clonus 2). The total UMN score for each patient therefore ranged from 0 to 31. A limb with very brisk reflexes (score > 3), or spasticity, or abnormal reflex Hoffman, or extensor plantar response was considered as having UMN signs (Brooks, 1994). Functional disability was assessed on the same day using the ALSFRS-R (maximum healthy score 48) (Cedarbaum et al., 1999).

Cutaneous Silent Period

We have described our protocol for study of the CutSP in detail in a previous report (Castro et al., 2021). Surface electrodes (reference 9013L0203, Natus Inc) were used for recording EMG activity and nerve action potentials. Eligible muscles (ADM and TA strength ≥ 4 on the MRC scale) from limbs on both sides were investigated. For the upper limb, recordings were made with the active electrode over the belly of the ADM muscle, and the reference electrode on the dorsum of the hand (in order to avoid artefact stimulation originating from the proximal ring electrode). Ground electrode (reference 9013L0862, Natus Inc) was placed on the wrist. For the lower limbs, recordings were made with the active electrode over the belly of the TA muscle (7-8 cm below the lower extremity of the ipsilateral patella) and the reference electrode 5-7 cm distally to the active electrode, over the tibial bone. The ground electrode (reference 019-400500, Natus Inc) was placed over the patella. Adhesive tape was used to secure the electrodes. Standard amplifier filter settings of 30-Hz and 10-kHz were used, and signals were digitized at a sampling frequency of 3 kHz.

Sensory orthodromic stimulation, using a constant current square wave of 0.2 ms duration, was applied by ring electrodes (reference 9013S0302, Natus Inc) on the Vth finger for the upper limbs; and using a conventional superficial bipolar bar stimulating electrode (reference 9013L0362, Natus Inc) over the sural nerve (cathode posterior to the lateral malleolus and anode 2 cm distally) for the lower limbs. Sensory threshold was tested by applying progressively greater stimuli intensities from 0 mA to the moment subject could identify 3 of 6 randomly timed stimuli, increasing stimulus intensity by steps of 0.1 mA. Subjects were blind to the stimulus intensity used. When necessary, threshold determination was repeated. For studies of the CutSP the stimulus intensity was then set to 15x the sensory thresholds in upper and lower limbs. Skin temperature was maintained >30ºC in each tested limb.

Since CutSP parameters are not influenced by muscle activation in the range of 10–60% of maximum voluntary contraction (Kofler et al., 2007, Rodi and Springer, 2011), patients were asked to maintain a stable contraction of the target muscle of around 50% of maximum force, monitored by audio feedback of their EMG activity. Electrical stimulation was delivered at irregular intervals, in order to avoid fatigue (Kofler et al., 2019a). Recordings for analysis were made in a 1 second window, with a period of 100 ms pre-stimulus signal. Ten consistent responses, recorded from each muscle (Castro et al., 2021), were rectified, averaged, and analyzed offline, using custom MatLab functions (MatLab R2018a, The Mathworks, Inc.,Natick, Massachusetts). CutSP onset latency was defined as the onset of a fall in the amplitude of the EMG trace to less than 80% of the baseline signal preceding the peripheral stimulus (Castro et al., 2021). The duration of the CutSP was calculated from its onset latency to the return of the EMG signal to 80% of baseline (Castro et al., 2021). EMG signal from studied muscles was quantified for testing differences between groups.

Transcranial Magnetic Stimulation

A Magpro x100 (MagVenture, Inc, Alpharetta, Georgia) was used for TMS. Stimulation was performed over the contralateral hand and lower limb muscle cortical areas, defined in preliminary recordings by the lowest resting motor threshold (RMT), using a round coil (inner diameter 35 mm; outer diameter 121 mm). MEPs were obtained using the recording settings described above. RMT was calculated for each

muscle, defined as the minimum stimulus intensity needed to elicit at least 50% of responses with a minimum amplitude of 0.1 mV (Rothwell et al., 1999). Stimulation was then performed at 20% above the RMT. Ten consecutive traces were recorded in each muscle, separated by more than 30 seconds interval, with the target muscle at rest, defined by audio monitoring. Recordings with artefacts or noise from adjacent muscle contraction were discarded. The MEP with highest peak-to-peak amplitude was selected to define motor latency and motor evoked amplitude. Central motor conduction time (CMCT) was calculated using the F-wave method (Robinson et al., 1988), by stimulating the ulnar nerve at wrist and the peroneal nerve at fibula (20 supramaximal stimuli,1 Hz). Taking into account normative data from our laboratory (de Carvalho et al., 2003), TMS was considered abnormal when there was no clear reproducible MEP, when MEP amplitude was below 5% of the compound muscle action potential (CMAP) peak-to-peak amplitude, or the CMCT time was greater than 8 ms for the ADM and 16 ms for the TA.

Statistical analysis

Neurophysiological data are shown with median values, and first and third interquartile ranges (1st and 3rd IQR). Gender differences were analyzed with $\chi 2$ test. The Shapiro-Wilk test was applied to test for the data distribution and, since most neurophysiological results did not follow a normal distribution, we applied non-parametric tests. Correlations between variables were tested using the Spearman correlation coefficient. Comparisons between two groups were performed using the Mann-Whitney U test. The Kruskal-Wallis H test was used for multiple group comparisons. Post-hoc pairwise comparisons were performed using Dunn's procedure, with a Bonferroni correction for multiple comparisons. A p value < 0.05 was considered statistically significant.

Two binomial logistic regression analyses were performed, one for the upper limb and one for the lower limb studies, to ascertain the effects of CutSP and TMS on the likelihood of patients having UMN signs (dependent variable). CutSP parameters of ADM and TA muscles included in the models were: onset latency, duration and amount of EMG suppression. TMS was included as a dichotomous variable (normal vs abnormal, see Methods). Linearity of the continuous variables with respect to the logit of the dependent variable was assessed via the Box-Tidwell procedure (Box and

Tidwell, 1962). A Bonferroni correction was applied using all eight terms in both models, resulting in statistical significance being accepted when $p < 0.00625$. All analyses were performed in IBM SPSS for Microsoft Windows, Version 26.0 (Armonk, NY: IBM Corp).

5.2.3. Study III

Subjects

We recruited a group of healthy subjects without history of neurological disease or who were taking drugs that could alter central nervous system excitability.

All subjects were right-handed, according to the Edinburgh Handedness Inventory (Oldfield, 1971).

Motor task and EMG recordings

Subjects were lying supine, in a quiet room, with arms stretched along the body, and hands resting comfortably on the bed, while trying to relax as much as possible. They were instructed to perform brief, 2 to 3 seconds, isometric full force contractions of only one hand (finger abduction) or one foot (foot dorsiflexion). This was considered the active muscle. No instruction was given regarding the contralateral limb, which was considered the mirror muscle. Three trials were performed considering one side as active, followed by three consecutive recordings with the other side as active. Order (right-left and hand-foot) was randomly chosen between subjects. An interval of 5 to 10 seconds was allowed for resting between each trial.

Surface electrodes (reference 9013L0203, Natus Inc) were used for recording EMG activity. For the upper limb, recordings were made with the active electrode over the belly of the ADM muscle, while the reference electrode was placed on the volar side of the proximal inter-phalangeal joint of the 5th finger. The ground electrode was placed on the wrist. For the lower limb, recordings were performed with the active electrode over the belly of the TA muscle and the reference electrode 5-7 cm distally, over the tibial bone. The ground electrode was placed on the ankle. Standard amplifier filter settings of 30-Hz and 10-kHz were used. Signals were digitized at sampling frequencies of 3 kHz and 24 kHz in order to assess the algorithm performance in commonly used ranges of sampling frequencies in clinical neurophysiology. Recordings were made on a 10 second window and stored for offline analysis.

Additionally, two experienced neurophysiologists (JC and IdeC), independently marked the beginning of muscle activation, for comparison with the proposed algorithm.

Mathematical Algorithm for signal analysis

The signals obtained were stored and exported as txt files, which were then analyzed offline using a custom built MatLab algorithm (MatLab R2018a, The Mathworks, Inc., Natick, Massachusetts).

The calculations of the starting and finishing points of muscle activation were based on a mathematical formula previously described in the literature (Garvey et al., 2001). In a small percentage of signals analyzed (6%), it was necessary to apply a 50Hz band pass filter to the signal due to the presence of electrical artifacts. Latency determinations were defined by the algorithm and both operators who were blind to the algorithm results and to the other operator determination.

The MatLab *trapz* function was used to estimate the amount of EMG signal in both sides, by calculating the area under the curve of the absolute value of the raw EMG signal during the estimated active muscle contraction. To control for differences in force across subjects, the amount of EMG signal in the mirror muscle during the motor task was defined as a percentage of the EMG signal of the active muscle according to the formula: $Mirror\ EMG\ = \frac{EMG\ signal\ of\ the\ mirror\ muslce}{EMG\ signal\ of\ the\ target\ muscle}\ x\ 100.$

An example of the custom function output can be seen in Figure 20.

Figure 20 – Example of our custom algorithm output

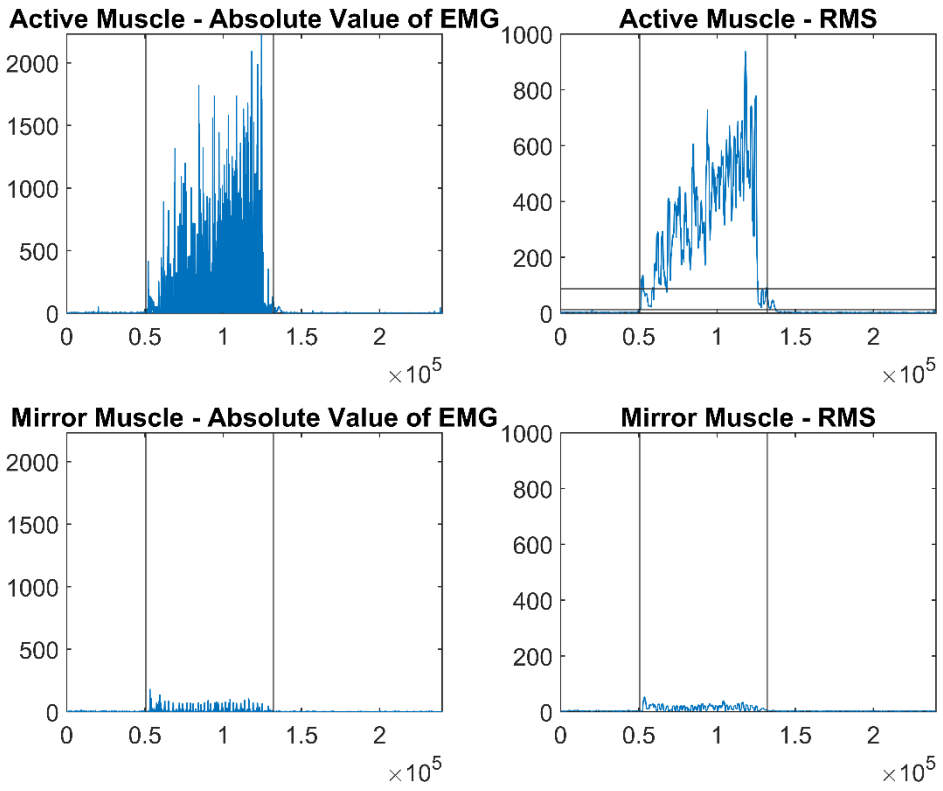

EMG – Electromyography signal; RMS – root mean square. Note: Adapted from Castro et al. (2023a), with permission.

The detailed code used for the construction of the algorithm, along with comments, can be found in the supplementary material.

Statistical analysis

Descriptive data is shown with mean values and standard deviations, or median with interquartile range (IQR), as appropriate. Inter-rater reliability was assessed with a two-way mixed model Intraclass Correlation Coefficient (ICC (2,k); Absolute Agreement) (McGraw and Wong, 1996). ICC reliability was considered poor for values lower than 0.5, moderate for values between 0.5-0.75, good for values 0.75-0.9 and excellent for values higher than 0.9 (Portney, 2020). We used the 95% Limits of Agreement, as proposed by Bland and Altman (1986), to evaluate the mean differences in the latency of the beginning of muscle activation as marked by the proposed algorithm and by the two neurophysiologists.

Regarding the amount of mirror EMG signal, the Shapiro-Wilk test was applied to test for the normality of data distribution. Given that the data was not normally distributed, non-parametric tests were used. Differences in gender and sides were

assessed with a Mann-Whitney U test. Correlation of mirror activity with age was evaluated with a Spearman rank-order correlation. A p value < 0.05 was considered statistically significant.

For calculations of normative data, we performed a logarithmic transformation log(x+1) of the mirror muscle signal amplitudes (McDonald, 2014). The resulting data followed a normal distribution. After the analysis, the data was back-transformed, in order to obtain meaningful values.

All analyses were performed in IBM SPSS for Microsoft Windows, Version 26.0 (Armonk, NY: IBM Corp).

5.2.4. Study IV

Clinical Assessment

Clinical and EMG assessments (MdeC) were carried out prior to the neurophysiological investigation, which was always scheduled within one month of the initial clinical evaluation. A clinical UMN score, as described by Geraldo et al. (2018), was derived: the total UMN score for each patient ranged from 0 to 31. Functional disability was assessed on the same day using the ALSFRS-R scale (maximum healthy score 48) (Cedarbaum et al., 1999).

Cognitive assessment

As part of our clinical routine, we evaluate cognition in ALS patients. We use the validated Portuguese version of the Edinburgh Cognitive and Behavioral ALS Screen (ECAS) (Tomsic, 2015), which is a multi-domain neuropsychological battery specifically developed for assessing cognitive status in ALS patients (Abrahams et al., 2014). This battery assesses domains that are described as impaired in ALS (executive functions, social cognition, verbal fluency, and language), but also other domains (memory and visuospatial performance).

Mirror movements

Patients were positioned supine in a silent room, with their arms extended along their body and hands resting comfortably on the bed. They were instructed to perform brief isometric full force contractions in only one hand (fifth finger abduction, ADM) or one foot (foot dorsiflexion, TA), which was considered the active muscle. The subjects were instructed to maintain the contralateral part of the body fully relaxed. This was monitored by the device loudspeaker. Each subject performed three trials (10 seconds maximal contraction and 15 seconds resting) in each muscle of one side, followed by the same protocol on the opposite side. The order of muscle (ADM or TA) and side (right or left) contraction was randomly assigned between subjects.

Surface electrodes (reference 9013L0203, Natus Inc) were used for recording EMG activity. For the upper limb, recordings were made with the active electrode over the belly of the ADM, while the reference electrode was placed on the palmar side of the proximal inter-phalangeal joint of the 5th finger. The ground electrode was placed on the wrist. For the lower limb, recordings were performed with the active electrode

over the belly of the TA muscle and the reference electrode 5-7 cm distally, over the tibial bone. The ground electrode was placed on the ankle. Standard amplifier filter settings of 30-Hz and 10-kHz were used. Signals were digitized at a sampling frequency of 3 kHz. Recordings were made on a 10 second window and stored for offline analysis.

Mirror activity was quantified using a custom built MatLab algorithm (MatLab R2018a, The Mathworks, Inc., Natick, Massachusetts) developed by our group, and published elsewhere (Castro et al., 2023a). Briefly, our algorithm detects the starting and finishing points of the active muscle contraction and estimates the amount of EMG signal between those two points by calculating the area under the curve for both the active and the mirror muscles. The amount of mirror activity is then expressed as a percentage of the EMG signal of the active muscle.

Transcranial Magnetic Stimulation

A Magpro x100 (MagVenture, Inc, Alpharetta, Georgia USA) was used for TMS. Stimulation was performed over the contralateral hand and lower limb muscle cortical areas, defined in preliminary recordings by the lowest resting motor threshold (RMT), using a round coil (inner diameter 35 mm; outer diameter 121 mm). MEPs were obtained using the recording settings described above. RMT was calculated for each muscle, defined as the minimum stimulus intensity needed to elicit at least 50% of responses with a minimum amplitude of 0.1 mV (Rothwell et al., 1999). Stimulation was set at 120% of RMT. Ten consecutive traces were recorded in each muscle, separated by more than 30 seconds interval, with the target muscle at rest, as controlled by audio monitoring. Recordings with artefacts or noise from adjacent muscle contraction were discarded. The MEP with highest peak-to-peak amplitude was selected to define motor latency and motor evoked amplitude. Amplitude was recorded as a ratio between MEP and CMAP peak-to-peak amplitudes. CMCT was calculated using the F-wave method (Robinson et al., 1988), by stimulating the ulnar nerve at wrist and the peroneal nerve at fibula (20 supramaximal stimuli,1 Hz). Taking into account normative data from our laboratory (de Carvalho et al., 2003), TMS was considered abnormal for the studied limb if one of the following were met: no reproducible MEP; MEP amplitude below 5% of CMAP amplitude; CMCT longer than 8 ms for the ADM or 16 ms for the TA.

Ipsilateral Silent Period

We assessed the Ipsilateral Silent Period (iSPs) in both ADM muscles, using the same TMS setting. Stimulation was applied, during maximum voluntary contraction of the ipsilateral ADM, and recording 6 to 8 responses, allowing for a 20 second rest between trials. Traces were recorded for offline analysis, and then rectified and averaged. The latencies of the iSP were derived using the mathematical method proposed by Garvey et al. (2001). The onset latency was calculated from the cortical stimulus to a consistent fall in the amplitude of the EMG trace to less than the mean amplitude of the 100 ms of EMG preceding the stimulus – [MCD*2.66]. The duration of the iSP was calculated from its onset latency to the return of the EMG signal to this mean pre-stimulus EMG amplitude – [MCD*2.66]. iSPs were classified as abnormal when either onset latency or duration were outside the normal limits for our laboratory (latency higher than 48.8 ms; duration lower than 12.4 ms or longer than 61.8 ms).

Statistical analysis

Descriptive data is shown with mean values and standard deviations, or median and first and third interquartile (1st and 3rd IQR), as appropriate. Data distribution was assessed with the Shapiro-Wilk test and, since most neurophysiological results did not follow a normal distribution, we subsequently used non-parametric tests. We considered *p* values lower than 0.05 as significant. Correlations between variables were tested using the Spearman correlation coefficient. Comparisons between 2 groups were performed using the Mann-Whitney U test. The Kruskal-Wallis H test was used for comparisons of more than 2 groups. Post-hoc pairwise comparisons were performed using Dunn's procedure. False discovery rates for multiple comparisons were controlled by the Benjamini-Hochberg procedure (Benjamini and Hochberg, 2018), using a false discovery rate of 5%.

5.2.5. Study V

Clinical Assessment

Clinical and EMG assessments (MdeC) were carried out prior to the investigation protocol, within a time interval shorter than one month. A clinical upper motor neuron (UMN) score, as described by Geraldo et al. (2018), was derived. The total UMN subscore for the lower limbs (UMN LL) is 14 (Reflexes 0-3; Spasticy 0-3; Babinsky 0-1). Functional disability was assessed on the same day using the ALSFRS-R (maximum healthy score 48) (Cedarbaum et al., 1999).

Neurophysiological measurements

All neurophysiological studies were conducted in a quiet room, using a Dantec Keypoint G4, with Keypoint.Net software (Natus Medical Inc., Pleasanton, California). The EMG signal was recorded at a sampling frequency of 6 kHz and bandpass-filtered between 20 Hz and 10 kHz.

Studies were performed with the subject in a reclined comfortable supine position, with the hip flexed to 150º, the knee flexed to 160º and the ankle at 110º of plantar flexion (Burke et al., 1999). Subjects were instructed to keep their leg relaxed throughout the procedures with visual and auditory feedback used to identify any background EMG activity.

For the control H reflex and all conditioning paradigms, 10 consecutive recordings were performed, with an irregular rate of stimulation, with no less than 10 seconds between each pair of stimuli. The average unconditioned and conditioned H amplitude was then calculated.

H Reflex

The H reflex was obtained from the right soleus muscle, after percutaneous stimulation of the posterior tibial nerve (PTN) in the popliteal fossa, with a square wave stimulus of 1 ms duration, positioning the anode electrode over the knee (Pierrot-Deseilligny and Burke, 2012). Recordings were made with superficial Ag/AgCl adhesive electrodes (reference 9013L0203, Natus Inc), with the active electrode over the belly of the soleus muscle, and the reference electrode over the Achilles tendon. The ground electrode was placed over the anterior aspect of the knee. Stimulus intensity was adjusted in order to obtain maximum H amplitude (H_{max}).

Recurrent inhibition

The alpha-motoneurons possess collateral axons that synapse on a group of inhibitory interneurons in the ventral horn of the spinal cord (Figure 21A). These interneurons are called Renshaw cells (Renshaw, 1946), which project back into both homonymous motor neurons and synergist motor neurons in neighbouring segments, providing a negative feedback (Pierrot-Deseilligny and Burke, 2012). Recurrent inhibition can be either homonymous or heteronymous (Knikou, 2008, Pierrot-Deseilligny and Burke, 2012).

We studied the homonymous recurrent inhibition, using the paired H reflex technique (Pierrot-Deseilligny and Bussel, 1975). Paired percutaneous electrical stimuli were performed over the PTN, in the popliteal fossa. The first stimulus (S1) was given at a fixed intensity that elicited a maximum control H reflex. A second stimulus (S2) was applied, with an interstimulus interval (ISI) of 10 ms, with a supramaximal intensity for the soleus M-wave. The recording setting was the same as of the standard H reflex. The average of the conditioned H (H') amplitude was calculated. The amount of recurrent inhibition (H'_{RI}) was calculated by the ratio H'/H_{max} as proposed previously (Bussel and Pierrot-Deseilligny, 1977).

Presynaptic inhibition of Ia terminals

In man, Ia terminals mediating the afferent volley of the H reflex are subject to presynaptic inhibition, controlled by supraspinal pathways (see Pierrot-Deseilligny and Burke (2012) for a detailed description). These mechanisms are modulated by GABAergic spinal interneurons (Rudomin and Schmidt, 1999), and are essential to motor control programs (Figure 21B).

To assess presynaptic inhibition, we used the D1 inhibition (Mizuno et al., 1971), that has been extensively used to study this mechanism in other diseases. A conditioning stimulus (S1), consisting of a train of 3 electrical stimuli to the common peroneal nerve (CPN), using surface electrodes over the fibular head (square wave of 1 ms duration, ISI 3 ms, 1.3x the motor threshold for the Tibialis anterior). A second stimulus (S2) was applied over the PTN, 21 ms after the initial stimulus of the conditioning train, with the same intensity used for H_{max}. The recording setting was the same as of the standard H reflex. The average conditioned H (H') amplitude was

calculated. The amount of inhibition (H'_{Pre}) was given by the absolute decrease in amplitude as a percentage of M_{max}, calculated by the formula $H'_{Pre} = \frac{H_{Max} - H'}{M_{Max}} \times 100$.

Figure 21 – Wiring diagrams of the different techniques used for testing H reflex conditioning paradigms, and illustrative examples of recordings

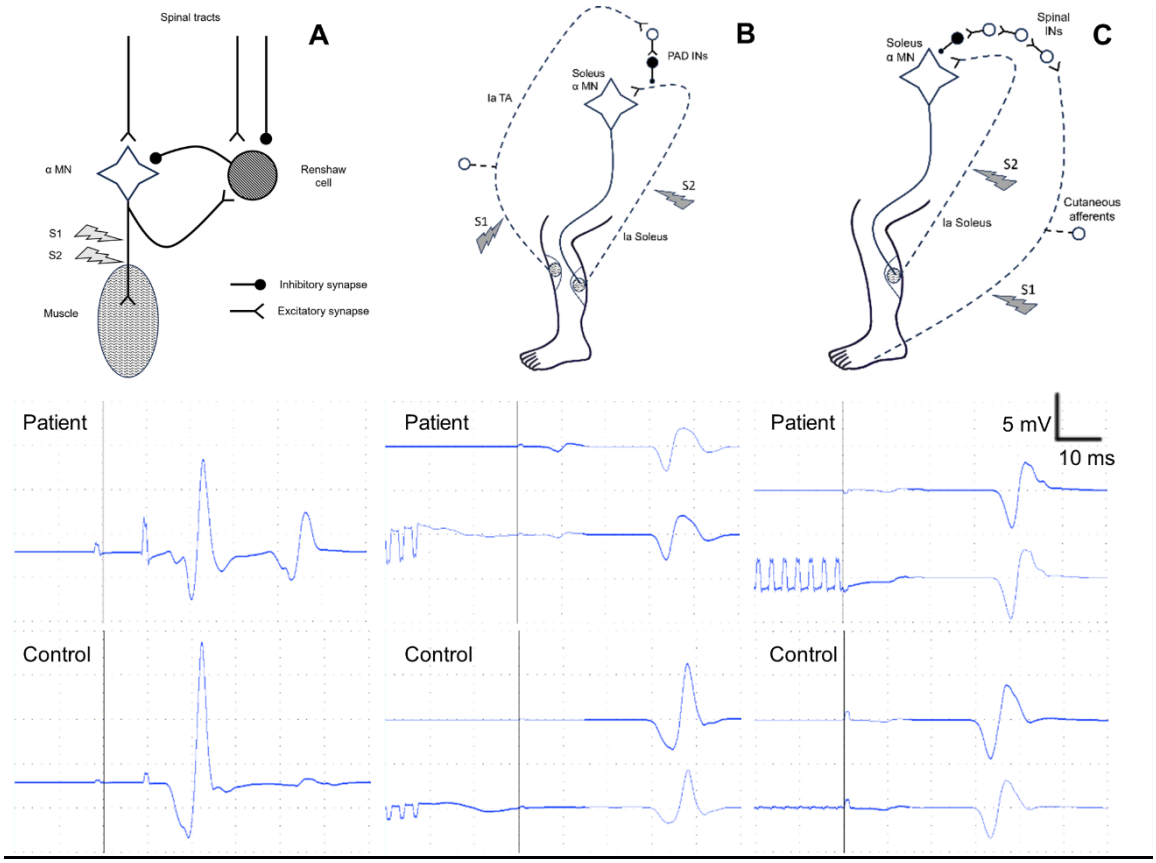

A – Recurrent inhibition: The first stimulus (S1) was given at an intensity that elicited a maximum control H reflex. A second stimulus (S2) was applied, with an interstimulus interval (ISI) of 10 ms, with a supramaximal intensity for the soleus M-wave. S2 does not evoke an H reflex by itself because of the collision of antidromic motor impulses with the orthodromic volley. However, when S2 is preceded by a submaximal conditioning stimulus, an orthodromic reflex volley in response to S1 is produced in motor axons that collides with the antidromic motor volley produced by S2. The collision allows for the potential generation of a reflex response to S2 in the alpha motoneurons that fired as part of the H reflex generated by S1; B – Presynaptic inhibition of Ia afferents: The conditioning stimulus induces the afferent volley in the tibialis anterior (TA) Ia afferent fibres and activates primary afferent depolarization (PAD) interneurons (INs) responsible for the presynaptic inhibition of Ia soleus fibres before the synapse with the soleus motoneuron; C – Inhibition after cutaneous stimulation: Conditioning stimulus induces the afferent volley in the cutaneous/nociceptive fibres in the sural nerve from the skin of the lateral side of the fifth toe activating spinal INs projecting on soleus motoneuron.

Inhibition after cutaneous stimulation

Both physiological and anatomical evidence support the presence of last-order GABAergic interneurons that play a crucial role in modulating the synaptic efficacy of large cutaneous afferents within the dorsal horn of the spinal cord (Eccles et al., 1963,

Rudomin and Schmidt, 1999) (Figure 21C). In man, an electrical stimulus applied to the lateral sural nerve has been shown to reduce the soleus H reflex amplitude (Bathien and Hugon, 1964, Crone et al., 1990, Klomjai et al., 2014). Although stimulation of the sural nerve can also cause facilitation of the H reflex, it has been demonstrated that using repetitive sural nerve stimulation increases the amount of H reflex inhibition at specific timepoints (Delwaide et al., 1981).

Considering the added effect on the H reflex amplitude when using repetitive stimulation, we used the protocol proposed by Klomjai et al. (2014). A conditioning stimulus (S1), consisting of a train of 17 stimuli, was applied over the lateral dorsal aspect of the right foot using surface electrodes (square wave of 1 ms duration, ISI 3 ms, 3x the perception threshold). A second stimulus (S2) was applied over the PTN, 50 ms after the initial stimulus of the conditioning train, with the same intensity used for H_{max}. The recording parameters were the same of the standard H reflex. The average conditioned H (H') amplitude was calculated. The amount of inhibition (H'_{Pos}) was given by the absolute decrease in amplitude as a percentage of M_{max}, calculated by the formula $H'_{Pos} = \frac{H_{Max} - H'}{M_{Max}} \times 100$. Given that a noxious cutaneous stimulus often is accompanied by a withdrawal movement of the stimulated limb, and this could in turn alter the motoneuron pool excitability and influence the H reflex (Burke, 2016), care was taken to ensure that the conditioning stimulus did not produce any movement of the limb, both by visual inspection and by monitoring EMG signal from tibialis anterior and soleus muscles.

Statistical analysis

Descriptive data is shown with median and first and third interquartile (1st and 3rd IQR). Gender differences were analyzed with χ2 test. Data distribution was assessed with the Shapiro-Wilk test. Given the non-normality distribution of our variables, we used non-parametric tests. Comparisons between 2 groups were performed with a Mann-Whitney U test, using an exact sample distribution (Dinneen and Blakesley, 1973). Correlations between variables were tested using the Spearman correlation coefficient. Multiple linear regression models were created to assess the degree to which differences in the different conditioning paradigms were predicted by variation in clinical UMN dysfunction (UMN Score), age and gender. We considered *p*

values lower than 0.05 as significant. All analyses were performed in IBM SPSS for Microsoft Windows, Version 26.0 (Armonk, NY: IBM Corp).

5.3. Ethical statement

All studies included in this dissertation followed the ethical principles as declared in the Declaration of Helsiniki (2013), and were approved by Ethics commission of the Lisbon Academic Medical Center (Ref. 405/2019 and 385/20). All subjects recruited agreed to participate in the studies performed and have signed a written informed consent.

6. Results

6.1. Study I

Forty-six MND patients (14 women) and 28 healthy controls (16 women) were included in the study. Demographic variables are shown in Table 3. Age was similar among the groups (p = 0.99). Regarding gender, there was a marginal difference (p = 0.049), since PMA included more men than the other groups, as expected.

Table 3 – Characteristics of the subjects studied

	N	Age (Mean ± SD (range)	Gender	
			Female	Male
Controls	28	61.7 ±10.1 (45-76)	16 (57%)	12 (43%)
ALS	16	61.2 ±13.6 (38-79)	6 (38%)	10 (62%)
PMA	15	61.0 ±13.9 (33-79)	2 (13%)	13 (87%)
PLS + UMN-ALS	15	62.1 ±8.5 (45-76)	6 (40%)	9 (60%)

ALS- amyotrophic lateral sclerosis; PMA – progressive muscular atrophy; PLS – primary lateral sclerosis; UMN-ALS – predominant upper motor signs ALS (spastic lower limbs and/or upper limbs). Note: Adapted from Castro et al. (2021), with permission.

However, gender do not affect CutSP (Floeter, 2003) and we did not find any differences between men and women in the healthy control group (p > 0.05).

CutSP was absent in one PMA patient with both experimental protocols, in another PMA patient in the baseline condition, in one ALS patient in the baseline condition, and in one healthy control in the baseline condition. The amount of EMG signal during maximum contraction, as well as the degree of contraction during the CutSP measurement was similar in the different groups for the different experimental conditions (Table 4; p > 0.05).

Results of the CutSP measurements are summarized in Table 5. In the baseline condition, all MND groups showed delayed onset latencies, when compared to healthy controls (p = 0.001). There was no significant difference in the CutSP duration among groups. The one-way ANOVA showed a significant difference between groups regarding EMG suppression in the baseline condition (p = 0.005). Despite a trend for less EMG suppression during the CutSP in all MND groups, the Tukey HSD post-hoc

analysis revealed that only in the PLS + UMN-ALS group was statistical significance achieved when compared to healthy controls (65.8 vs 74.6%; p = 0.004) (Figure 22).

Table 4 – Values of EMG signal during full contraction and degree of contraction in both experimental protocols; values are represented by mean ± SD

	Healthy Controls	ALS	PMA	PLS+UMN-ALS
EMG signal during full contraction (mV)	381.3 ± 215.0	285.5 ± 128.7	351.6 ± 164.5	234.7 ± 71.8
Degree of contraction in Baseline condition (%)	35.6 ± 12.7	49.3 ± 11.7	42.7 ± 17.9	40.2 ± 15.3
Degree of contraction in Test condition (%)	37.3 ± 12.4	50.5 ± 19.6	49.2 ± 18.8	44.0 ± 17.0

ALS- amyotrophic lateral sclerosis; PMA – progressive muscular atrophy; PLS – primary lateral sclerosis; UMN-ALS – predominant upper motor signs ALS (spastic lower limbs and/or upper limbs). Note: Adapted from Castro et al. (2021), with permission.

During simultaneous contralateral ADM contraction, no change was observed in the control group. However, onset latency shortened in the PMA group (p = 0.001, Table 5). In the test condition, with co-contraction of the contralateral ADM, the one-way ANOVA showed significant differences between groups regarding the onset latency of the CutSP (p = 0.004).

Table 5 – Results of cutaneous silent period measurements in each group; values are represented by mean ± SD

	Baseline condition				Test condition			
	Healthy Controls	ALS	PMA	PLS+UMN-ALS	Healthy Controls	ALS	PMA	PLS+UMN-ALS
CutSP onset Latency (ms)	72.5 ±6.1*	83.9 ±12.3	83.6 ±13.7	84.7 ±12.2	73.7 ±11.5**	83.3 ±15.7	76.1 ±11.3	87.9 ±13.4
CutSP duration (ms)	65.1 ±19.1	64.4 ±21.0	63.6 ±19.5	69.1 ±23.9	62.9 ±15.8	60.8 ±23.7	72.3 ±17.2	61.5 ±25.9
EMG Suppression (%)	74.6 ±5.8***	69.0 ±8.1	70.1 ±9.4	65.8 ±8.3	74.6 ±6.0***	68.0 ±7.3	69.3 ±8.0	65.3 ±9.2

* Onset-latency was significantly shorter in healthy controls as compared with any other group in the baseline condition (p = 0.001). ** Onset-latency was significantly shorter in healthy controls than in the PLS+UMN-ALS group in the test condition (p=0.004). *** EMG suppression was significantly lower in the PLS+UMN-ALS group (p=0.04 and p=0.001, in the baseline and test condition, respectively) and in the ALS group in the test condition (p=0.04) than in the control group. CutSP – cutaneous silent period; ALS- amyotrophic lateral sclerosis; PMA – progressive muscular atrophy; PLS – primary lateral sclerosis; UMN-ALS – predominant upper motor signs ALS (spastic lower limbs and/or upper limbs). Note: Adapted from Castro et al. (2021), with permission.

Figure 22 – Cutaneous silent period variables in each group

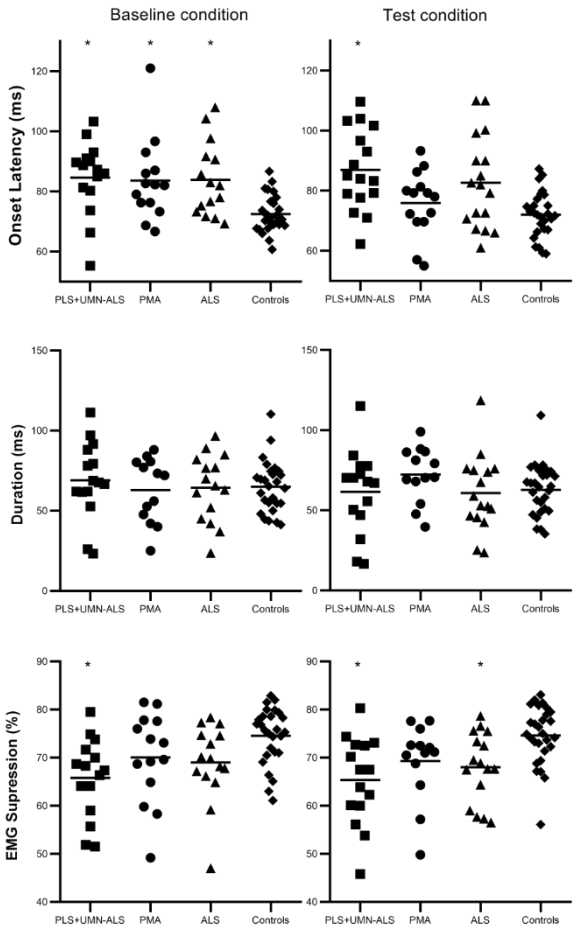

Each point corresponds to one subject; Asterisks denote significant changes when compared to healthy controls ($p < 0.05$). Note: Adapted from Castro et al. (2021), with permission.

However, the post-hoc tests revealed that only the PLS + UMN-ALS group had prolonged onset latency of the CutSP (Figure 23) when compared to healthy controls ($p = 0.004$). In this experiment, the amount of EMG suppression tended to further decrease in all MND groups, while staying the same in the healthy subjects group, when compared to the values observed at baseline. Consequently, the difference in the amount of EMG suppression achieved statistical significance not only for PLS + UMN-ALS group ($p < 0.001$) but also for the ALS group ($p = 0.04$) (Figure 22).

Figure 23 – Cutaneous silent period examples for each group and experimental condition

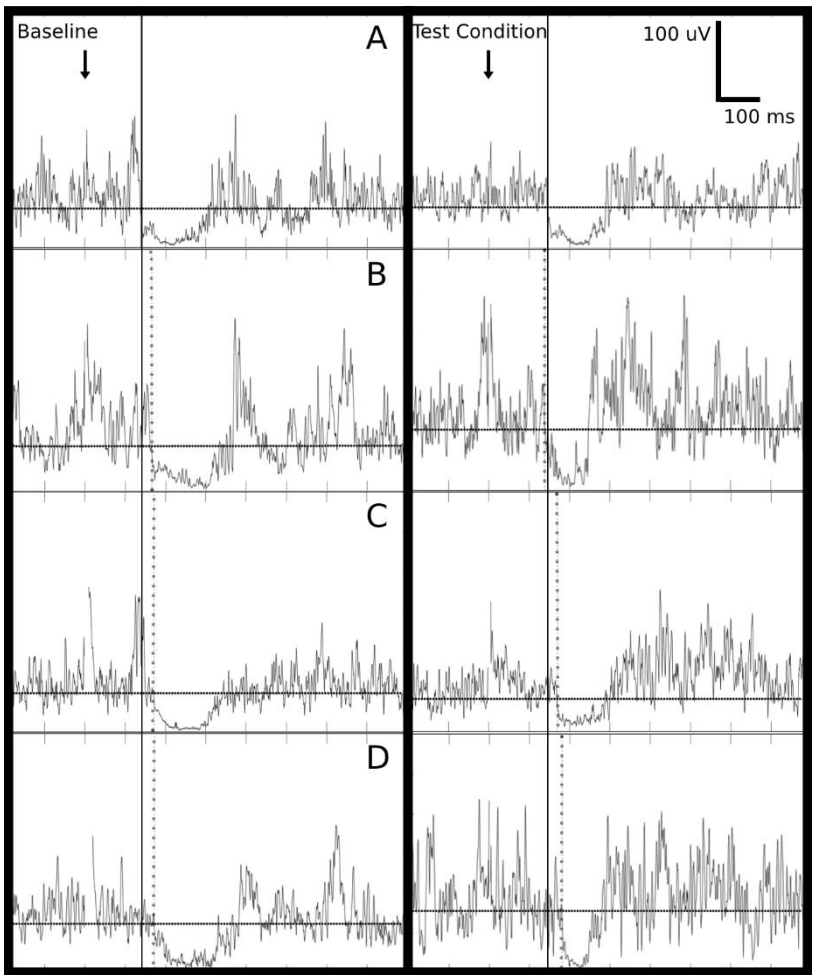

A – Control subject; B – PMA subject; C – ALS subject; D – PLS+UMN-ALS subject; Vertical solid line – Onset latency for the control subject Cutaneous silent period (CutSP); Vertical dotted lines – Onset latency for each CutSP example; Horizontal dashed lines – 80% of pre-stimulus average EMG signal. In the test condition, onset latencies for the PMA and ALS groups shortened, with no significant difference from controls. Note: Adapted from Castro et al. (2021), with permission.

6.2. Study II

Twenty-four ALS patients, 7 women (29%; median age 59.5 years, IQR 52.5-69.0) were studied. They were consecutively observed patients respecting inclusion and exclusion criteria and consenting.

CutSP measurements

Measurements of the CutSP were obtained in a total of 74 muscles, 45 ADM and 29 TA, after excluding results from weak muscles (MRC <4, see methods) or those with an absent CutSP (7 TA muscles). CutSP onset latency was longer in TA (median 103.3 ms, IQR 89.0-108.3) than in ADM (median 77.0 ms, IQR 72.7-80.3) ($p < 0.001$). But CutSP duration (TA, median 58.3 ms, IQR 45.0-72.0; ADM, median 64 ms, IQR 52.3-75.7) and EMG suppression (TA, median 77.1%, IQR 70.7-81.4; ADM, median 75.1%, IQR 72.1-78.2) were similar ($p = 0.71$ and 0.65, respectively).

The CutSP measurements were also obtained in healthy subjects. For the ADM muscles, we used the values of 27 muscles from 28 healthy subjects (16 women; median age 63.5, IQR 52.5-69.0), reported from our previous study (Castro et al., 2021). For the TA muscles, values were obtained in 26 TA muscles from 13 healthy subjects (7 women; median age 57.0 years, IQR 39.0-62.0). CutSP was absent in one ADM from a healthy control subject.

Comparison of ALS and healthy subjects groups, disclosed a marginal difference in gender in the ADM groups ($p = 0.043$), since the control group had a higher number of females. Nevertheless, there was no difference between men and women in our healthy control group ($p > 0.05$), and gender does not seem to influence CutSP (Floeter, 2003). There were no significant differences in age between groups, for both ADM and TA sets. Regarding CutSP measurements, ALS patients had significantly higher onset latencies, for both ADM ($p = 0.006$) and TA ($p = 0.005$) muscles, compared to healthy controls (Table 6).

Table 6 – Cutaneous silent period measurements in ALS patients and healthy subjects

	ADM		TA	
	ALS patients (n=45)	Healthy subjects (n=27)	ALS patients (n=29)	Healthy subjects (n=26)
CutSP onset latency (ms)	77.0* (72.7-803)	71.3 (68.7-76.7)	103.3** (89.0-108.3)	87.2 (78.7-99.0)
CutSP duration (ms)	64.0 (52.3-75.7)	65.3 (54.7-74.7)	58.3 (45.0-72.0)	61.5 (49.3-74.0)
EMG suppression (% amplitude)	77.1 (70.7-81.4)	75.7 (71.0-78.6)	75.1 (72.1-78.2)	75.5 (72.9-79.8)

All values represented are Median (IQR); CutSP – cutaneous silent period; ALS – amyotrophic lateral sclerosis; n – number of muscles included; ADM – abductor digit minimi; TA – tibialis anterior; *p =0.006 (Mann-Whitney test); ** p =0.005 (Mann-Whitney test); *** p =0.007 (Mann-Whitney test). Note: Adapted from Castro et al. (2023b), with permission.

Clinical UMN signs

Since abnormalities in CutSP could be explained by inhibitory effects at segmental spinal levels, we categorized the tested muscles into 2 groups, according to the presence, or absence of clinical UMN signs in the respective spinal segment (see Methods). From the set of 45 ADM and 29 TA muscles from ALS patients, 27 ADM and 21 TA had clinical signs of UMN involvement in the respective limb. We compared CutSP measurements in limbs with and without UMN signs (Figure 24), and each of these subgroups with values from healthy subjects. The Kruskal-Wallis H test showed statistically significant differences between the above 3 subgroups for

ADM (p = 0.004) and TA (p = 0.004) regarding CutSP onset latency. There were also significant differences in the amount of EMG suppression for the TA muscles (p = 0.022). Pairwise comparisons are shown in Table 7.

Onset latencies were significantly higher in muscles with UMN signs when compared to controls (ADM and TA, p = 0.001). There was a significant decrease in the amount of EMG suppression in muscles with UMN signs when compared to muscles without UMN signs, p = 0.08 (Figure 25). There were no significant differences between muscles without UMN signs and control subjects. In the 7 TA muscles with no CutSP, clinical signs of UMN lesion were positive in 4 legs.

Figure 24 – Cutaneous silent period examples for each muscle studied, with and without UMN signs in the respective limb

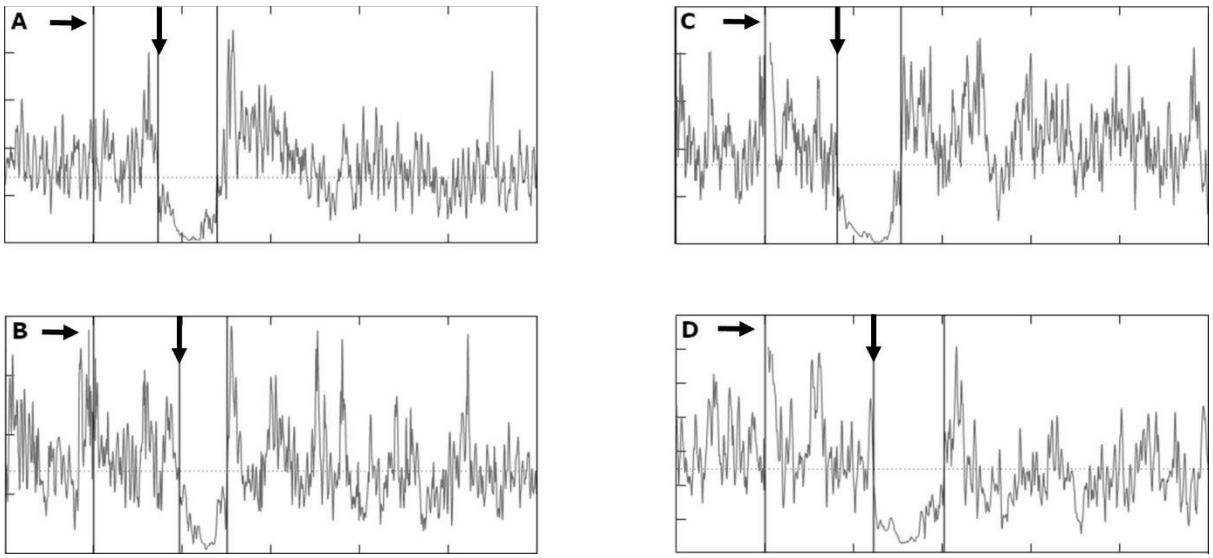

A – ADM without UMN signs; B – ADM with UMN signs; C – TA without UMN signs; D – TA with UMN signs; Horizontal arrows – electrical stimulus; Vertical arrows – Cutaneous silent period onset latency; Dotted horizontal line - 80% of pre-stimulus average EMG signal. Note: Adapted from Castro et al. (2023b), with permission.

In every studied muscle the needle EMG changes were mild or moderate according to the inclusion criteria. Nevertheless, in order to assess a possible influence of LMN degeneration in the CutSP findings, we analyzed neurophysiological data that evaluates LMN function. The degree of muscle contraction, evaluated by the envelope EMG signal, and ADM and TA CMAP amplitudes, following nerve stimulation, were similar between muscles with vs without CutSP, as well as between muscles in limbs with vs without clinical UMN signs ($p > 0.05$).

TMS studies

TMS recordings were investigated, as a further measure of UMN dysfunction, in the spinal segments. A reproducible motor evoked response was absent in 2 ADM and 7 TA muscles. Abnormal TMS responses were found in 73% of ADM and 42% of TA muscles (absent responses in eligible muscles was considered an abnormal result). RMT for ADM recordings (median 50.0%, IQR 50.0-58.0) was lower than in the TA recordings (median 75.0%, IQR 65.0-80.0). In addition, the MEP latency (median 23.3 ms, IQR 22.6-24.7) and CMTC (median 8.5 ms, IQR 7.4-9.2) were shorter in ADM than in TA recordings (median 32.2 ms, IQR 31.3-35.7 and median 14.4 ms, IQR 13.3-116.0, respectively) ($p < 0.001$). Median motor amplitudes recorded in ADM (median

1.3 mV, IQR 0.7-2.3) were similar to TA (median 0.7 mV, IQR 0.5-1.2) (p = 0.36). We compared TMS results in muscles with vs without UMN signs (Table 7). There were no significant differences between groups (p > 0.005).

Table 7 – Cutaneous silent period measurements and TMS results in healthy subjects and in muscles with or without UMN clinical signs

	ADM			TA		
	UMN signs (n=27)	No UMN signs (n=18)	Healthy subjects (n=27)	UMN signs (n=21)	No UMN signs (n=8)	Healthy subjects (n=26)
CutSP onset latency (ms)	78.0* (73.0-87.7)	75.2 (71.3-78.0)	71.3 (68.7-76.7)	104.3* (91.3-109.7)	91.3 (81.5-103.5)	87.2 (78.7-99.0)
CutSP duration (ms)	70.0 (53.3-83.7)	61.5 (51.3-66.0)	65.3 (54.7-74.7)	58.3 (43.0-71.0)	65.5 (50.7-75.2)	61.5 (49.3-74.0)
EMG suppression (% amplitude)	78.7 (69.8-82.9)	74.6 (71.4-81.3)	75.7 (71.0-78.6)	72.8** (70.4-75.6)	78.7 (77.1-80.1)	75.5 (72.9-79.8)
	UMN signs (n=25)	No UMN signs (n=18)		UMN signs (n=18)	No UMN signs (n=11)	
TMS threshold (%)	53.0 (50.0-65.0)	50.0 (45.0-55.0)		72.5 (65.0-80.0)	75.0 (65.0-90)	
TMS latency (ms)	24.0 (22.7-24.3)	23.0 (22.6-24.7)		32.7 (31.4-35.7)	32.1 (30.9-36.6)	
TMS amplitude (mV)	1.3 (0.5-2.3)	1.3 (1.0-2.0)		0.9 (0.6-1.2)	0.6 (0.5-1.3)	
TMS CMCT (ms)	8.6 (7.4-9.4)	8.5 (7.9-9.2)		14.6 (12.8-16)	14.2 (13.4-17.2)	

A limb with very brisk reflexes (score > 3), or spasticity or abnormal reflex Hoffman or extensor plantar response) was considered as having UMN signs (Brooks, 1994). All values represented are Median (IQR); CutSP – cutaneous silent period; n – number of muscles included; ADM – abductor digit minimi; TA – tibialis anterior; UMN signs – clinical signs of upper motor neurons lesion (see methods for definition); *p = 0.001 (post-hoc comparison UMN signs – healthy subjects); ** p = 0.008 (post-hoc comparison UMN signs – No UMN signs). Note: Adapted from Castro et al. (2023b), with permission.

We also categorized muscles into 2 groups, according to the presence or absence of TMS abnormalities in the respective limb. From the set of 45 ADM and 29 TA muscles from ALS patients, 33 ADM and 10 TA had abnormal TMS results, as defined in the methods. We compared CutSP measurements in limbs with normal and abnormal TMS results. The Kruskal-Wallis H test comparing limbs with and without UMN signs in ALS patients, and with controls, showed statistically significant differences between groups for ADM (p = 0.022) and TA (p < 0.001) CutSP onset latency. Pairwise comparisons are shown in Table 8. In ADM muscles with abnormal TMS results, CutSP onset latencies were prolonged when compared with healthy subjects (p = 0.007). In TA muscles with abnormal TMS, CutSP onset latencies were significantly prolonged when compared either with muscles with normal TMS results (p = 0.004) or with healthy controls (p < 0.001).

Figure 25 – Distribution of cutaneous silent period parameters in healthy subjects and in patients with or without UMN clinical signs

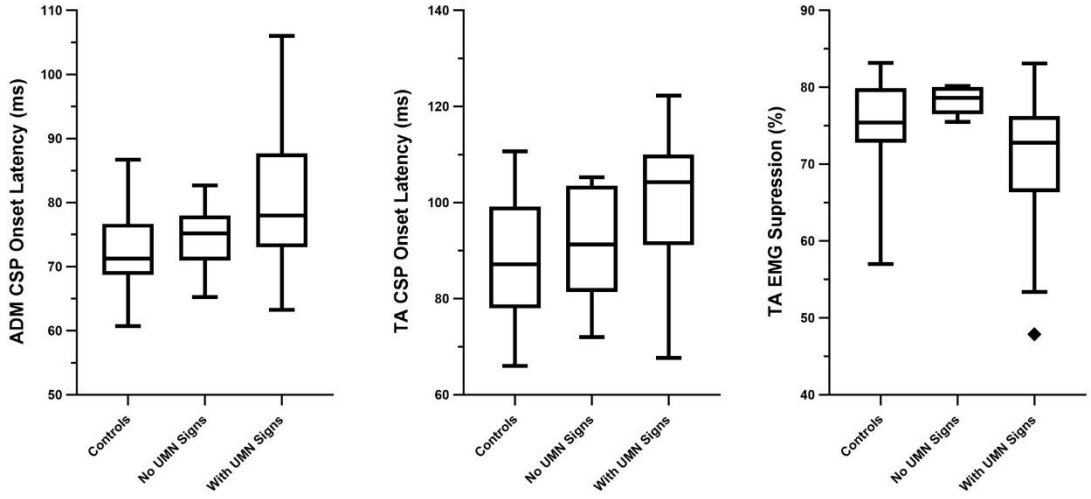

ADM – abductor digit minimi; TA – tibialis anterior; UMN – Upper motor neuron; ms – milliseconds. Note: Adapted from Castro et al. (2023b), with permission.

Correlation analysis

The median total UMN score and ALSFRS-R score were 10.5 (IQR 6.5-14.0) and 45.0 (44.0-45.5), respectively. No significant correlations were found between these scores and CutSP parameters ($p > 0.05$ for all tests).

As previously done, we considered the UMN score in each specific anatomical region. For the cervical region, we identified a significant correlation between upper limb UMN score and CutSP duration in the ADM muscles ($r_s = 0.30$, $p = 0.045$). For the lumbosacral region, there was a significant correlation between lower limb UMN scores and CutSP onset latency ($r_s = 0.54$, $p = 0.002$) and also with EMG suppression ($r_s = -0.40$, $p = 0.031$) in TA muscles. There were no significant correlations between TMS parameters and UMN score in both anatomical regions.

We also investigated correlations between TMS parameters and CutSP findings. For the ADM, we found a significant correlation between CutSP onset latency and CMCT ($r_s = 0.36$, $p = 0.018$) and RMT ($r_s = 0.34$, $p = 0.025$). For the TA there was no significant correlation between CutSP measurements and TMS findings.

Table 8 – Results from healthy subjects and limbs with vs without TMS changes

	ADM			TA		
	Abnormal TMS# (n=33)	Normal TMS (n=12)	Healthy subjects (n=27)	Abnormal TMS# (n=10)	Normal TMS (n=19)	Healthy subjects (n=26)
CutSP onset latency (ms)	77.3* (72.7-80.3)	75.2 (72.2-80.9)	71.3 (68.7-76.7)	107.5** (103.7-112.3)	91.3 (82.3-105.3)	87.2 (78.7-99.0)
CutSP duration (ms)	66.7 (52.3-78.0)	61.5 (53.7-67.4)	65.3 (54.7-74.7)	52.5 (42.7-65.0)	66.0 (45.0-78.0)	61.5 (49.3-74.0)
EMG suppression (% amplitude)	77.2 (72.2-80.9)	73.5 (68.8-83.2)	75.7 (71.0-78.6)	72.7 (71.7-75.6)	76.0 (72.2-79.1)	75.5 (72.9-79.8)

All values represented are Median (IQR). Absent responses in eligible muscles were considered an abnormal result. CutSP – cutaneous silent period; n – number of muscles included; ADM – abductor digit minimi; TA – tibialis anterior; # - including absent responses; TMS – transcranial magnetic stimulation; *p = 0.007 (post-hoc comparison Abnormal TMS – Healthy subjects); ** p = 0.004 (post-hoc comparison Abnormal TMS – Normal TMS) and p < 0.001 (post-hoc comparison Abnormal TMS – Healthy subjects) Note: Adapted from Castro et al. (2023b), with permission.

Binomial logistic regression analyses

All continuous independent variables were found to be linearly related to the logit of the dependent variable (clinical UMN signs), and there were no significant outliers (standardized residuals < 2.0 standard deviations).

For the upper limb, the logistic regression model was statistically significant, $\chi^2(4) = 18.198$, $p < 0.05$. Using the Nagelkerke R^2 to evaluate the goodness of fit of the logistic regression model, this model explained 45.0% of the variance in the presence of clinical UMN signs and correctly classified 73.3% of cases (Nagelkerke, 1991). Of the four variables included, only two were statistically significant: CutSP onset latency and CutSP duration (Table 9). Increasing onset latency and duration were associated with an increased likelihood of having clinical UMN signs in upper limbs. For the lower limb, the logistic regression model was statistically significant, $\chi^2(4) = 11.035$, $p < 0.05$. Using the Nagelkerke R^2 to evaluate the goodness of fit of the logistic regression model, this model explained 45.7% of the variance in the presence of clinical UMN signs and correctly classified 79.3% of cases (Nagelkerke, 1991). Despite this, none of the four variables included achieved statistical significance. There was, however, a trend ($p = 0.082$) for the decrease in the amount of EMG suppression to be associated with an increased likelihood of having clinical UMN signs.

Table 9 – Logistic regression analysis for the presence of UMN signs in the upper limb

	B	SE	Wald	*df*	*p*	Odds Ratio	Lower 95% CI	Upper 95% CI
CutSP onset latency	0.194	0.068	8.215	1	0.004*	1.214	1.063	1.387
CutSP duration	0.086	0.036	5.814	1	0.016*	1.089	1.016	1.168
EMG suppression	0.023	0.066	0.122	1	0.727	1.023	0.899	1.164
TMS	0.310	0.831	0.139	1	0.709	1.364	0.268	6.948
Constant	-21.998	8.487	6.718	1	0.010	0.000		

In the model, TMS was included as a dichotomous variable (normal vs abnormal); * - statistically significant predictors of the presence of UMN signs using this model. ADM – abductor digit minimi; UMN – clinical signs of upper motor neurons lesion (see methods for definition); TMS – transcranial magnetic stimulation changes (see methods for definition); 95% CI: confidence interval for odds ratio. Note: Adapted from Castro et al. (2023b), with permission.

In this model, TMS defined as normal vs abnormal was not predictive of the clinical UMN signs for both upper and lower limbs. We tested an additional model, which included TMS threshold, MEP amplitude and CMCT. The results of this model were similar to the ones described above.

6.3. Study III

Fifty-seven subjects (42 females; mean age 56.9 ± 13.8 SD; 20-83) were recruited. In 41 subjects, the upper limbs were studied. In a subset of 16 subjects, all 4 limbs were evaluated. Records were obtained from bilateral ADM and TA muscles at sampling frequencies of 3 and 24 Hz, as detailed in Table 10.

Table 10 – Number of muscles recordings in each sampling frequency

	3Hz				24 HZ	
	Right ADM	Left ADM	Right TA	Left TA	Right ADM	Left ADM
Gender	29 ♀ 14 ♂		10 ♀ 6 ♂		29 ♀ 12 ♂	
Age	56.6 ± 15.1		53.8 ± 17.2		57.3 ± 12.5	
Muscles	43	43	16	16	41	41

Age values are mean and SD; ADM – Abductor digiti minimi; TA – Tibialis anterior. Note: Adapted from Castro et al. (2023a), with permission.

Latency measurements

ICC values for the onset latency (proposed algorithm and both operators), were calculated for the ADM muscles, considering all recordings done in both sampling frequencies. For both 3 Hz and 24 Hz, the ICC value was 0.998 ($p < 0.001$). Concordance between the ADM measurements of the Algorithm against both operators, for the two frequencies, can be seen in Figure 26.

Bland-Altman plots were constructed in order to further evaluate the agreement in measurements. We compared measurements from one operator (JC) against the other operator (IdC) and against the Algorithm for both frequencies Figure 27. The limits of agreement were very similar for both comparisons JC vs IdeC 82.9 ms and JC vs Algorithm 88.4 ms for 24 Hz and JC vs IdeC 63.9 ms and JC vs Algorithm 83.5 ms for 3 Hz.

Figure 26 – Comparison of latency measurements in both sampling frequencies between one operator (JC) and the other operator (IdeC) and the proposed algorithm

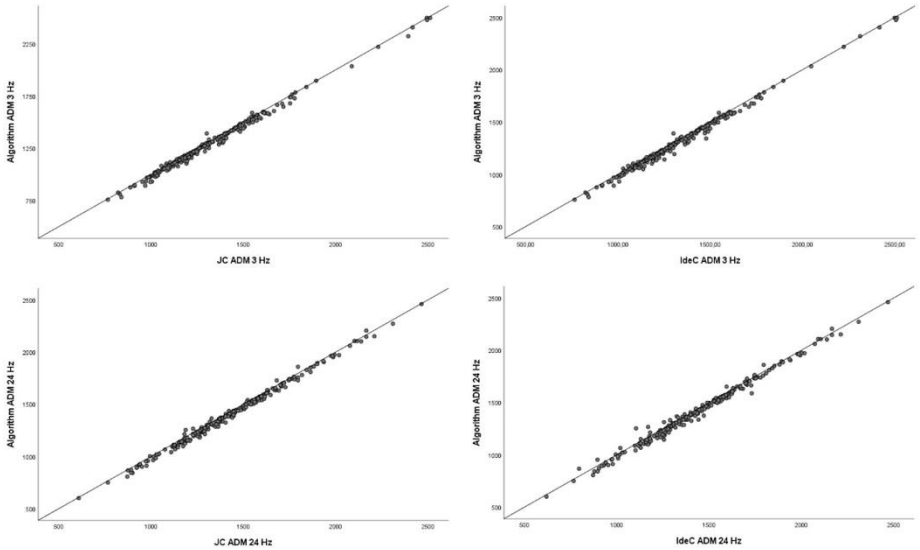

ADM – Abductor digiti minimi; Note: Adapted from Castro et al. (2023a), with permission.

Figure 27 – Bland-Altman plots of the difference in latency as marked by the custom algorithm vs one operator (JC) as well as one operator (JC) vs other operator (IdeC), for both sampling

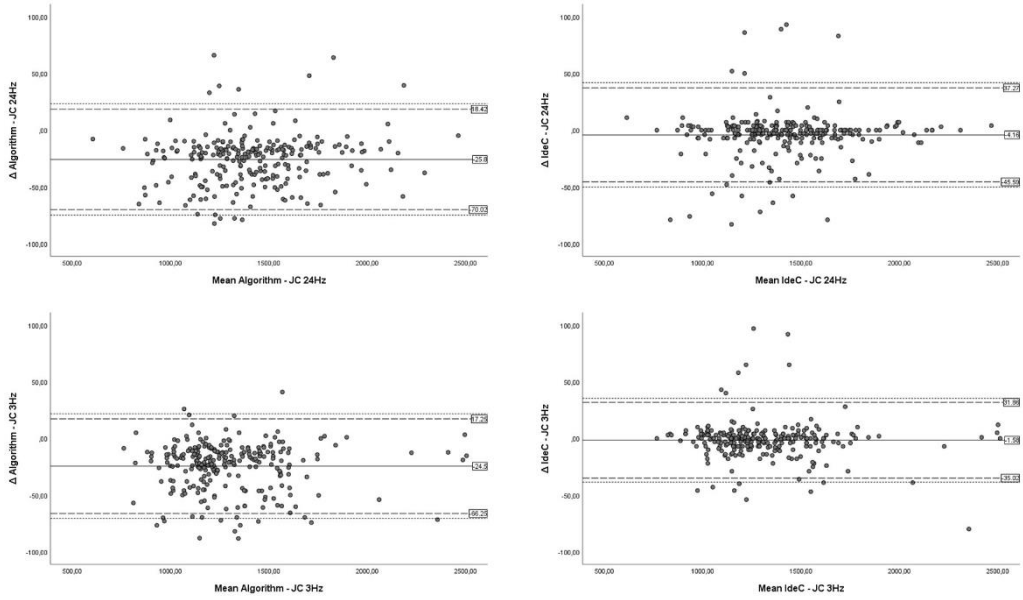

Solid lines represent the mean difference; Upper dashed lines represent the mean differences + 1.96 SD (with upper 95% CI – dotted line), and lower dashed lines represent the mean differences – 1.96 SD (with lower 95% CI – dotted line). Note: Adapted from Castro et al. (2023a), with permission.

Amplitude measurements

Given the similar results in latency measurements between both frequencies analyzed, amplitude measurements were evaluated in 3 Hz signals. For each subject, the amplitude considered was the average of the three recordings. The amount of EMG mirror signal for each muscle as a percentage of the full contraction signal is displayed in Table 11.

Table 11 – Amount of mirror activity for each muscle

		Mirror activity		
		Mirror EMG (%)	Logarithmic scale (%)	After exponentiation (%)
Mirror muscle	Right ADM	6.4 3.0 - 10.2	0.83 ± 0.31 (0.09 - 1.19)	6.8 ± 2.0 (1.7 - 27.4)
	Left ADM	2.6 1.6 - 5.0%	0.64 ± 0.28 (0.22 - 1.44)	4.4 ± 1.9 (1.2 – 15.4)
	Right TA	2.1 0.8 - 4.0	0.49 ± 0.29 (-0.08 - 1.06)	3.1 ± 1.9 (0.8 – 10.4)
	Left TA	0.8 0.5 - 1.2	0.26 ± 0.12 (0.02 - 0.50)	1.8 ± 1.3 (1.1 – 2.1)

Median and IQR of the amount of mirror activity; Mean ± standard deviation and 95% limits of normality for both the transformed (Logarithmic scale) and the exponentiated variables (all values are in % of the amount of EMG from the active muscle); ADM – Abductor digiti minimi; TA – Tibialis anterior. Note: Adapted from Castro et al. (2023a), with permission.

There was no difference in amplitude of the mirror activity between genders. A Spearman's rank-order correlation was run to assess the relationship between age and the amount of mirror activity. Preliminary analysis showed that all relationships were monotonic, as assessed by visual inspection of a scatterplot. There was a statistically significant, moderate positive correlation between age and mirror activity in the ADM ($r_s(86) = 0.300$, $p = 0.005$) and in the TA ($r_s(32) = 0.475$, $p = 0.006$) muscles (Figure 28). Regarding differences between sides, there was significantly more mirror activity in the right muscles (when the left muscle was active). Differences between mirror activity, regarding the active side, were assessed with the Mann-Whitney U test. In the upper limbs, median mirror activity in the right ADM (6.4%) was significantly higher than in the left ADM (2.6%), $U = 577$, $z = -3.002$, $p = 0.003$. In the lower limbs, median mirror activity in the right TA (2.1%) was significantly higher than in the left TA (0.8%), $U = 64.5$, $z = -2.399$, $p = 0.016$ (Figure 29).

Figure 28 - Scatterplots of age and mirror activity in the studied muscles

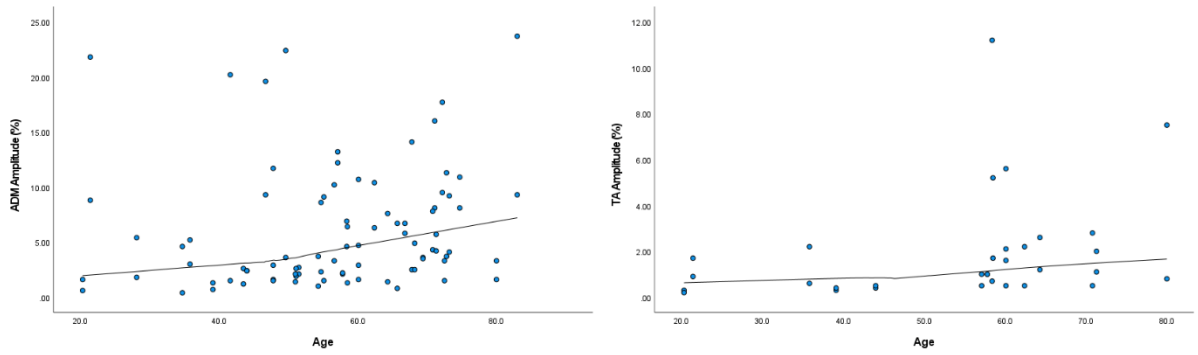

Values are represented as a percentage of the amount of EMG signal of the active muscle; ADM – Abductor digiti minimi; TA – Tibialis anterior; Trend lines were generated using loess modeling (90% of points fit, Epanechnikov kernel). Note: Adapted from Castro et al. (2023a), with permission.

Given the non-normality of the amount of mirror signal distribution, we performed a logarithmic transformation of the data, for the calculation of normative data. We chose a log10 transformation for this purpose. Given the small amount of mirror EMG signal in some subjects, we opted for a log(x+1), to avoid the approach to negative infinity as x approached 0. The resulting variables were approximately normally distributed (Shapiro-Wilk test $p > 0.01$, Skewness and Kurtosis < 1).

Normative data was calculated as Mean ± 1.96SD in the transformed data. Values in logarithmic scale and after exponentiation are presented in Table 11. The upper limit of normality for mirror EMG signal in our group was 27.4% for right ADM, 15.4% for left ADM, 10.4% for right TA and 2.1% for left TA.

Figure 29 - Boxplot of the amount of mirror activity per muscle and side

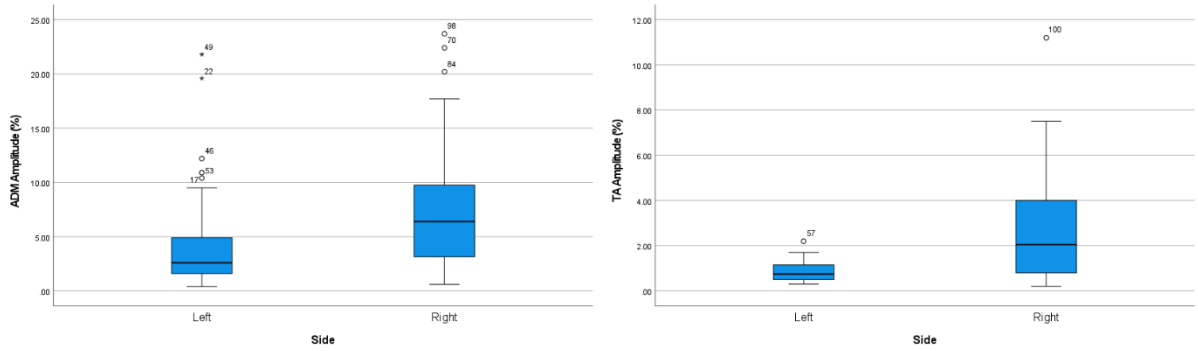

Values are represented as a percentage of the amount of EMG signal of the active muscle; ADM – Abductor digiti minimi; TA – Tibialis anterior. Note: Adapted from Castro et al. (2023a), with permission.

6.4. Study IV

Forty-two ALS patients, 14 women (33%), with a median age of 59.5 years (IQR 52.0-71.0), and a median disease duration of 13.5 months (IQR 8.0-24-0), were studied. The median ALSFRS-R at the time of the assessment was 44.0 (IQR 40.0-45.0). Forty patients were right-handed, as assessed by the Edinburgh Handedness Inventory (Oldfield, 1971), 1 patient was left-handed and 1 was ambidextrous. These patients were early affected patients consecutively recruited in our Unit.

Mirror activity

Measurements of mirror activity were obtained from 72 ADM and 56 TA muscles (Table 12), after excluding results from cervical or lumbo-sacral segments in which at least one muscle was weak (MRC <4, see methods).

Table 12 – Amount of mirror activity in ALS subjects, and percentage of muscles with abnormal mirror activity considering previously published normative values

	N	Mirror activity (%) Cut-Off values*	Mirror activity (%) ALS	Muscles with abnormal mirror activity
Right ADM	36	27.4	11.1 6.6 – 18.9	3 (8%)
Left ADM	36	15.4	10.2 4.2 – 22.6	12 (33%)
Right TA	28	10.4	7.9 2.6 – 18.3	13 (46%)
Left TA	28	2.1	5.7 1.6 – 20.1	17 (61%)

ADM – Abductor digiti minimi; TA – Tibialis anterior; Mirror activity is expressed as a percentage of the EMG signal of the active muscle (see Methods); *Cut-off values published previously (Castro et al., 2023a); Values are median and IQR.

There were no significant differences in the amount of mirror activity between genders. There was also no significant correlation between mirror activity and age, disease duration, UMN score and ALSFRS-R, as assessed by the Spearman rank-order correlation ($p > 0.05$ for all correlations).

When compared with the data obtained from our healthy subjects group (Castro et al., 2023a), the ALS population had a significantly stronger mirror activity in all 4 muscles (Figure 30). Moreover, there was an abnormal amount of mirror activity in 3 right ADM (8%), 12 left ADM (33%), 13 right TA (46%) and 17 left TA (61%). There were no significant inter-side differences: right ADM (11.1%) vs left ADM (10.2%), U = 618, z = -0.338, p = 0.735; right TA (7.9%) vs left TA (5.7%), U = 347, z = -0.737, p =

0.461. Given the absence of inter-side differences, subsequent analyses were performed with 2 sets of muscles (ADM and TA), disregarding side.

Figure 30 – Comparison of mirror activity between ALS subjects and healthy controls for each studied muscle

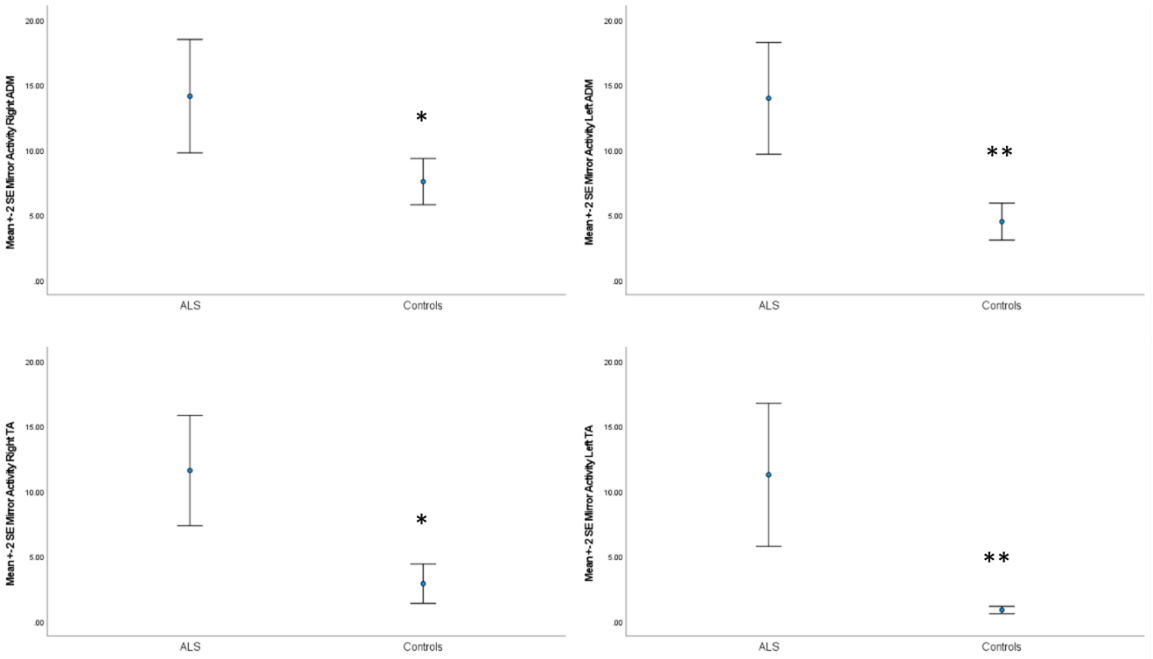

Bars represent mean ± 2 standard error of mean. ADM – Abductor digiti minimi; TA – Tibialis anterior; Mann-Whitney U test was used for group comparisons: * - $p = 0.003$; ** - $p < 0.001$.

Cognitive data

In a subgroup of 21 ALS patients (14 male; mean age 62.32 ± 11.68 years) neuropsychological status was measured with the ECAS battery (mean disease duration at evaluation 29.57 ± 20.90 months). The subjects' ECAS total score ranged between 21 and 128 with a median of 88 (IQR 64–116), while the median ALS-Specific score (executive functions and social cognition; fluency; language) was 60 (IQR 41–85). In this group of patients, 57.1% were found to have cognitive impairment on the ECAS total score and 61.9% on ALS-specific score.

When comparing the amount of mirror activity between subjects with or without cognitive impairment (ECAS ALS-specific score and ECAS total score), we found no significant differences in both muscles.

Transcranial magnetic stimulation

Conventional TMS was performed in all subjects. Values for RMT, amplitude and CMCT are displayed in Table 13. A reproducible motor evoked response was absent in 7 ADM and 15 TA of the assessed muscles. Abnormal TMS responses were found in 68% of ADM and 52% of TA muscles.

Table 13 – Transcranial magnetic stimulation and Ipsilateral Silent Period values for ALS subjects

	RMT (%)	MEP/CMAP Ampl. Ratio (mV)	CMCT (ms)	iSP Onset Latency (ms)	iSP Duration (ms)
ADM	52 50-60	0.12 0.07-0.22	8.8 7.8-9.9	42.2 39.3-48.5	40.4 27.8-48.5
TA	75 63-85	0.12 0.08-0.22	14.6 13.3-17.7	--	--

ADM – Abductor digiti minimi; TA – Tibialis anterior; RMT – resting motor threshold; MEP – Motor evoked potential; CMCT – central motor conduction time; iSP – ipsilateral silent period; mV – millivolts; ms – milliseconds; TMS normative cut-off values: MEP/CMAP Ampl. ratio < 0.05, CMCT > 8 ms for ADM and 16 ms for TA (de Carvalho et al., 2003); iSP normative cut-off values: Onset latency > 48.8, Duration < 12.4 ms or > 61.8 ms; values are median and IQR.

We compared the amount of mirror activity from limbs with normal and abnormal TMS results, and with our normative data from healthy subjects investigated with the same method (Castro et al., 2023a) (Figure 31). The Kruskal-Wallis H test showed significant differences between the 3 groups, both in ADM ($\chi 2(2) = 43.606$, $p < 0.001$) and in TA ($\chi 2(2) = 39.162$, $p < 0.001$). Subsequent pairwise comparisons (Table 14) disclosed significant differences between all groups, both in ADM and TA muscles. Patients with normal TMS results had more mirror activity than healthy subjects, while patients with abnormal TMS results had more mirror activity than patients with normal TMS results.

Figure 31 – Comparison of mirror activity between limbs with vs without transcranial magnetic stimulation changes

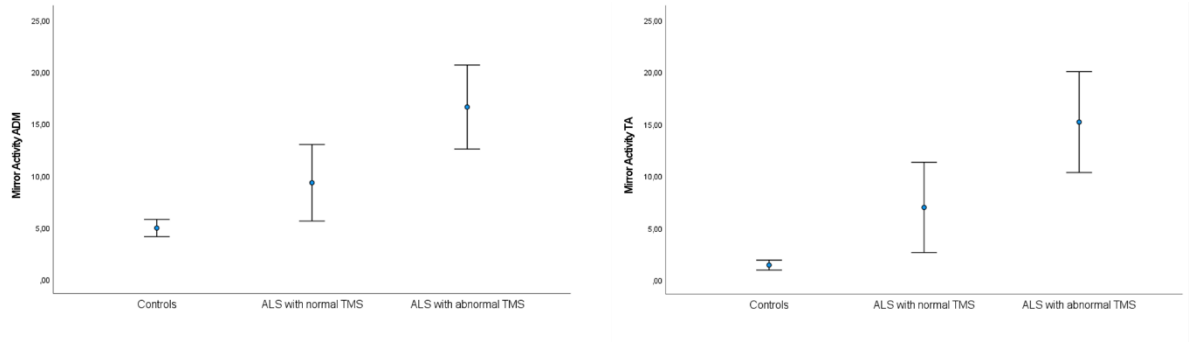

ADM – Abductor digiti minimi; TA – Tibialis anterior; TMS – Transcranial magnetic stimulation; Bars represent mean ± 2 standard error of mean; Pairwise group comparisons are shown in Table 14.

Table 14 – Comparison of mirror activity between groups according to transcranial magnetic results (pairwise comparisons using Dunn's procedure)

	Mirror activity (%) Healthy subjects	Mirror activity (%) ALS normal TMS	Mirror activity (%) ALS abnormal TMS	Healthy subjects vs ALS normal TMS (*p* value)	Healthy subjects vs ALS abnormal TMS (*p* value)	ALS normal TMS vs ALS abnormal TMS (*p* value)
ADM	3.6 2.0-7.7	5.4 3.3-12.3	12.1 7.6-23.2	0.034	0.003	0.005
TA	1.0 0.5-2.0	2.0 1.0-5.0	12.0 7.7-21.4	0.01	0.002	0.002

ADM – Abductor digiti minimi; TA – Tibialis anterior; TMS – Transcranial magnetic stimulation; ms – milliseconds; Mirror activity is expressed as a percentage of the EMG signal of the active muscle (see Methods); Values are median and IQR; *p* values shown are adjusted values using the Benjamini-Hochberg procedure (FDR 5%).

Ipsilateral Silent Period

iSPs were studied in 70 ADM muscles. Values of onset latency and duration are shown in Table 13. A reproducible iSP was absent in 18 (26%) of the assessed ADM muscles. Considering our normative values, abnormal iSPs were found in 36 (51.4%) ADM muscles (absent iSP was considered an abnormal result).

Figure 32 – Comparison of mirror activity between upper limbs with vs without abnormalities on the ipsilateral silent period

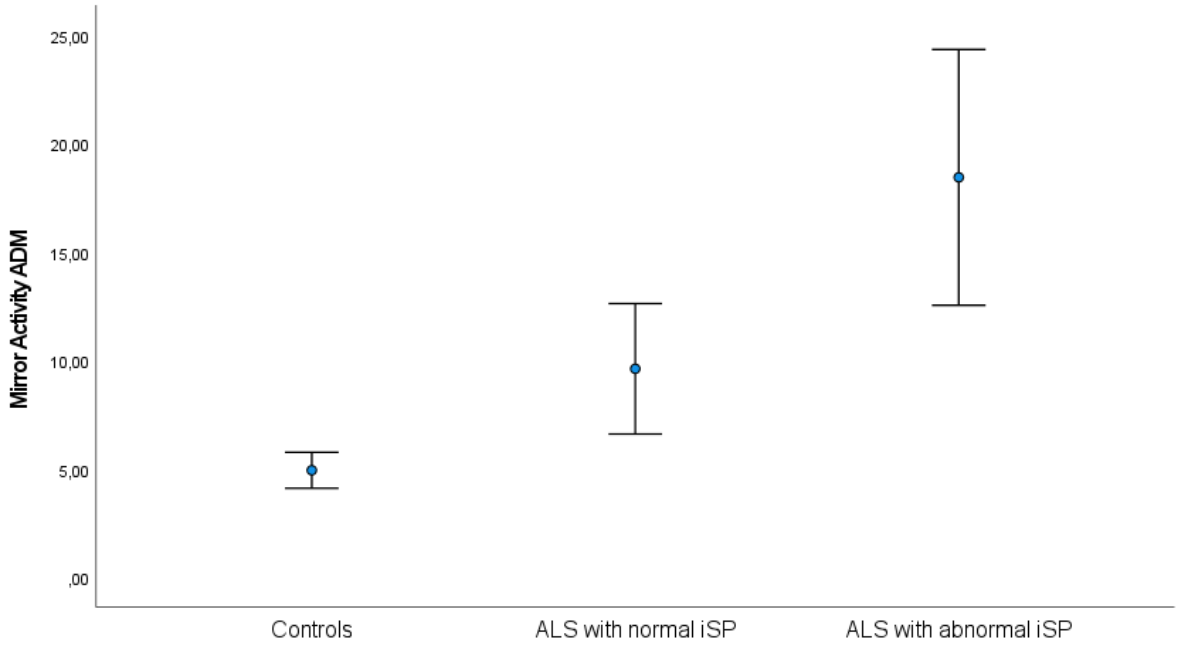

ADM – Abductor digiti minimi; iSP – Ipsilateral silent period; Bars represent mean ± 2 standard error of mean; Pairwise group comparisons are shown in Table 15.

We categorized muscles into 2 groups according to the presence or absence of iSP abnormalities. We compared the amount of mirror activity from muscles with normal and abnormal iSP values, and with data from our healthy subjects group (Figure 32). The Kruskal-Wallis H test showed significant differences between the 3 groups ($\chi 2(2) = 35.577$, $p < 0.001$). Subsequent pairwise comparisons disclosed significant differences between groups, as shown in Table 15.

Table 15 – Comparison of mirror activity between groups according to ipsilateral silent period results (pairwise comparisons using Dunn's procedure)

	Mirror activity (%) Healthy subjects	Mirror activity (%) ALS normal iSP	Mirror activity (%) ALS abnormal iSP	Healthy subjects vs ALS normal iSP (*p* value)	Healthy subjects vs ALS abnormal iSP (*p* value)	ALS normal iSP vs ALS abnormal iSP (*p* value)
ADM	3.6 2.0-7.7	6.9 3.4-11.5	14.3 8.2-22.2	0.008	0.003	0.009

ADM – Abductor digiti minimi; TA – Tibialis anterior; iSP – ipsilateral silent period; Mirror activity is expressed as a percentage of the EMG signal of the active muscle (see Methods); values are median and IQR; *p* values shown are adjusted values using the Benjamini-Hochberg procedure (FDR 5%).

Patients with normal iSP values had more mirror activity than healthy subjects, while patients with abnormal iSP values had more mirror activity than patients with normal iSP values.

Figure 33 displays an illustrative example of an absent and a normal iSP, with the mirror activity of the corresponding ADM muscle.

Figure 33 – Illustrative example of absent and normal ipsilateral silent period, with the corresponding mirror activity

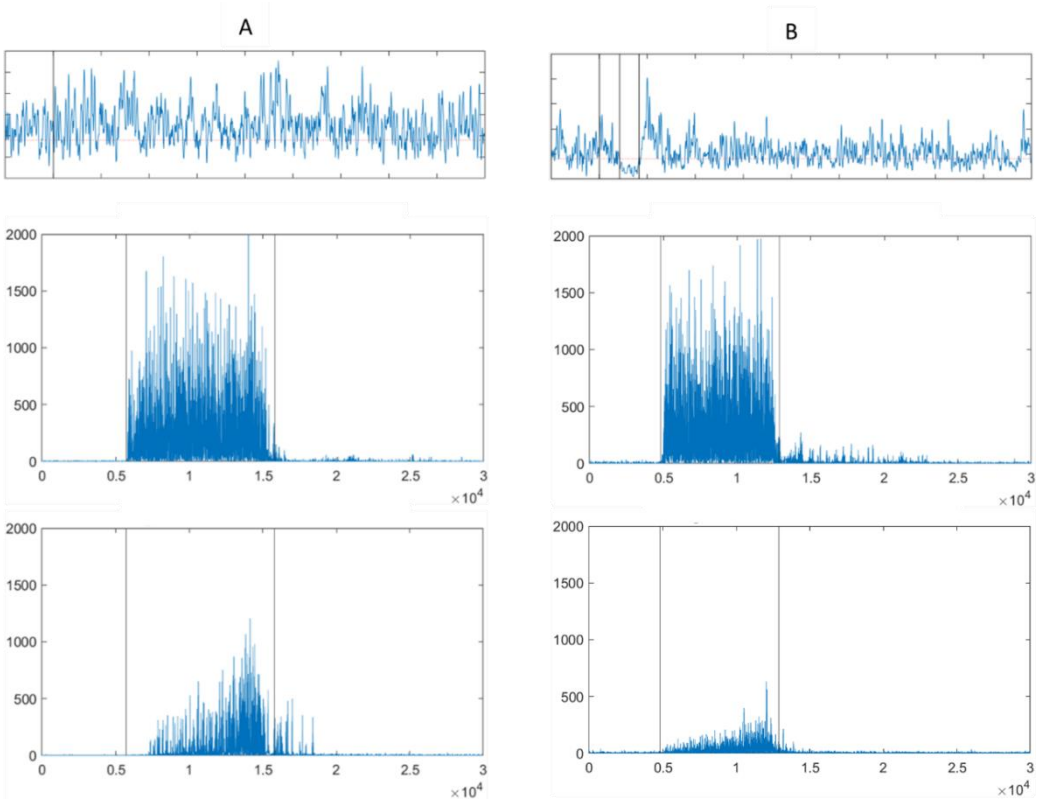

A – ALS subject with absent ipsilateral silent period (iSP) (top trace) on the right Abductor digiti minimi (ADM), contraction of the left (active) ADM (middle trace), and clear mirror activity on the right (mirror) ADM (bottom trace). B – ALS subject with normal iSP (top trace) on the right ADM, contraction of the left (active) ADM (middle trace), and less mirror activity on the right (mirror) ADM (bottom trace).

6.5. Study V

Fifteen ALS patients, 3 women (median age 57.0, IQR 45.0-62.0) and ten healthy controls, 5 women (median age 57.0, IQR 51.0-66.0), were included in the study. Median disease duration was 15 months (IQR 7.0-19.0). Patients were, generally, in a good overall status (median ALFRS-R 44, IQR 40-46). Median clinical UMN score in the lower limbs was 6 (IQR 3.0-8.0). Table 16 details the clinical characteristics of ALS patients. There were no statistically significant differences regarding gender (p = 0.115) or age (p = 0.536) between groups.

Table 16 – Clinical features of ALS patients

	Gender	Age	Site of onset	Disease duration	ALSFRS-R	UMN score LL
1	Male	52	Upper limb	15	47	2
2	Male	69	Thoracic	2	48	6
3	Female	71	Upper limb	19	39	7
4	Male	72	Bulbar	9	44	5
5	Female	58	Bulbar	65	40	10
6	Male	43	Upper limb	6	39	9
7	Male	61	Upper limb	15	43	2
8	Male	37	Upper limb	18	44	2
9	Female	62	Upper limb	7	38	8
10	Male	57	Bulbar	6	43	6
11	Male	30	Lower limb	16	44	3
12	Male	45	Lower limb	17	46	10
13	Male	58	Bulbar	88	45	4
14	Male	57	Lower limb	12	43	7
15	Male	51	Upper limb	34	46	8

H reflex

A reproducible soleus H reflex was obtained in all subjects. Measured body heights were statistically similar between patients and controls. Values from standard H reflex and conditioning paradigms are shown in Table 17.

M_{max} (8.0 mV vs 9.3 mV, in patients and controls respectively, p = 0.40), H_{max} (4.0 mV vs 3.6 mV, in patients and controls respectively, p = 0.89) and H-reflex latency (33.7 ms vs 30.9 ms, in patients and controls respectively, p = 0.55) were similar between ALS subjects and controls. H_{max}/M_{max} was also not significantly different in ALS patients (0.44 vs 0.40, in patients and controls respectively, p =

0.43). Taken together, these findings suggest that the patients included did not have a significant loss of functioning, recruitable LMNs.

Table 17 – Values from H reflex and conditioning paradigms in ALS and healthy subjects

	H Latency (ms)	H_{max} (mV)	M_{max} (mV)	H_{max}/M_{max} ratio	H'_{RI} (H'/H)	H'_{Pre} (% M_{max})	H'_{Post} (% M_{max})
ALS	33.7 (29.6 - 34.9)	4.0 (2.6 - 5.1)	8.0 (5.0 - 11.9)	0.44 (0.40 - 0.54)	0.35 (0.14 - 0.51)	1.0 (-1.0 - 3.0)	0.0 (-2.0 – 3.0)
Controls	30.9 (28.4 - 32.0)	3.6 (3.0 - 4.6)	9.3 (7.1 - 10.0)	0.40 (0.33 - 0.30)	0.11 (0.11 - 0.18)	5.0 (4.0 - 8.0	2.5 (1.0 - 5.0)

ALS – Amyotrophic lateral sclerosis; ms – milliseconds; mV – millivolts; H'RI – amount of recurrent inhibition (H'/H_{max}); H'_{Pre} – amount of presynaptic inhibition of Ia terminals $H'_{Pre} = \frac{H_{Max} - H'}{M_{Max}} \times 100$; H'_{Pos} – amount of inhibition after cutaneous stimulation $H'_{Pos} = \frac{H_{Max} - H'}{M_{Max}} \times 100$. * - p = 0.036; ** - p = 0.001; *** - p = 0.031;

Conditioning paradigms

Contrary to the H/M ratio, H'_{RI} (ratio H'/H) was significantly increased in ALS subjects, when compared to healthy subjects (0.35 vs 0.11; U = 37.5; z = -2.085; p = 0.036), indicating a decrease in the strength of recurrent inhibition in these patients. None of the 3 patients who had an H'_{RI} lower than the median of the control group had UMN signs in the tested lower limb.

Regarding the paradigm used for assessing presynaptic inhibition of Ia terminals, there was a significant decrease in H'_{Pre} in ALS patients when compared to healthy subjects (1.0 vs 5.0; U = 19.0; z = -3.120; p = 0.001), denoting less effective presynaptic inhibition. As noted for H'_{RI}, only two ALS patients had H'_{Pre} higher than the median of the control group, and neither of them had UMN signs in the lower limbs.

As for the paradigm of inhibition after cutaneous stimulation, ALS patients also had a significant decrease in H'_{Pos} when compared to healthy subjects (0.0 vs 2.5; U = 36.0; z = -2.176; p = 0.031), also denoting less inhibition. In this paradigm, 4 patients had higher H'_{Pos} values than the median of the control group, but only two had no UMN signs in the studied limb. Of the remaining two, both had increased deep tendon reflexes (knee and ankle), and one also presented with increased muscle tone (scored 2 in the modified Aswhorth scale).

Figure 34 displays the results for all conditioning paradigms.

Figure 34 – Results from H reflex conditioning paradigms

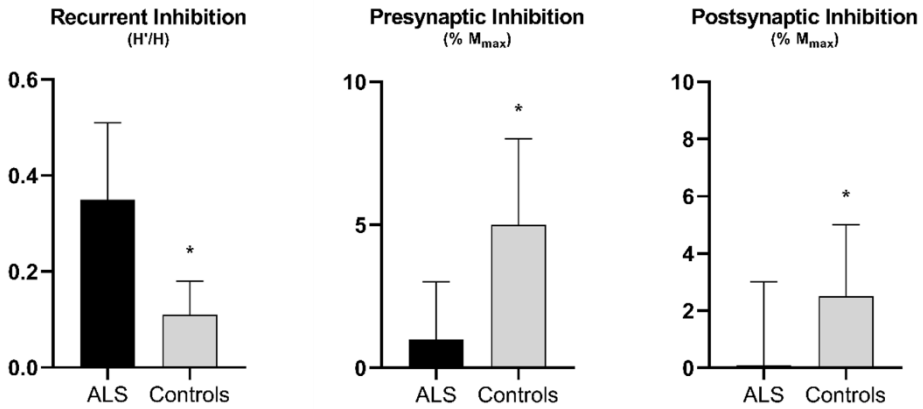

ALS – Amyotrophic Lateral Sclerosis; ms – milliseconds; filled bars represent median; error bars represent 1st or 3rd quartile as appropriate. * - denotes a significant difference between groups (see text).

Influence of UMN dysfunction on H reflex conditioning paradigms

To evaluate the impact of upper motor neuron dysfunction on H-reflex inhibition, distinct regression analyses were conducted, each focusing on a specific condition paradigm. Models were run with dependent variables H'_{RI}, H'_{Pre} and H'_{Pos} (Table 18).

Changes in H'_{RI}, and H'_{Pre} were closely related to changes in the UMN score (Figure 35). The UMN score was a significant predictor of both H'_{RI} ($\beta = 0.648$; $p = 0.010$) and H'_{Pre} ($\beta = -0.850$; $p < 0.001$). Age and disease duration were not related to the dependent variables in any of the models. An increase in the UMN score is associated with an increase in H'_{RI} and a decrease in H'_{Pre}, meaning lower inhibition. Interestingly, changes in H'_{Post} were not related to changes in the UMN score ($\beta = -0.131$; $p = 0.661$).

Table 18 – Regression models for the different conditioning paradigms of the H reflex, incorporating upper motor neuron score, age and disease duration

Dependent variable	Independent variables	Beta	t	p	Model statistics		
					Adjusted R^2	F	p
H'_{RI}	UMNs	0.648	3.094	**0.010**	0.401	4.127	**0.035**
	Age	-0.356	-1.700	0.117			
	Disease duration	-0.267	-1.286	0.225			
H'_{Pre}	UMNs	-0.850	-5.930	**<0.001**	0.720	12.988	**< 0.001**
	Age	-0.012	-0.087	0.932			
	Disease duration	0.289	2.037	0.066			
H'_{Pos}	UMNs	-0.131	-0.450	0.661	-0.157	0.366	0.779
	Age	-0.227	-0.780	0.452			
	Disease duration	-0.107	-0.371	0.718			

Regression models for H'RI, and H'Pre were significant, with satisfactory 'goodness of fit'. Multicollinearity was excluded in all models (VIF < 1.5 for all independent variables).

Figure 35 – Scatterplots of the amount of recurrent inhibition and presynaptic inhibition with the upper motor neuron score from the lower limbs

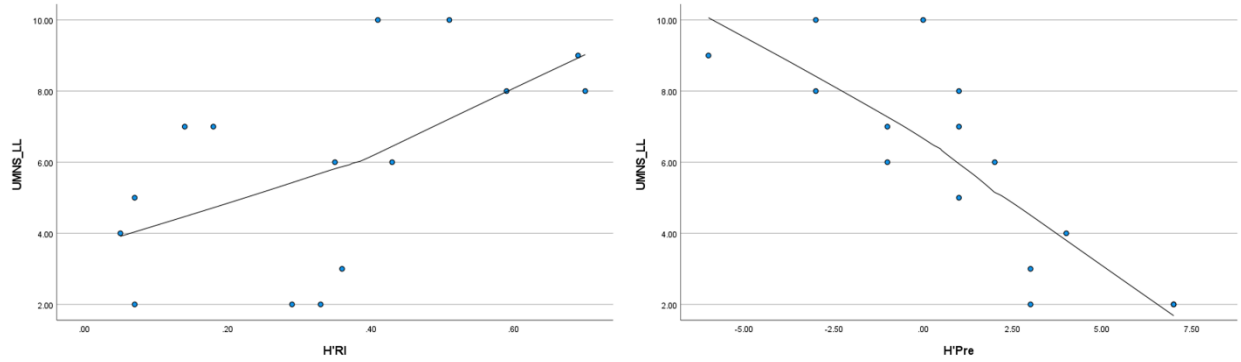

UMNS_LL – upper motor neuron score from the lower limbs; H'RI – amount of recurrent inhibition; H'Pre – amount of presynaptic inhibition; Note: Trend lines generated using loess modelling (99% of points fit, Epanechnikov kernel). Spearman's rank-order correlation for each pair of variables is H'_{RI} ($r_s(15) = 0.641$, $p = 0.010$) and H'_{Pre} ($r_s(15) = -0.853$, $p < 0.001$).

7. Discussion

7.1. Cutaneous silent period

Two studies have been conducted assessing the CutSP in ALS patients (Castro et al., 2021, 2023b). The onset latency of the CutSP, both in the upper and lower limbs was consistently increased in patients, when compared to healthy controls. No changes in CutSP duration were apparent. These finding are consistent with previous reports in the literature in ALS subjects (Gilio et al., 2008, Kim and Kwak, 2010, Cengiz et al., 2018) for the upper limbs. To best of our knowledge, this was the first report of CutSP in the lower limbs of ALS patients. Additionally, the amount of EMG suppression was also decreased in muscles with marked UMN signs. In both studies, changes in CutSP were significantly linked with the amount of UMN signs, suggesting that an interplay between UMN dysfunction and spinal mechanisms is present in ALS.

In the first study (Castro et al., 2021), patients were classified according to clinical involvement of UMN: ALS without spasticity; PMA; PLS plus ALS with predominant spasticity. The CSP onset latency was significantly increased in all groups (Figure 22). This was also evident even in the PMA patients, supporting a subclinical UMN lesion, as demonstrated in neuropathological studies of PMA (Ince et al., 2003). The amount of suppression of the EMG signal during CutSP is decreased in patients with spasticity, indicating that marked UMN dysfunction can not only slow but also reduce the amount of inhibition in CutSP. Interestingly, during co-contraction of the contralateral ADM, onset CutSP latencies decreased in patients without UMN signs, particularly in the PMA group, a finding not seen in healthy controls. With this paradigm, only the PLS + UMN-ALS group had an increased onset latency when compared to healthy controls ($p = 0.004$) and in this group of patients the amount of EMG suppression tended to decrease.

In the second study (Castro et al., 2023b), we classified limbs regarding the presence or absence of UMN signs. CutSP was significantly increased in limbs with UMN signs when compared to controls. In limbs without UMN signs median onset latencies were higher than in healthy controls, although the difference did not reach statistical significance. The same results were observed when limbs were categorized as normal or abnormal regarding TMS results, i.e., CutSP onset latency was

significantly increased in limbs with abnormal TMS results. Again, as with the results of limbs without UMN signs, in limbs with normal TMS results median onset latencies were higher than in healthy controls, although the not significantly. Interestingly, the differences in TMS variables between limbs with and without UMN signs were not significant. Furthermore, in the binomial logistic regression model, CutSP onset latency and duration were strong predictors of clinical signs of UMN lesion in upper limbs in ALS. For the lower limbs this binomial logistic regression disclosed a trend for a reduced EMG suppression to predict clinical UMN signs. Indeed, in 7 TA muscles EMG suppression was so slight that CutSP was considered absent (methods). The results from the lower limbs are, however, influenced by the smaller number of eligible TA muscles with CutSP response (29 muscles). Interestingly, neither TMS parameters nor TMS classification as normal vs abnormal, were predictors of clinical UMN signs.

Taken together, the findings of both studies clearly demonstrate that changes in CutSP are present in ALS patients and are more significant with increasing UMN dysfunction. TMS tests the function of the strong corticomotoneuronal connections (Porter, 1985), which are critical to rapid discrete digital movements. However, the UMN syndrome in ALS is physiologically complex (Swash, 2012), affecting the central nervous system beyond the classical “corticospinal” syndrome (Swash et al., 2020). The direct pathway between Betz cells and the spinal motor neurons represents less than 5% of the corticospinal tract (Brodal, 1981), while other projections forming the propriospinal motor system (Pierrot-Deseilligny, 2002) are crucial to the modulation of other inputs (vestibular, cerebellar, sensory) to the spinal command motor systems (Swash et al., 2020). This limits the role of conventional TMS in the assessment of UMN signs in ALS. Thus, although changes in UMN function can have unexpected clinical impact on motor function, spinal segmental changes, probably linked to disfunction of inhibitory interneurons, can be assessed with CutSP studies. Another interesting finding that merits further discussion is the observation that a contralateral contraction during CutSP measurements decreases abnormal onset latencies in patients without clinical UMN signs. One possible explanation for this is that in this group of patients, with minor dysfunction of the UMN, the activation of the motor cortex of the ipsilateral test hand increases the descending motor output from the contralateral motor cortex, creating a compensatory mechanism at the spinal level. Since this effect is not present in healthy subjects, a reduced transcallosal inhibition in

ALS patients, an early finding in ALS (Karandreas et al., 2007, Hübers et al., 2021a, van den Bos et al., 2021), could account for this phenomenon.

A possible effect of partial denervation of the muscles studied, due to anterior horn cell degeneration, a characteristic feature of ALS, needs consideration. We observed abnormalities in the CutSP even when there were no clinical or TMS UMN abnormalities. This is consistent with the neuropathological observations in PMA (Ince et al., 2003)], in which degeneration of the corticospinal tract was found in the absence of any clinically detectable dysfunction. The physiological disturbances underlying the classical features of the UMN syndrome are complex and include the effects of propriospinal pathway damage (Kuypers, 1973). Not all need be present in any individual with the UMN syndrome (Swash, 2012, Swash et al., 2020). The CutSP is particularly sensitive to segmental spinal damage. It is therefore likely, as suggested by Pierrot-Deseilligny (2002), that this technique can be used to detect specific aspects of abnormality in fragments of descending motor pathways in ALS syndromes.

From a physiological point of view is interesting to note that contralateral muscle contraction does not change CSP parameters in healthy controls. Another group has shown that contralateral upper limb contraction caused absent H-reflex response in the tested hand in a group of subjects, while increasing the motor response on TMS, but not affecting motor responses evoked by electromagnetic electrical cervicomedullary stimulation between the mastoid processes (Hortobágyi et al., 2003). All together, these changes indicate that contralateral muscle contraction at the same segmental level caused robust presynaptic inhibition of Ia afferents resulting from descending activity (Hortobágyi et al., 2003) but since the CSP is unchanged by contralateral contraction, post-synaptic inhibition is the most probable mechanism for this reflex.

7.2. Mirror movements

Adequate control of lateralization of voluntary movements is typical from individuals with a mature, healthy motor system. During intended unimanual movements, young children, and adults with neurological diseases, display visible involuntary movements that mirror the intended ones. However, even healthy adults display some MM that is, most of the time, of so low amplitude that is not clinically

visible. With that in mind, and with the purpose of objectively quantifying MA, we developed a mathematical algorithm to analyze the EMG signal from a given muscle, bilaterally (Castro et al., 2023a) and calculating MA as a percentage of the amount of EMG signal of the active muscle.

We analysed EMG signal from 57 healthy subjects, specifically studying MA during an isometric full force contraction. We evaluated MA in upper limbs (ADM) and lower limbs (TA). The performance of the algorithm regarding latency was excellent, with very high ICC values between automated and manual measurements. The analysis of the Bland-Altman plots showed that the 95% limits of agreement between the algorithm and an experienced human operator were very similar. The performance of the algorithm was similar for both sampling frequencies tested. Despite an excellent performance in ignoring cases where there was incomplete relaxation or spontaneous muscle activity, e.g., fasciculations, there were a small number of issues with latency markings, particularly when the beginning of the contraction was not very well defined. There were significant positive correlations with age, as expected, since it has been suggested that this mirror phenomenon may reappear in older adults (Bodwell et al., 2003). When comparing sides, we found that when the left muscles were active, the amount of mirror activity was significantly greater. Given that all our selected subjects were right-handed, our findings are in accordance with what has been already reported, supporting a higher dominant-to-non dominant hemispheric inhibition (Armatas et al., 1994, 1996). This side-to-side difference in MA can originate in an asymmetry in callosal interconnectivity (Armatas et al., 1996), a possible result of hemisphere specialization (Aboitiz et al., 1992). These results extend these findings, demonstrating that there is higher dominant-to-non dominant hemispheric inhibition also in the lower limbs. Limits of normality are also proposed as follows: 27.4% for the right ADM, 15.4% for the left ADM, 10.4% for the right TA and 2.1% for the left TA.

After the development of this algorithm, we proceeded to analyze MA in ALS. We studied a group of 42 ALS patients in a high functional status (median ALSFRS-R – 44), with normal CMAP amplitudes and MRC ≥ 4 in the assessed muscles. To the best of our knowledge, this is the first attempt to quantify EMG signal in MM in ALS patients. We found significantly increased mirror activity in ALS subjects in both upper and lower limbs, in line with what has previously been reported (Krampfl et al., 2003, Krampfl et al., 2004, Wittstock et al., 2007, Meister et al., 2011, Wittstock et al., 2011,

Wittstock et al., 2020, Hübers et al., 2021a, Hübers et al., 2021b). Subsequent analysis showed that MA was significantly increased in both upper and lower limbs of ALS patients with abnormal TMS results, but also in upper limbs with abnormal iSP, as compared with patients with normal results. However, even in muscles from ALS patients with normal TMS and iSP values, MA was also significantly increased when compared to controls. Interestingly, contrary to our previous findings in healthy subjects (Castro et al., 2023a) and to what has also been reported using clinical assessment (Armatas et al., 1994, 1996), we did not find differences in mirror activity between sides in ALS subjects.

Our results support early inhibitory transcallosal pathway dysfunction in ALS patients (Karandreas et al., 2007, Filippini et al., 2010, Castro et al., 2021, Hübers et al., 2021b, van den Bos et al., 2021). This dysfunction favors mirror phenomenon (Cernacek, 1961, Hübers et al., 2021a), and is associated with abnormal iSPs, since iSPs reflect the function of inhibitory pathways between both cortices, that pass through the posterior corpus callosum (Meyer et al., 1998, Hupfeld et al., 2020). Moreover, our findings are consistent with the concept that transcortical inhibition is associated with cortical motoneuronal loss, since TMS changes are related to stronger MM. Our earlier studies investigating the silent period after cutaneous stimulation have indicated that delayed onset-latency is associated with clinical and TMS signs of UMN lesion (Castro et al., 2021, 2023b). In addition, in patients without clinical signs of UMN lesion, preserved transcallosal inhibition causes onset-latency shortening by ipsilateral cortical activation (Castro et al., 2021). These neurophysiological findings are consistent in associating dysfunction of transcallosal inhibition with UMN loss, in ALS.

Imaging and TMS studies have suggested that, in ALS, there is an early impairment of callosal pathways, in addition to the involvement of the primary motor cortex (Caiazzo et al., 2014, van den Bos et al., 2021). Recent studies observing clinical signs of MM have shown that functional deficits precede structural changes of the corpus callosum (Wittstock et al., 2020, Hübers et al., 2021a). The present work strengthens the possibility that MM may be a simple early marker of callosal dysfunction. Additionally, the increase in mirror activity in ALS patients precedes changes in corticospinal tract function, as assessed by TMS, possibly suggesting early UMN lesion.

7.3. Segmental motoneuron dysfunction

Segmental motoneuron dysfunction was investigated in a group of 15 ALS subjects, using different conditioning paradigms of the H reflex. All patients were in a high functional status (median ALSFRS-R – 44, maximum 48), with little involvement of LMN in the lower limbs (TA strength ≥ 4+ MRC, no significant difference in soleus M_{max} from controls).

Although it has been argued that H reflex studies should be performed during a sustained voluntary contraction of the target muscle (Knikou, 2008), we chose to do all our experiments at rest. It would be very difficult to maintain a stable and reproducible contraction in different subjects, and changes in motoneuron pool excitability brought about by differences in voluntary activation would impede an adequate interpretation of the findings.

Values from standard H reflex studies were similar between ALS patients and healthy controls, in particular the H_{max}/M_{max} ratio, in line with results reported in the literature (Raynor and Shefner, 1994, Simon et al., 2015). It has been suggested that this paradox could reflect a preferential loss of large, rapidly conducting axons in LMN of ALS patients (Simon et al., 2015). Our findings not only strengthen this explanation, but also suggest, given that even in patients with minimal affection of LMN the H_{max}/M_{max} ratio is normal, that the dynamics of the H reflex could be altered very early in the disease course.

Recurrent inhibition

Recurrent inhibition is a negative feedback mechanism, important in movement control, locally mediated by the activity of Renshaw cells. Changes in homonymous (Raynor and Shefner, 1994, Özyurt et al., 2020) and heteronymous (Sangari et al., 2022) recurrent inhibition have been reported in ALS. We also found a significant decrease in the strength of recurrent inhibition in ALS patients when compared to healthy controls, using the paired H reflex technique. The supramaximal stimulus (S2) would not, by itself generate an H reflex, due to the known collision phenomenon. However, the descending volley generated by the conditioning stimulus (S1), will collide with the ascending volley from S2, and leave those alpha motoneurons unimpeded to generate an H reflex. The conditioned H

response (H') could, at most, be of the same amplitude as the H response generated by S1 (H1). Given that S2 is a supramaximal stimulus that depolarizes all Ia afferents, one would expect that this should always be the case. Since the H' is, most of the time, of smaller amplitude than the unconditioned one, this reflects the activity of the activated Renshaw cells by S1, inhibiting the alpha motoneuron from firing.

There is some debate regarding the intensity of S1 that should be used in this paradigm (Mazzocchio and Rossi, 1996) We chose to use a fixed intensity that reliably evoked an H_{max}, for two reasons. First, there is a linear increase of recurrent inhibition with increasing conditioning reflex size (Hultborn et al., 1979), and as suggested by Mazzocchio and Rossi (1989), this level of intensity is probably when there are more Renshaw cells active, and thus more recurrent inhibition. Second, despite H' being maximal at lower intensities of S1 (Pierrot-Deseilligny and Bussel, 1975), it is generally accepted that motoneuron recruitment in the H reflex response follows the size principle (Buchthal and Schmalbruch, 1970, Simon et al., 2015), from which one can surmise that different motoneurons are recruited if different stimuli are employed.

In homonymous recurrent inhibition, post-spike after-hyperpolarization can have some influence on the amplitude of H' (Bussel and Pierrot-Deseilligny, 1977, Rossi and Mazzocchio, 1991). However, it has been demonstrated that the amplitude of H' decreases with the increase of H1, which can only be explained by the recurrent inhibition brought by the conditioning stimulus, and that changes in H' only depend on changes of H1 magnitude (Bussel and Pierrot-Deseilligny, 1977, Rossi and Mazzocchio, 1991, Pierrot-Deseilligny and Burke, 2012). It is also unlikely that group Ib inhibition could account for the results found, since this type of inhibition should have subsided at interstimulus intervals longer than 9 ms (Pierrot-Deseilligny and Burke, 2012).

We found a significant relationship between the amount of recurrent inhibition (H'_{RI}) and the degree of UMN involvement in the lower limbs. The amount of H'_{RI} was correlated (Figure 35) and highly predicted by the UMN LL score, suggesting that that these signs are linked with changes in recurrent inhibition. It has been shown that the activity of Renshaw cells can be depressed by activation of corticospinal fibers with a

single pulse of TMS, probably mediated through an oligosynaptic interneuronal chain (Mazzocchio et al., 1994).

Presynaptic inhibition of Ia terminals

Presynaptic inhibition of Ia terminals is mediated by a last order interneuron that is GABA-ergic and acts on Ia afferents through primary afferent depolarization (Rudomin and Schmidt, 1999, Pierrot-Deseilligny and Burke, 2012). In ALS, it has been suggested that presynaptic inhibition is reduced (Morin and Pierrot-Deseilligny, 1988, Howells et al., 2020). Our findings are concordant with this. In our group of patients, presynaptic inhibition of Ia terminals is significantly decreased when compared to controls (Figure 34). We used the protocol described by Mizuno et al. (1971) for assessing the D1 inhibition. It has been shown that this process is maximal at approximately 20 ms (Howells et al., 2020), and there is compelling evidence attributing this phenomenon to a presynaptic process (Iles, 1996, Aymard et al., 2000), and not to postsynaptic or recurrent inhibition (Pierrot-Deseilligny and Burke, 2012).

We found a very strong relationship between the decrease in presynaptic inhibition and involvement of the UMN. Similar to H'_{RI}, the amount of H'_{Pre} was highly correlated (Figure 35) and very strongly predicted by the UMN LL score, pointing to a decrease in presynaptic inhibition linked to an increase in the UMN signs.

Inhibition after cutaneous stimulation

It has been demonstrated that stimulating the sural nerve (a purely cutaneous nerve), leads to an ipsilateral inhibition of the soleus H reflex (Bathien and Hugon, 1964, Hugon, 1973, Delwaide et al., 1981). The spinal localization of this pathway is likely given that, at the intervals between the conditioning and test stimuli used, the cutaneous effect is likely spinal in origin (Burke et al., 1991). This has also been demonstrated in complete spinal cord lesions in humans (Logigian et al., 1999). Furthermore, Lourenco et al. (2007) suggested that stimulation of cutaneous afferents activated inhibitory spinal interneurons in human upper limb, although the exact pathway of this mechanism is not fully understood. However, an exteroceptive silent period in the soleus EMG activity at the same moment in time as the H reflex inhibition (Pierrot-Deseilligny et al., 1973), and a decrease in motor evoked potentials amplitudes have been reported (Manconi et al., 1998). In fact, strong transient

inhibition of alpha-motoneurons during active contraction is achieved after noxious cutaneous stimulation, which has been termed the cutaneous silent period (Kofler et al., 2019a). This reflex response is not modulated by simultaneous contralateral contraction (Castro et al., 2021), which is known to cause robust presynaptic inhibition of Ia afferents (Hortobágyi et al., 2003). Although presynaptic inhibition of Ia afferents by the cutaneous fiber stimulation cannot be completely ruled out (Delwaide et al., 1981), taking these considerations together, the localization of the inhibitory pathway after cutaneous stimulation is likely postsynaptic. In our group of ALS patients the inhibition of the H reflex after cutaneous stimulation is significantly less than in controls; indeed, it was almost non-existent (Figure 34). However, contrary to what has been demonstrated for the CutSP in ALS (Castro et al., 2021, 2023b), the decrease of H'_{Pos} is not correlated with the extent of UMN signs.

UMN influence on H reflex conditioning paradigms

The amount of UMN involvement seems to be linked with some of the spinal mechanisms tested in this work. This was observed for homonymous recurrent inhibition and for presynaptic inhibition of Ia terminals but it was not the case for inhibition after cutaneous stimulation. Regarding the latter finding, some considerations are relevant. In ALS It has been demonstrated that changes in sensory afferents are present, as shown by altered N9 potentials in somatosensory evoked potentials (Iglesias et al., 2015), while sensory-motor integration at the spinal level is also impaired (Sangari et al., 2016). These findings could explain the decrease in the cutaneous influence over the alpha motoneuron, and the lack of correlation with UMN signs. However, one should also note that in our results, the amount of inhibition after cutaneous stimulation in ALS patients was almost non-existent (median H'_{Pos} 0.0, IQR -2 – 3). From a statistical point of view, it would be inappropriate to mathematically link two variables when one of them is near zero. In that case, doubt arises regarding whether or not there is a true correlation, or perhaps we are just not able to demonstrate it. Whatever the reason, the lack of inhibition after cutaneous stimulation seems clearly to be an abnormality in ALS.

In sporadic ALS, widespread loss of neurons in the ventral horn has been described, with interneurons being affected to a similar extent and in parallel with motor neurons (Stephens et al., 2006). It is thus unclear whether changes in spinal

mechanisms in ALS/MND are due to direct damage of interneurons or to abnormal control of those interneurons by other neurons. There is evidence that different supraspinal pathways actively modulate Renshaw cells (Mazzocchio et al., 1994) and presynaptic inhibitory interneurons (Hultborn et al., 1987), so it is possible that the dysfunction of spinal mechanisms is due to a decrease in signals from supraspinal structures to the interneurons. Nevertheless, supraspinal drives seem to suppress both recurrent inhibition (Koehler et al., 1978) and presynaptic inhibition (Hultborn et al., 1987). A loss of these drives would not decrease these inhibitory pathways.

There is growing evidence that ALS may involve an interneuronopathy (Turner and Kiernan, 2012), which could also explain the loss of spinal inhibition of alpha motoneurons. Inhibitory interneurons in the spinal cord use GABA and glycine as their neurotransmitter (Jankowska, 1992, Rudomin and Schmidt, 1999). In the mouse spinal cord, over 80% of V1 interneurons are glycinergic (Alvarez et al., 2005). Recently, it has been proposed that spinal microcircuit imbalance brought about by the initial loss of fast fatigable motoneurons, and consequent compensatory excitation of alpha motoneurons by spinal premotor circuits, could even be one of the drivers of initial disease progression in ALS (Brownstone and Lancelin, 2018). In fact, fast fatigable motoneurons receive stronger inputs from the V1 inhibitory population than other motoneurons, and are affected in presymptomatic models of SOD1 mice, before motor neuron degeneration (Chang and Martin, 2009, 2011, Allodi et al., 2021). Cavarsan et al. (2023), have also recently shown that glycinergic interneurons are affected in the very early stages of disease, and that the ones most altered, where located more ventrally (putative location of Renshaw cells) and the ones in lamina IX (putative location of Ia interneurons). Interestingly, the postsynaptic inhibition after cutaneous stimulation is also mediated by glycinergic synapses (Curtis et al., 1967, Jankowska, 1992, Rudomin and Schmidt, 1999).

In ALS tendon reflexes are often brisk in muscles that are not weak, muscle tone is very often normal (Verschueren et al., 2021), and the extensor Babinski response, which is not a monosynaptic reflex, is frequently absent (Swash, 2012, Swash et al., 2020). These findings are often ascribed to the simultaneous degeneration of LMNs. If a defect in spinal inhibition of alpha motoneurons is a common feature of ALS, we would expect to see increased tendon reflexes in all

patients, regardless of whether or not they have other UMN signs. If hyperreflexia results from an interneuronopathy, affecting spinal inhibitory interneurons, then this negates the notion that hyperactive tendon reflexes are a specific sign of corticospinal tract damage. Indeed, our group of patients had only mild LMN involvement in the lower limbs, as noted by normal M_{max} amplitudes and normal or near normal strength in leg muscles. As for UMN signs, only 2 had a positive Babinski sign, and 1 had significant spasticity, while 12 (80%) had hyperreflexia.

Considering all these factors, we suggest that hyperreflexia in ALS could be an abnormality that originates at the spinal pre-motoneuronal level, rather than being primarily a corticospinal abnormality.

7.4. Limitations

Regarding the studies included in this dissertation there are a number of limitations that need to be pointed out.

In study I, we only assessed the CutSP in one muscle (ADM) in each patient. However, the findings reported in this work were subsequently confirmed in study II, and also in study V, reinforcing the notion that changes in CutSP are present in ALS.

In study II, the number of patients included (24) was not particularly large, although with some clinical variability, which could have had some influence on the results found. Some concern was raised regarding the use of the sural nerve, an S1 sensory nerve, to record the motor response from a muscle predominantly innervated by the L5 myotome. However, this does not seem particularly problematic given that the afferent volley reaching one spinal segment descends and ascends through several spinal cord segments (Logigian et al., 1999).

In study III, the number of muscles analyzed, particularly TA, was not very large. This hinders the definition of normal values per age group, which can be somewhat problematic in a neurophysiological measure that is influenced by age. The use of the normative values proposed in this work should only be applied to subjects within the age range of healthy controls analyzed here. Although we did not use force measurements of muscle contractions, care was taken to ensure that subjects performed maximum contractions. Another limitation, inherent to the study design, is that the algorithm was constructed to analyze EMG signal from a simple isometric full force contraction. Despite that, we believe that with some simple adjustments, it can be used to measure MA in more advanced kinematic paradigms for studying motor overflow.

In study IV, the main limitation is that we did not include patients without clinical UMN signs, particularly patients with PMA. Given that transcallosal dysfunction is present in ALS (*vide* Mirror movements discussion section) possibly even in PMA (Castro et al., 2021), it would be of interest to see if these patients had similar results.

In study V, the main limitation is the somewhat low number of subjects, patients and controls, included. However, power calculations performed using the data reported on recurrent inhibition (Raynor and Shefner, 1994) and on presynaptic

inhibition (Howells et al., 2020), showed that the total number of subjects to be included should vary between 20 and 28 (effect size 1.21 to 0.97; power 80%; α = 0.05).

8. Conclusions

With the work developed in the context of this dissertation, it was shown that the function of some inhibitory circuits, depending on inhibitory interneurons, are altered in ALS patients, and that these changes are closely linked to UMN dysfunction. Mathematical algorithms were developed for precise, objective, and reproducible measurements of different neurophysiological techniques, such as the cutaneous silent period or the quantification of mirror activity.

Regarding the clinical implications of the findings here reported and the literature research done over the course of this thesis, some further reflections are merited.

ALS is a neurodegenerative, devastating, and usually fatal disease, for which no effective treatment currently exists. Since the initial descriptions by Charcot in the 19th century, a large amount of knowledge of the disease has been gained. Despite several pathophysiological processes involved in ALS are currently known, there is no agreement as to the site of origin of the characteristic neurodegeneration of this disease. Several hypotheses have been put forward (Figure 36), with some authors suggesting a “dying-forward” hypothesis, others suggest a “dying-back" hypothesis, and some investigators propose that UMN and LMN occur independently (Kiernan et al., 2011). There can be, however, a conciliatory hypothesis that has also been suggested: a corticofugal synaptopathy, or “dying-outward” hypothesis (Baker, 2014).

A number of features are central in ALS pathophysiology. There are different presentations of the disease, ranging from affection of UMN and LMN in the classical form of the disease, dysfunction only of the corticospinal tract neurons in PLS, to degeneration mostly restricted to anterior horn cells in PMA. Independent of the disease presentation, degenerative changes are present mainly in anterior horn cells and brainstem motor neurons that receive monosynaptic connections from the motor cortex, and in the corticospinal tract neurons within the primary motor cortex. ALS progression is typically contiguously between regions be it in the cortex, brainstem or spinal cord (Gromicho et al., 2020), resembling a prion-like disease (Kanouchi et al., 2012). Another striking fact is that sporadic ALS exists only in the human species affecting parts of the nervous system that are more recent from an evolutionary

standpoint. This is further strengthened by the notion that only nonhuman primates display certain features of the disease seen in humans (Uchida et al., 2012). The corticomotoneuronal synapse sets primates apart from other mammals. What sets apart humans from nonhuman primates is both the quantity of corticomotoneuronal synapses and the length of axons in the corticospinal tract (Lemon and Griffiths, 2005, Lemon, 2008). Mutations in mitochondrial DNA have been associated with neurodegenerative diseases in general (Cha et al., 2015) and ALS in particular (Jankovic et al., 2021), with a focus on aberrant synaptic mitochondria (Candelise et al., 2022, Gelon et al., 2022, Zhao et al., 2022). Hence, the corticomotoneuronal synapse serves not only as a critical connection between the corticospinal tract and anterior horn cells but, due to its susceptibility, also may act as an efficient breeding ground for neurodegeneration.

Figure 36 - The "dying-forward" and "dying-back" hypotheses in ALS

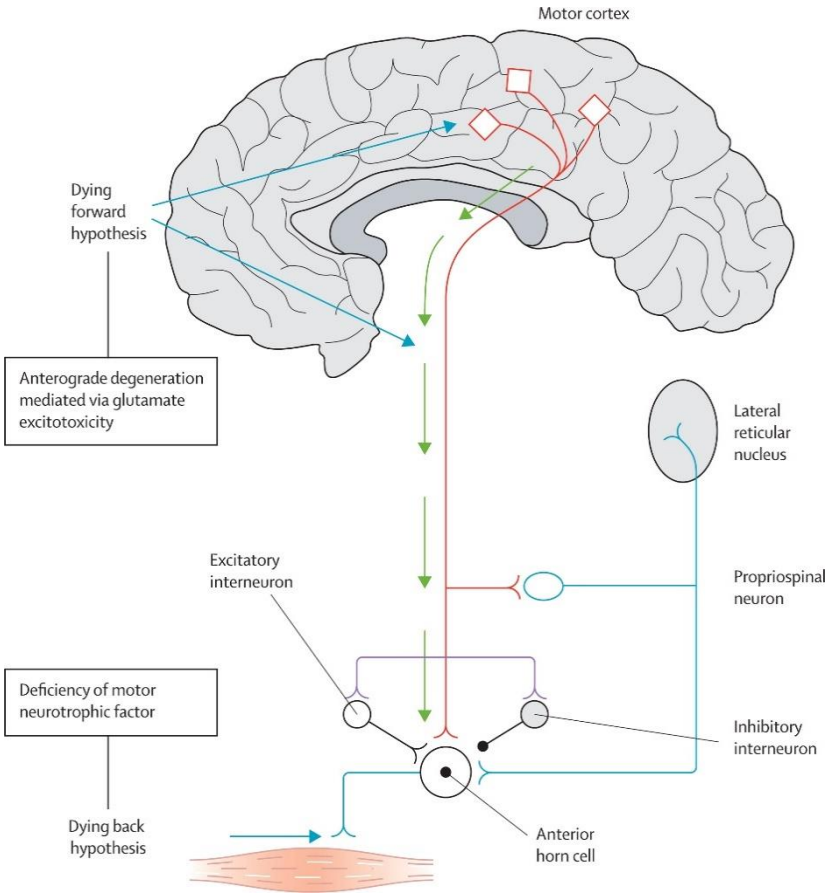

Note: Adapted from Kiernan et al. (2011), with permission.

Recently, it has been suggested that ALS-related motor deficits are best understood as a failure of complex and intricate motor task performance, involving management of synergistic motor activity, rather than reflecting weakness of individual muscles (Eisen and Lemon, 2021). In fact, as far back as the beginning of the 20th century, the role of inhibition in movement control has been recognized. Already in 1932, in his Nobel lecture (Inhibition as a coordinative factor), Sir Charles Sherrington deeply emphasized the importance of central inhibition in the control of voluntary movement (Sherrington, 1932).

"The role of inhibition in the working of the central nervous system has proved to be more and more extensive and more and more fundamental as experiment has advanced in examining it. Reflex inhibition can no longer be regarded merely as a factor specially developed for dealing with the antagonism of opponent muscles acting at various hinge-joints. Its role as a coordinative factor comprises that, and goes beyond that. In the working of the central nervous machinery inhibition seems as ubiquitous and as frequent as is excitation itself."

However, the role of inhibitory control of motoneurons in ALS has been largely overlooked, until very recently.

In the last 20 years a significant amount of evidence has been gained regarding inhibitory interneurons, which not only regulate corticospinal motoneurons in the cortex, but also are instrumental mediators of the communication between upper and lower motoneurons. In the animal model, there is evidence that interneuron degeneration is an early feature, even preceding symptoms and motoneuron dysfunction (Chang and Martin, 2009, Nieto-Gonzalez et al., 2011, McGown et al., 2013, Salamatina et al., 2020, Cavarsan et al., 2023). In humans, degeneration of cells surrounding motoneurons is also a key factor (Crabé et al., 2020).

Neurophysiological studies have similarly demonstrated early involvement of inhibitory cortical circuits in ALS. We have shown that mirror activity is particularly increased in ALS patients, suggesting a significant compromise of transcallosal inhibitory pathways. Additionally, the normalization of the cutaneous silent period with the activation of the motor cortex of the ipsilateral test hand also points to the same conclusion. These changes provide further evidence that hyperexcitability of cortical

motoneurons are probably due to dysfunction of inhibitory mechanisms of control instead of intrinsic changes of the motoneuron itself.

Studies showing dysfunction of spinal segmental interneurons have also been published, albeit to a much lesser extent. The cutaneous silent period is an inhibitory spinal reflex, integrating a complex pre-attentional protective reflex process. We have shown that this mechanism is altered in ALS and that the magnitude of change is linked to the amount of UMN dysfunction. Although still a matter of debate, we have likewise provided convincing evidence that this mechanism is probably postsynaptic in nature, i.e., its inhibitory influence is exerted directly on the alpha motoneuron. Using modulation paradigms of the H reflex, we have demonstrated that function of different interneurons, from Renshaw cells to primary afferent depolarization interneurons, are altered, compromising spinal systems of motor control that act directly on the alpha motoneuron by inhibiting its excitation. These changes involve recurrent, presynaptic, and postsynaptic mechanisms, leaving the corticomotoneuronal synapse particularly susceptible to hyperexcitation.

The findings of this work strengthen the notion that an interneuronopathy (Turner and Kiernan, 2012) can be deemed a major feature of ALS, and can possibly be one of the first events and drivers of motoneuron degeneration in this devastating disease. In the end, these discoveries might have therapeutic importance. Developing approaches to safeguard the integrity of inhibitory circuits, while also counteracting excitatory circuits, both at the cortical and at the spinal levels, could unveil fresh avenues for therapeutic intervention in ALS. Neurophysiological measures that can accurately and objectively disclose changes in these circuits are thus of paramount importance to identify and monitor both progression and, eventually, treatment efficacy.

9. Future perspectives

One of the most frequent conclusions when doing scientific studies is the necessity for further research. I value this tradition deeply, and, considering the discoveries within the studies presented in this dissertation, it is evident that additional research is, indeed, imperative.

As thoroughly detailed in this thesis, inhibitory mechanisms are significantly altered in ALS. With this in mind, there are several avenues of investigation, particularly with regard to pharmacological modulations. It is expected that administration of GABA or glycine agonists improve at least some of the changes in inhibitory mechanisms, be them spinal or cortical. Additionally, drugs that are aimed at improving UMN dysfunction, such as antispastic medication also could shed some light to the specific physiology of the pathways here explored.

In more detail, changes in CutSP have been reported after the use of a selective serotonin reuptake inhibitor, escitalopram (Pujia et al., 2014), implying the monoaminergic system in the CutSP physiology. Given that a compromise of serotonergic pathways in ALS has been suggested (Vermeiren et al., 2018), it would be of interest to explore the effects of this drug in ALS patients. Baclofen, a $GABA_B$ agonist, is commonly used to treat spasticity. It has been shown that Baclofen failed to induce changes in the CutSP of incomplete spinal cord injury patients (Stetkarova and Kofler, 2013). However, in diseases mediated by GABAergic dysfunction, such as stiff-person, the CutSP is clearly altered (Bocek et al., 2016). It would also be of interest to study the influence of baclofen in the CutSP in ALS patients.

As for the H reflex, apart from the obvious interest in pharmacological studies as detailed for the CutSP, an interesting approach would be to assess the effect of TMS modulation of segmental spinal mechanisms in ALS. Modulation of the H reflex in humans after cortical stimulation is a well-known phenomenon (Costa et al., 2011, Andrews et al., 2020). Additionally, some of the mechanisms explored in our work, are also modulated by cortical stimulation (Valls-Sole et al., 1994, Andrews et al., 2015, Bringman et al., 2022). These approaches would surely help to shed some light on the interplay between supraspinal influences and spinal inhibitory mechanisms in the specific context of ALS.

Finally, given the possibility that early stages ALS may in part reflect an inability to perform complex motor tasks (Eisen and Lemon, 2021), it would be valuable to investigate if performance of fine motor skills is, in fact, impaired in ALS. Correlating these findings with measures of inhibitory interneuron function could provide insightful and valuable clues to ALS pathophysiology.

10. References

1. , Andersen PM, Abrahams S, Borasio GD, de Carvalho M, Chio A, et al. EFNS guidelines on the clinical management of amyotrophic lateral sclerosis (MALS) revised report of an EFNS task force. Eur J Neurol 2012;19(3):360-75.

2. Aboitiz F, Scheibel AB, Fisher RS, Zaidel E. Individual differences in brain asymmetries and fiber composition in the human corpus callosum. Brain Res 1992;598(1-2):154-61.

3. Abrahams S, Newton J, Niven E, Foley J, Bak TH. Screening for cognition and behaviour changes in ALS. Amyotroph Lateral Scler Frontotemporal Degener 2014;15(1-2):9-14.

4. Al-Chalabi A, Calvo A, Chio A, Colville S, Ellis CM, Hardiman O, et al. Analysis of amyotrophic lateral sclerosis as a multistep process: a population-based modelling study. Lancet Neurol 2014;13(11):1108-13.

5. Allodi I, Montañana-Rosell R, Selvan R, Löw P, Kiehn O. Locomotor deficits in a mouse model of ALS are paralleled by loss of V1-interneuron connections onto fast motor neurons. Nat Commun 2021;12(1):3251.

6. Alvarez FJ, Jonas PC, Sapir T, Hartley R, Berrocal MC, Geiman EJ, et al. Postnatal phenotype and localization of spinal cord V1 derived interneurons. J Comp Neurol 2005;493(2):177-92.

7. Alves I, Gromicho M, Oliveira Santos M, Pinto S, Pronto-Laborinho A, Swash M, et al. Demographic changes in a large motor neuron disease cohort in Portugal: a 27 year experience. Amyotroph Lateral Scler Frontotemporal Degener 2023:1-11.

8. Amado DA, Davidson BL. Gene therapy for ALS: A review. Mol Ther 2021;29(12):3345-58.

9. Amassian VE, Cracco RQ. Human cerebral cortical responses to contralateral transcranial stimulation. Neurosurgery 1987;20(1):148-55.

10. Amassian VE, Stewart M, Quirk GJ, Rosenthal JL. Physiological basis of motor effects of a transient stimulus to cerebral cortex. Neurosurgery 1987;20(1):74-93.

11. Andrews JC, Sankar T, Stein RB, Roy FD. Characterizing the effect of low intensity transcranial magnetic stimulation on the soleus H-reflex at rest. Exp Brain Res 2020;238(12):2725-31.

12. Andrews JC, Stein RB, Roy FD. Reduced postactivation depression of soleus H reflex and root evoked potential after transcranial magnetic stimulation. J Neurophysiol 2015;114(1):485-92.

13. Aran F. Recherches sur une maladie non encore décrite du système musculaire (atrophie musculaire progressive). Arch Gen de Méd 1850;24(5):172-214.

14. Armatas CA, Summers JJ, Bradshaw JL. Mirror movements in normal adult subjects. J Clin Exp Neuropsychol 1994;16(3):405-13.

15. Armatas CA, Summers JJ, Bradshaw JL. Handedness and performance variability as factors influencing mirror movement occurrence. J Clin Exp Neuropsychol 1996;18(6):823-35.

16. Armon C. Motor Neuron Disease. In: Gorelick P, Alter M, editors. Handbook of neuroepidemiology. New York: Marcel Dekker; 1994. p. 407-54.

17. Armon C. An evidence-based medicine approach to the evaluation of the role of exogenous risk factors in sporadic amyotrophic lateral sclerosis. Neuroepidemiology 2003;22(4):217-28.

18. Aymard C, Katz R, Lafitte C, Lo E, Penicaud A, Pradat-Diehl P, et al. Presynaptic inhibition and homosynaptic depression: a comparison between lower and upper limbs in normal human subjects and patients with hemiplegia. Brain 2000;123 (Pt 8)(8):1688-702.

19. Bacman SR, Bradley WG, Moraes CT. Mitochondrial involvement in amyotrophic lateral sclerosis: trigger or target? Mol Neurobiol 2006;33(2):113-31.

20. Bae JS, Simon NG, Menon P, Vucic S, Kiernan MC. The puzzling case of hyperexcitability in amyotrophic lateral sclerosis. J Clin Neurol 2013;9(2):65-74.

21. Baker MR. ALS—dying forward, backward or outward? Nature Reviews Neurology 2014;10(11):660-
.

22. Barker AT, Jalinous R, Freeston IL. Non-invasive magnetic stimulation of human motor cortex. Lancet 1985;1(8437):1106-7.

23. Bathien N, Hugon M. Étude, chez l'homme, de la dépression d'un réflexe monosynaptique par stimulation d'un nerf cutańe. J Physiol (Paris) 1964;56(3):285-6.

24. Bendotti C, Carri MT. Lessons from models of SOD1-linked familial ALS. Trends Mol Med 2004;10(8):393-400.

25. Benjamini Y, Hochberg Y. Controlling the False Discovery Rate: A Practical and Powerful Approach to Multiple Testing. J R Stat Soc, B: Stat Methodol 2018;57(1):289-300.

26. Bensimon G, Doble A. The tolerability of riluzole in the treatment of patients with amyotrophic lateral sclerosis. Expert Opin Drug Saf 2004;3(6):525-34.

27. Bensimon G, Lacomblez L, Meininger V. A controlled trial of riluzole in amyotrophic lateral sclerosis. ALS/Riluzole Study Group. N Engl J Med 1994;330(9):585-91.

28. Berardelli A, Rona S, Inghilleri M, Manfredi M. Cortical inhibition in Parkinson's disease. A study with paired magnetic stimulation. Brain 1996;119 (Pt 1):71-7.

29. Bernard-Marissal N, Moumen A, Sunyach C, Pellegrino C, Dudley K, Henderson CE, et al. Reduced calreticulin levels link endoplasmic reticulum stress and Fas-triggered cell death in motoneurons vulnerable to ALS. J Neurosci 2012;32(14):4901-12.

30. Bland J, Altman D. Statistical Methods for Assessing Agreement between Two Methods of Clinical Measurement. The Lancet 1986;327(8476):307-10.

31. Bloom JS, Hynd GW. The role of the corpus callosum in interhemispheric transfer of information: excitation or inhibition? Neuropsychol Rev 2005;15(2):59-71.

32. Bocek V, Cvickova B, Peisker T, Stetkarova I. ID 140 – Left-side asymmetry in cortical and spinal inhibitory circuits in stiff-person syndrome: A case report. Clinical Neurophysiology 2016;127(3):e62.

33. Bodwell JA, Mahurin RK, Waddle S, Price R, Cramer SC. Age and features of movement influence motor overflow. J Am Geriatr Soc 2003;51(12):1735-9.

34. Boillee S, Vande Velde C, Cleveland DW. ALS: a disease of motor neurons and their nonneuronal neighbors. Neuron 2006;52(1):39-59.

35. Borchelt DR, Lee MK, Slunt HS, Guarnieri M, Xu ZS, Wong PC, et al. Superoxide dismutase 1 with mutations linked to familial amyotrophic lateral sclerosis possesses significant activity. Proc Natl Acad Sci U S A 1994;91(17):8292-6.

36. Boroojerdi B, Battaglia F, Muellbacher W, Cohen LG. Mechanisms influencing stimulus-response properties of the human corticospinal system. Clin Neurophysiol 2001;112(5):931-7.

37. Bourke SC, Tomlinson M, Williams TL, Bullock RE, Shaw PJ, Gibson GJ. Effects of non-invasive ventilation on survival and quality of life in patients with amyotrophic lateral sclerosis: a randomised controlled trial. Lancet Neurol 2006;5(2):140-7.

38. Box GEP, Tidwell PW. Transformation of the Independent Variables. Technometrics 1962;4(4):531-50.

39. Bradley WG, Borenstein AR, Nelson LM, Codd GA, Rosen BH, Stommel EW, et al. Is exposure to cyanobacteria an environmental risk factor for amyotrophic lateral sclerosis and other neurodegenerative diseases? Amyotroph Lateral Scler Frontotemporal Degener 2013;14(5-6):325-33.

40. Brasil AA, de Carvalho MDC, Gerhardt E, Queiroz DD, Pereira MD, Outeiro TF, et al. Characterization of the activity, aggregation, and toxicity of heterodimers of WT and ALS-associated mutant Sod1. Proc Natl Acad Sci U S A 2019;116(51):25991-6000.

41. Bringman CL, Shields RK, DeJong SL. Corticospinal modulation of vibration-induced H-reflex depression. Exp Brain Res 2022;240(3):803-12.

42. Brodal A. Neurological Anatomy in Relation to Clinical Medicine. Oxford: Oxford University Press, 1981.

43. Bromberg MB. MUNIX and MUNE in ALS. Clin Neurophysiol 2013;124(3):433-4.

44. Brooks BR. El Escorial World Federation of Neurology criteria for the diagnosis of amyotrophic lateral sclerosis. Subcommittee on Motor Neuron Diseases/Amyotrophic Lateral Sclerosis of the World Federation of Neurology Research Group on Neuromuscular Diseases and the El Escorial "Clinical limits of amyotrophic lateral sclerosis" workshop contributors. J Neurol Sci 1994;124 Suppl:96-107.

45. Brooks BR, Miller RG, Swash M, Munsat TL, World Federation of Neurology Research Group on Motor Neuron D. El Escorial revisited: revised criteria for the diagnosis of amyotrophic lateral sclerosis. Amyotroph Lateral Scler Other Motor Neuron Disord 2000;1(5):293-9.

46. Brouwer B, Ashby P. Corticospinal projections to upper and lower limb spinal motoneurons in man. Electroencephalography and Clinical Neurophysiology 1990;76(6):509-19.

47. Brownstone RM, Lancelin C. Escape from homeostasis: spinal microcircuits and progression of amyotrophic lateral sclerosis. J Neurophysiol 2018;119(5):1782-94.

48. Buchthal F, Schmalbruch H. Contraction times of twitches evoked by H-reflexes. Acta Physiol Scand 1970;80(3):378-82.

49. Burke D. Clinical uses of H reflexes of upper and lower limb muscles. Clin Neurophysiol Pract 2016;1:9-17.

50. Burke D, Dickson HG, Skuse NF. Task-dependent changes in the responses to low-threshold cutaneous afferent volleys in the human lower limb. J Physiol 1991;432:445-58.

51. Burke D, Hallett M, Fuhr P, Pierrot-Deseilligny E. H reflexes from the tibial and median nerves. The International Federation of Clinical Neurophysiology. Electroencephalogr Clin Neurophysiol Suppl 1999;52:259-62.

52. Bussel B, Pierrot-Deseilligny E. Inhibition of human motoneurons, probably of Renshaw origin, elicited by an orthodromic motor discharge. J Physiol 1977;269(2):319-39.

53. Caiazzo G, Corbo D, Trojsi F, Piccirillo G, Cirillo M, Monsurro MR, et al. Distributed corpus callosum involvement in amyotrophic lateral sclerosis: a deterministic tractography study using q-ball imaging. J Neurol 2014;261(1):27-36.

54. Candelise N, Salvatori I, Scaricamazza S, Nesci V, Zenuni H, Ferri A, et al. Mechanistic Insights of Mitochondrial Dysfunction in Amyotrophic Lateral Sclerosis: An Update on a Lasting Relationship. Metabolites 2022;12(3).

55. Cantello R, Gianelli M, Civardi C, Mutani R. Magnetic brain stimulation: the silent period after the motor evoked potential. Neurology 1992;42(10):1951-9.

56. Caramia MD, Cicinelli P, Paradiso C, Mariorenzi R, Zarola F, Bernardi G, et al. "Excitability" changes of muscular responses to magnetic brain stimulation in patients with central motor disorders. Electroencephalogr Clin Neurophysiol 1991;81(4):243-50.

57. Carson RG. Neural pathways mediating bilateral interactions between the upper limbs. Brain Res Brain Res Rev 2005;49(3):641-62.

58. Castro J, de Carvalho M. P69-S Cutaneous silent period behavior in different motor neuron diseases phenotypes. Clin Neurophysiol 2019;130(7):e112-e3.

59. Castro J, Pedrosa T, de Castro I, Swash M, de Carvalho M. Mirror movements - A simple algorithm for mirror activity signal processing and normative values. Neurosci Lett 2023a;803:137186.

60. Castro J, Swash M, de Carvalho M. The cutaneous silent period in motor neuron disease. Clin Neurophysiol 2021;132(2):660-5.

61. Castro J, Swash M, de Carvalho M. The cutaneous silent period as a measure of upper motor neuron dysfunction in amyotrophic lateral sclerosis. Neurophysiol Clin 2023b;53(4):102843.

62. Cavarsan CF, Steele PR, Genry LT, Reedich EJ, McCane LM, LaPre KJ, et al. Inhibitory interneurons show early dysfunction in a SOD1 mouse model of amyotrophic lateral sclerosis. J Physiol 2023;601(3):647-67.

63. Cedarbaum JM, Stambler N, Malta E, Fuller C, Hilt D, Thurmond B, et al. The ALSFRS-R: a revised ALS functional rating scale that incorporates assessments of respiratory function. BDNF ALS Study Group (Phase III). J Neurol Sci 1999;169(1-2):13-21.

64. Cengiz B, Kuruoğlu R. A new parameter to discriminate amyotrophic lateral sclerosis patients from healthy participants by motor cortical excitability changes. Muscle Nerve 2020;61(3):354-62.

65. Cengiz B, Mercan M, Kuruoglu R. Spinal excitability changes do not influence the mechanisms of split-hand syndrome in amyotrophic lateral sclerosis. Muscle Nerve 2018;58(4):503-8.

66. Cernacek J. Contralateral motor irradiation--cerebral dominance. Its changes in hemiparesis. Arch Neurol 1961;4(2):165-72.

67. Cha MY, Kim DK, Mook-Jung I. The role of mitochondrial DNA mutation on neurodegenerative diseases. Exp Mol Med 2015;47(3):e150.

68. Chang Q, Martin LJ. Glycinergic innervation of motoneurons is deficient in amyotrophic lateral sclerosis mice: a quantitative confocal analysis. Am J Pathol 2009;174(2):574-85.

69. Chang Q, Martin LJ. Glycine receptor channels in spinal motoneurons are abnormal in a transgenic mouse model of amyotrophic lateral sclerosis. J Neurosci 2011;31(8):2815-27.

70. Charcot J-M. Sclerose laterale amyotrophique. Oeuvres Completes. Bureaux du Progres Medical 1874;2:249-66.

71. Chio A, Logroscino G, Hardiman O, Swingler R, Mitchell D, Beghi E, et al. Prognostic factors in ALS: A critical review. Amyotroph Lateral Scler 2009;10(5-6):310-23.

72. Chio A, Logroscino G, Traynor BJ, Collins J, Simeone JC, Goldstein LA, et al. Global epidemiology of amyotrophic lateral sclerosis: a systematic review of the published literature. Neuroepidemiology 2013;41(2):118-30.

73. Cincotta M, Giovannelli F, Borgheresi A, Balestrieri F, Vanni P, Ragazzoni A, et al. Surface electromyography shows increased mirroring in Parkinson's disease patients without overt mirror movements. Mov Disord 2006;21(9):1461-5.

74. Cincotta M, Ziemann U. Neurophysiology of unimanual motor control and mirror movements. Clin Neurophysiol 2008;119(4):744-62.

75. Civardi C, Collini A, Mazzini L, Monaco F, Geda C. Single-pulse transcranial magnetic stimulation in amyotrophic lateral sclerosis. 2020;61(3):330-7.

76. Claus D, Weis M, Jahnke U, Plewe A, Brunhölzl C. Corticospinal conduction studied with magnetic double stimulation in the intact human. J Neurol Sci 1992;111(2):180-8.

77. Coan G, Mitchell CS. An Assessment of Possible Neuropathology and Clinical Relationships in 46 Sporadic Amyotrophic Lateral Sclerosis Patient Autopsies. Neurodegener Dis 2015;15(5):301-12.

78. Cohen HJ, Taft LT, Mahadeviah MS, Birch HG. Developmental changes in overflow in normal and aberrantly functioning children. J Pediatr 1967;71(1):39-47.

79. Compta Y, Valls-Solé J, Valldeoriola F, Kumru H, Rumià J. The silent period of the thenar muscles to contralateral and ipsilateral deep brain stimulation. Clin Neurophysiol 2006;117(11):2512-20.

80. Corcia P, Bede P, Pradat PF, Couratier P, Vucic S, de Carvalho M. Split-hand and split-limb phenomena in amyotrophic lateral sclerosis: pathophysiology, electrophysiology and clinical manifestations. J Neurol Neurosurg Psychiatry 2021a;92(10):1126-30.

81. Corcia P, Beltran S, Bakkouche SE, Couratier P. Therapeutic news in ALS. Rev Neurol (Paris) 2021b;177(5):544-9.

82. Corcia P, Lunetta C, Couratier P, Vourc'h P, Gromicho M, Desnuelle C, et al. Familial clustering of primary lateral sclerosis and amyotrophic lateral sclerosis: Supplementary evidence for a continuum. Eur J Neurol 2021c;28(8):2780-3.

83. Costa J, Guzmán J, Valldeoriola F, Rumià J, Tolosa E, Casanova-Molla J, et al. Modulation of the soleus H reflex by electrical subcortical stimuli in humans. Exp Brain Res 2011;212(3):439-48.

84. Costa J, Swash M, de Carvalho M. Awaji criteria for the diagnosis of amyotrophic lateral sclerosis:a systematic review. Arch Neurol 2012;69(11):1410-6.

85. Crabé R, Aimond F, Gosset P, Scamps F, Raoul C. How Degeneration of Cells Surrounding Motoneurons Contributes to Amyotrophic Lateral Sclerosis. Cells 2020;9(12).

86. Cracco RQ, Amassian VE, Maccabee PJ, Cracco JB. Comparison of human transcallosal responses evoked by magnetic coil and electrical stimulation. Electroencephalogr Clin Neurophysiol 1989;74(6):417-24.

87. Crone C, Hultborn H, Mazieres L, Morin C, Nielsen J, Pierrot-Deseilligny E. Sensitivity of monosynaptic test reflexes to facilitation and inhibition as a function of the test reflex size: a study in man and the cat. Exp Brain Res 1990;81:35-45.

88. Curtis DR, Hösli L, Johnston GA. Inhibition of spinal neurons by glycine. Nature 1967;215(5109):1502-3.

89. Daskalakis ZJ, Christensen BK, Fitzgerald PB, Roshan L, Chen R. The mechanisms of interhemispheric inhibition in the human motor cortex. J Physiol 2002;543(Pt 1):317-26.

90. Davidson T, Tremblay F. Age and hemispheric differences in transcallosal inhibition between motor cortices: an ispsilateral silent period study. BMC Neurosci 2013;14:62.

91. de Carvalho M, Dengler R, Eisen A, England JD, Kaji R, Kimura J, et al. Electrodiagnostic criteria for diagnosis of ALS. Clin Neurophysiol 2008;119(3):497-503.

92. de Carvalho M, Kiernan MC, Pullman SL, Rezania K, Turner MR, Simmons Z. Neurophysiological features of primary lateral sclerosis. Amyotroph Lateral Scler Frontotemporal Degener 2020;21(sup1):11-7.

93. de Carvalho M, Scotto M, Swash M. Clinical patterns in progressive muscular atrophy (PMA): a prospective study. Amyotroph Lateral Scler 2007;8(5):296-9.

94. de Carvalho M, Swash M. Conventional neurophysiology in amyotrophic lateral sclerosis. In: Brown R, Swash M, Pasinelli P, editors. Amyotrophic Lateral Sclerosis. 2nd ed. London: Martin Dunitz; 2006.

95. de Carvalho M, Swash M. Fasciculation potentials and earliest changes in motor unit physiology in ALS. J Neurol Neurosurg Psychiatry 2013;84(9):963-8.

96. de Carvalho M, Swash M. Lower motor neuron dysfunction in ALS. Clin Neurophysiol 2016;127(7):2670-81.

97. de Carvalho M, Swash M. Transcranial magnetic stimulation to monitor disease progression in ALS: a review. Amyotroph Lateral Scler Frontotemporal Degener 2023;24(5-6):362-8.

98. de Carvalho M, Turkman A, Swash M. Motor responses evoked by transcranial magnetic stimulation and peripheral nerve stimulation in the ulnar innervation in amyotrophic lateral sclerosis: the effect of upper and lower motor neuron lesion. J Neurol Sci 2003;210(1-2):83-90.

99. de Carvalho M, Turkman A, Swash M. Motor unit firing in amyotrophic lateral sclerosis and other upper and lower motor neurone disorders. Clin Neurophysiol 2012;123(11):2312-8.

100. DeJesus-Hernandez M, Mackenzie IR, Boeve BF, Boxer AL, Baker M, Rutherford NJ, et al. Expanded GGGGCC hexanucleotide repeat in noncoding region of C9ORF72 causes chromosome 9p-linked FTD and ALS. Neuron 2011;72(2):245-56.

101. Deletis V, Sala F. Intraoperative neurophysiological monitoring of the spinal cord during spinal cord and spine surgery: a review focus on the corticospinal tracts. Clin Neurophysiol 2008;119(2):248-64.

102. Delwaide PJ, Crenna P, Fleron MH. Cutaneous nerve stimulation and motoneuronal excitability: I, soleus and tibialis anterior excitability after ipsilateral and contralateral sural nerve stimulation. J Neurol Neurosurg Psychiatry 1981;44(8):699-707.

103. Devanne H, Lavoie BA, Capaday C. Input-output properties and gain changes in the human corticospinal pathway. Exp Brain Res 1997;114(2):329-38.

104. Dharmadasa T, Matamala JM, Howells J, Vucic S, Kiernan MC. Early focality and spread of cortical dysfunction in amyotrophic lateral sclerosis: A regional study across the motor cortices. Clin Neurophysiol 2020;131(4):958-66.

105. Di Lazzaro V, Oliviero A, Meglio M, Cioni B, Tamburrini G, Tonali P, et al. Direct demonstration of the effect of lorazepam on the excitability of the human motor cortex. Clin Neurophysiol 2000;111(5):794-9.

106. Di Lazzaro V, Oliviero A, Pilato F, Saturno E, Dileone M, Mazzone P, et al. The physiological basis of transcranial motor cortex stimulation in conscious humans. Clinical Neurophysiology 2004a;115(2):255-66.

107. Di Lazzaro V, Oliviero A, Pilato F, Saturno E, Dileone M, Meglio M, et al. Direct recording of the output of the motor cortex produced by transcranial magnetic stimulation in a patient with cerebral cortex atrophy. Clinical Neurophysiology 2004b;115(1):112-5.

108. Di Lazzaro V, Oliviero A, Profice P, Insola A, Mazzone P, Tonali P, et al. Direct demonstration of interhemispheric inhibition of the human motor cortex produced by transcranial magnetic stimulation. Exp Brain Res 1999;124(4):520-4.

109. Di Lazzaro V, Oliviero A, Profice P, Pennisi MA, Pilato F, Zito G, et al. Ketamine increases human motor cortex excitability to transcranial magnetic stimulation. J Physiol 2003;547(Pt 2):485-96.

110. Di Lazzaro V, Restuccia D, Oliviero A, Profice P, Ferrara L, Insola A, et al. Magnetic transcranial stimulation at intensities below active motor threshold activates intracortical inhibitory circuits. Exp Brain Res 1998;119(2):265-8.

111. Dinneen LC, Blakesley BC. A Generator for the Sampling Distribution of the Mann-Whitney U Statistic. J R Stat Soc Ser C Appl Stat 1973;22(2):269-73.

112. Distad BJ, Meekins GD, Liou LL, Weiss MD, Carter GT, Miller RG. Drug therapy in amyotrophic lateral sclerosis. Phys Med Rehabil Clin N Am 2008;19(3):633-51, xi-xii.

113. Eccles JC, Fatt P, Koketsu K. Cholinergic and inhibitory synapses in a pathway from motor-axon collaterals to motoneurones. J Physiol 1954;126(3):524-62.

114. Eccles JC, Schmidt RF, Willis WD. Depolarization of the Central Terminals of Cutaneous Afferent Fibers. J Neurophysiol 1963;26(4):646-61.

115. Eisen A. Chapter 1 Historical aspects of motor neuron diseases. In: Eisen AA, Shaw PJ, editors. Handb Clin Neurol. 82: Elsevier; 2007. p. 1-11.

116. Eisen A, Entezari-Taher M, Stewart H. Cortical projections to spinal motoneurons: changes with aging and amyotrophic lateral sclerosis. Neurology 1996;46(5):1396-404.

117. Eisen A, Krieger C. Classic Charcot amyotrophic lateral sclerosis. In: Eisen A, editor. Clinical Neurophysiology of Motor Neuron Diseases. Handbook of Clinical Neurophysiology. 4: Elsevier; 2004. p. 469-85.

118. Eisen A, Kuwabara S. The split hand syndrome in amyotrophic lateral sclerosis. J Neurol Neurosurg Psychiatry 2012;83(4):399-403.

119. Eisen A, Lemon R. The motor deficit of ALS reflects failure to generate muscle synergies for complex motor tasks, not just muscle strength. Neurosci Lett 2021;762:136171.

120. Eisen A, Shytbel W, Murphy K, Hoirch M. Cortical magnetic stimulation in amyotrophic lateral sclerosis. Muscle Nerve 1990;13(2):146-51.

121. Eisen A, Weber M. The motor cortex and amyotrophic lateral sclerosis. Muscle Nerve 2001;24(4):564-73.

122. Elamin M, Phukan J, Bede P, Jordan N, Byrne S, Pender N, et al. Executive dysfunction is a negative prognostic indicator in patients with ALS without dementia. Neurology 2011;76(14):1263-9.

123. Epstein CM, Schwartzberg DG, Davey KR, Sudderth DB. Localizing the site of magnetic brain stimulation in humans. Neurology 1990;40(4):666-70.

124. Espay AJ, Li JY, Johnston L, Chen R, Lang AE. Mirror movements in parkinsonism: evaluation of a new clinical sign. J Neurol Neurosurg Psychiatry 2005;76(10):1355-8.

125. Farmer SF, Ingram DA, Stephens JA. Mirror movements studied in a patient with Klippel-Feil syndrome. J Physiol 1990;428:467-84.

126. Feiereisen P, Duchateau J, Hainaut K. Motor unit recruitment order during voluntary and electrically induced contractions in the tibialis anterior. Exp Brain Res 1997;114(1):117-23.

127. Ferbert A, Priori A, Rothwell JC, Day BL, Colebatch JG, Marsden CD. Interhemispheric inhibition of the human motor cortex. J Physiol 1992;453:525-46.

128. Filippini N, Douaud G, Mackay CE, Knight S, Talbot K, Turner MR. Corpus callosum involvement is a consistent feature of amyotrophic lateral sclerosis. Neurology 2010;75(18):1645-52.

129. Fisher MA. H reflexes and F waves. Fundamentals, normal and abnormal patterns. Neurol Clin 2002;20(2):339-60, vi.

130. Fisher RJ, Nakamura Y, Bestmann S, Rothwell JC, Bostock H. Two phases of intracortical inhibition revealed by transcranial magnetic threshold tracking. Exp Brain Res 2002;143(2):240-8.

131. Floeter MK. Cutaneous silent periods. Muscle Nerve 2003;28(4):391-401.

132. Floyd AG, Yu QP, Piboolnurak P, Tang MX, Fang Y, Smith WA, et al. Transcranial magnetic stimulation in ALS: utility of central motor conduction tests. Neurology 2009;72(6):498-504.

133. Fujiyama H, Hinder MR, Schmidt MW, Garry MI, Summers JJ. Age-related differences in corticospinal excitability and inhibition during coordination of upper and lower limbs. Neurobiol Aging 2012;33(7):1484.e1-14.

134. Funalot B, Desport JC, Sturtz F, Camu W, Couratier P. High metabolic level in patients with familial amyotrophic lateral sclerosis. Amyotroph Lateral Scler 2009;10(2):113-7.

135. Gamez J, Cervera C, Codina A. Flail arm syndrome of Vulpian-Bernhart's form of amyotrophic lateral sclerosis. J Neurol Neurosurg Psychiatry 1999;67(2):258.

136. Gao C, Jiang J, Tan Y, Chen S. Microglia in neurodegenerative diseases: mechanism and potential therapeutic targets. Signal Transduction and Targeted Therapy 2023;8(1):359.

137. Garvey MA, Ziemann U, Becker DA, Barker CA, Bartko JJ. New graphical method to measure silent periods evoked by transcranial magnetic stimulation. Clin Neurophysiol 2001;112(8):1451-60.

138. Geevasinga N, Menon P, Ng K, Van Den Bos M, Byth K, Kiernan MC, et al. Riluzole exerts transient modulating effects on cortical and axonal hyperexcitability in ALS. Amyotroph Lateral Scler Frontotemporal Degener 2016;17(7-8):580-8.

139. Geevasinga N, Menon P, Yiannikas C, Kiernan MC, Vucic S. Diagnostic utility of cortical excitability studies in amyotrophic lateral sclerosis. Eur J Neurol 2014;21(12):1451-7.

140. Gelon PA, Dutchak PA, Sephton CF. Synaptic dysfunction in ALS and FTD: anatomical and molecular changes provide insights into mechanisms of disease. Front Mol Neurosci 2022;15:1000183.

141. Geraldo AF, Pereira J, Nunes P, Reimao S, Sousa R, Castelo-Branco M, et al. Beyond fractional anisotropy in amyotrophic lateral sclerosis: the value of mean, axial, and radial diffusivity and its correlation with electrophysiological conductivity changes. Neuroradiology 2018;60(5):505-15.

142. Gilio F, Bettolo CM, Conte A, Iacovelli E, Frasca V, Serrao M, et al. Influence of the corticospinal tract on the cutaneous silent period: a study in patients with pyramidal syndrome. Neurosci Lett 2008;433(2):109-13.

143. Gordon PH. Amyotrophic Lateral Sclerosis: An update for 2013 Clinical Features, Pathophysiology, Management and Therapeutic Trials. Aging Dis 2013;4(5):295-310.

144. Gordon PH, Cheng B, Katz IB, Pinto M, Hays AP, Mitsumoto H, et al. The natural history of primary lateral sclerosis. Neurology 2006;66(5):647-53.

145. Goutman SA, Hardiman O, Al-Chalabi A, Chio A, Savelieff MG, Kiernan MC, et al. Emerging insights into the complex genetics and pathophysiology of amyotrophic lateral sclerosis. Lancet Neurol 2022;21(5):465-79.

146. Grace GM, Orange JB, Rowe A, Findlater K, Freedman M, Strong MJ. Neuropsychological functioning in PLS: a comparison with ALS. Can J Neurol Sci 2011;38(1):88-97.

147. Gromicho M, Figueiral M, Uysal H, Grosskreutz J, Kuzma-Kozakiewicz M, Pinto S, et al. Spreading in ALS: The relative impact of upper and lower motor neuron involvement. Ann Clin Transl Neurol 2020;7(7):1181-92.

148. Gromicho M, Kuzma-Kozakiewicz M, Szacka K, Nieporecki K, Andersen PM, Grosskreutz J, et al. Motor neuron disease beginning with frontotemporal dementia: clinical features and progression. Amyotroph Lateral Scler Frontotemporal Degener 2021;22(7-8):508-16.

149. Gutierrez J, Pérez-Lalana R, Zaldivar T, Lara G, Arias A, Ferrer Y, et al. CUTANEOUS SILENT PERIODS IN PATIENTS WITH EARLY-STAGE ALS (2447). 2020;94(15 Supplement):2447.

150. Hallett M. Transcranial magnetic stimulation. Negative effects. Adv Neurol 1995;67:107-13.

151. Hanajima R, Ugawa Y, Machii K, Mochizuki H, Terao Y, Enomoto H, et al. Interhemispheric facilitation of the hand motor area in humans. J Physiol 2001;531(Pt 3):849-59.

152. Hanajima R, Ugawa Y, Terao Y, Ogata K, Kanazawa I. Ipsilateral cortico-cortical inhibition of the motor cortex in various neurological disorders. J Neurol Sci 1996;140(1-2):109-16.

153. Hanajima R, Ugawa Y, Terao Y, Sakai K, Furubayashi T, Machii K, et al. Paired-pulse magnetic stimulation of the human motor cortex: differences among I waves. J Physiol 1998;509 (Pt 2)(Pt 2):607-18.

154. Hannaford A, Pavey N, van den Bos M, Geevasinga N, Menon P, Shefner JM, et al. Diagnostic Utility of Gold Coast Criteria in Amyotrophic Lateral Sclerosis. Ann Neurol 2021;89(5):979-86.

155. Hardiman O, Al-Chalabi A, Chio A, Corr EM, Logroscino G, Robberecht W, et al. Amyotrophic lateral sclerosis. Nat Rev Dis Primers 2017;3(1):17071.

156. Heffernan C, Jenkinson C, Holmes T, Feder G, Kupfer R, Leigh PN, et al. Nutritional management in MND/ALS patients: an evidence based review. Amyotroph Lateral Scler Other Motor Neuron Disord 2004;5(2):72-83.

157. Heffernan C, Jenkinson C, Holmes T, Macleod H, Kinnear W, Oliver D, et al. Management of respiration in MND/ALS patients: an evidence based review. Amyotroph Lateral Scler 2006;7(1):5-15.

158. Henneman E, Somjen G, Carpenter DO. Functional Significance of Cell Size in Spinal Motoneurons. J Neurophysiol 1965;28:560-80.

159. Henriques AR, Gromicho M, Grosskreutz J, Kuzma-Kozakiewicz M, Petri S, Uysal H, et al. Association of the practice of contact sports with the development of amyotrophic lateral sclerosis. Amyotroph Lateral Scler Frontotemporal Degener 2023;24(5-6):449-56.

160. Hoffmann P. Ueber die Beziehungen der Sehnenreflexe zur willkürlichen Bewegung und zum Tonus. Zeitschrift für Biologie 1918;68:351-70.

161. Hortobágyi T, Taylor J, Petersen N, Russell G, Gandevia S. Changes in Segmental and Motor Cortical Output With Contralateral Muscle Contractions and Altered Sensory Inputs in Humans. J Neurophysiol 2003;90(4):2451-9.

162. Howells J, Sangari S, Matamala JM, Kiernan MC, Marchand-Pauvert V, Burke D. Interrogating interneurone function using threshold tracking of the H reflex in healthy subjects and patients with motor neurone disease. Clin Neurophysiol 2020;131(8):1986-96.

163. Hübers A, Böckler B, Abaei A, Rasche V, Lulé D, Ercan E, et al. Functional and structural impairment of transcallosal motor fibres in ALS: a study using transcranial magnetic stimulation, diffusion tensor imaging, and diffusion weighted spectroscopy. Brain Imaging Behav 2021a;15(2):748-57.

164. Hübers A, Kassubek J, Muller HP, Broc N, Dreyhaupt J, Ludolph AC. The ipsilateral silent period: an early diagnostic marker of callosal disconnection in ALS. Ther Adv Chronic Dis 2021b;12:20406223211044072.

165. Hübers A, Orekhov Y, Ziemann U. Interhemispheric motor inhibition: its role in controlling electromyographic mirror activity. Eur J Neurosci 2008;28(2):364-71.

166. Hugon M. Exteroceptive Reflexes to Stimulation of the Sural Nerve in Normal Man. In: Desmedt JE, editor. Human Reflexes, Pathophysiology of Motor Systems, Methodology of Human Reflexes. 3: S.Karger AG; 1973. p. 713-29.

167. Hui J, Lioumis P, Blumberger DM, Daskalakis ZJ. Non-invasive Central Neuromodulation with Transcranial Magnetic Stimulation. In: Pouratian N, Sheth SA, editors. Stereotactic and Functional Neurosurgery: Principles and Applications. Cham: Springer International Publishing; 2020. p. 205-22.

168. Hultborn H, Meunier S, Pierrot-Deseilligny E, Shindo M. Changes in presynaptic inhibition of Ia fibres at the onset of voluntary contraction in man. J Physiol 1987;389(1):757-72.

169. Hultborn H, Pierrot-Deseilligny E, Wigstrom H. Recurrent inhibition and afterhyperpolarization following motoneuronal discharge in the cat. J Physiol 1979;297(0):253-66.

170. Hupfeld KE, Swanson CW, Fling BW, Seidler RD. TMS-induced silent periods: A review of methods and call for consistency. J Neurosci Methods 2020;346:108950.

171. Huynh W, Simon NG, Grosskreutz J, Turner MR, Vucic S, Kiernan MC. Assessment of the upper motor neuron in amyotrophic lateral sclerosis. Clin Neurophysiol 2016;127(7):2643-60.

172. Iglesias C, Sangari S, El Mendili MM, Benali H, Marchand-Pauvert V, Pradat PF. Electrophysiological and spinal imaging evidences for sensory dysfunction in amyotrophic lateral sclerosis. BMJ Open 2015;5(2):e007659.

173. Iles JF. Evidence for cutaneous and corticospinal modulation of presynaptic inhibition of Ia afferents from the human lower limb. J Physiol 1996;491 (Pt 1)(Pt 1):197-207.

174. Ilieva H, Polymenidou M, Cleveland DW. Non-cell autonomous toxicity in neurodegenerative disorders: ALS and beyond. J Cell Biol 2009;187(6):761-72.

175. Ince PG, Evans J, Knopp M, Forster G, Hamdalla HH, Wharton SB, et al. Corticospinal tract degeneration in the progressive muscular atrophy variant of ALS. Neurology 2003;60(8):1252-8.

176. Inghilleri M, Berardelli A, Cruccu G, Manfredi M. Silent period evoked by transcranial stimulation of the human cortex and cervicomedullary junction. J Physiol 1993;466:521-34.

177. Inghilleri M, Cruccu G, Argenta M, Polidori L, Manfredi M. Silent period in upper limb muscles after noxious cutaneous stimulation in man. Electroencephalogr Clin Neurophysiol 1997;105(2):109-15.

178. Ingre C, Roos PM, Piehl F, Kamel F, Fang F. Risk factors for amyotrophic lateral sclerosis. Clin Epidemiol 2015;7:181-93.

179. Iyer PM, Egan C, Pinto-Grau M, Burke T, Elamin M, Nasseroleslami B, et al. Functional Connectivity Changes in Resting-State EEG as Potential Biomarker for Amyotrophic Lateral Sclerosis. PLoS One 2015;10(6):e0128682.

180. Jaiser SR, Mitra D, Williams TL, Baker MR. Mills' syndrome revisited. J Neurol 2019;266(3):667-79.

181. Jankovic M, Novakovic I, Gamil Anwar Dawod P, Gamil Anwar Dawod A, Drinic A, Abdel Motaleb FI, et al. Current Concepts on Genetic Aspects of Mitochondrial Dysfunction in Amyotrophic Lateral Sclerosis. Int J Mol Sci 2021;22(18).

182. Jankowska E. Interneuronal relay in spinal pathways from proprioceptors. Prog Neurobiol 1992;38(4):335-78.

183. Jenkins TM, Alix JJP, Fingret J, Esmail T, Hoggard N, Baster K, et al. Longitudinal multi-modal muscle-based biomarker assessment in motor neuron disease. J Neurol 2020;267(1):244-56.

184. Johnsen B, Pugdahl K, Fuglsang-Frederiksen A, Kollewe K, Paracka L, Dengler R, et al. Diagnostic criteria for amyotrophic lateral sclerosis: A multicentre study of inter-rater variation and sensitivity. Clin Neurophysiol 2019;130(2):307-14.

185. Julien JP. Neurofilament functions in health and disease. Curr Opin Neurobiol 1999;9(5):554-60.

186. Kanouchi T, Ohkubo T, Yokota T. Can regional spreading of amyotrophic lateral sclerosis motor symptoms be explained by prion-like propagation? J Neurol Neurosurg Psychiatry 2012;83(7):739-45.

187. Karandreas N, Papadopoulou M, Kokotis P, Papapostolou A, Tsivgoulis G, Zambelis T. Impaired interhemispheric inhibition in amyotrophic lateral sclerosis. Amyotroph Lateral Scler 2007;8(2):112-8.

188. Kiernan MC, Vucic S, Cheah BC, Turner MR, Eisen A, Hardiman O, et al. Amyotrophic lateral sclerosis. Lancet 2011;377(9769):942-55.

189. Kim HJ, Oh KW, Kwon MJ, Oh SI, Park JS, Kim YE, et al. Identification of mutations in Korean patients with amyotrophic lateral sclerosis using multigene panel testing. Neurobiol Aging 2016;37:209 e9- e16.

190. Kim WK, Kwak YT. Preservation of motor neuron excitability during the cutaneous silent period in amyotrophic lateral sclerosis. J Neurol 2010;257:92-3.

191. Kim WK, Liu X, Sandner J, Pasmantier M, Andrews J, Rowland LP, et al. Study of 962 patients indicates progressive muscular atrophy is a form of ALS. Neurology 2009;73(20):1686-92.

192. Klomjai W, Katz R, Lackmy-Vallée A. Basic principles of transcranial magnetic stimulation (TMS) and repetitive TMS (rTMS). Ann Phys Rehabil Med 2015;58(4):208-13.

193. Klomjai W, Lackmy-Vallee A, Katz R, Bussel B, Bensmail D, Lamy JC, et al. Changes in spinal inhibitory networks induced by furosemide in humans. J Physiol 2014;592(13):2865-79.

194. Knikou M. The H-reflex as a probe: pathways and pitfalls. J Neurosci Methods 2008;171(1):1-12.

195. Koehler W, Windhorst U, Schmidt J, Meyer-Lohmann J, Henatsch HD. Diverging influences on Renshaw cell responses and monosynaptic reflexes from stimulation of capsula interna. Neurosci Lett 1978;8(1):35-9.

196. Kofler M. Functional organization of exteroceptive inhibition following nociceptive electrical fingertip stimulation in humans. Clin Neurophysiol 2003;114(6):973-80.

197. Kofler M, Kumru H, Stetkarova I, Schindler C, Fuhr P. Muscle force up to 50% of maximum does not affect cutaneous silent periods in thenar muscles. Clin Neurophysiol 2007;118(9):2025-30.

198. Kofler M, Leis AA, Valls-Sole J. Cutaneous silent periods - Part 1: Update on physiological mechanisms. Clin Neurophysiol 2019a;130(4):588-603.

199. Kofler M, Leis AA, Valls-Sole J. Cutaneous silent periods - Part 2: Update on pathophysiology and clinical utility. Clin Neurophysiol 2019b;130(4):604-15.

200. Komissarow L, Rollnik JD, Bogdanova D, Krampfl K, Khabirov FA, Kossev A, et al. Triple stimulation technique (TST) in amyotrophic lateral sclerosis. Clin Neurophysiol 2004;115(2):356-60.

201. Krampfl K, Mohammadi B, Komissarow L, Dengler R, Bufler J. Mirror movements and ipsilateral motor evoked potentials in ALS. Amyotroph Lateral Scler Other Motor Neuron Disord 2004;5(3):154-63.

202. Krampfl K, Petri S, Gotz F, Mohammadi B, Bufler J. Amyotrophic lateral sclerosis (ALS) and mirror movements in a patient with polymicrogyria. Amyotroph Lateral Scler Other Motor Neuron Disord 2003;4(4):266-9.

203. Kujirai T, Caramia MD, Rothwell JC, Day BL, Thompson PD, Ferbert A, et al. Corticocortical inhibition in human motor cortex. J Physiol 1993;471:501-19.

204. Kuo YL, Dubuc T, Boufadel DF, Fisher BE. Measuring ipsilateral silent period: Effects of muscle contraction levels and quantification methods. Brain Res 2017;1674:77-83.

205. Kuypers HGJM. The Anatomical Organization of the Descending Pathways and their Contributions to Motor Control Especially in Primates. Human Reflexes, Pathophysiology of Motor Systems, Methodology of Human Reflexes; 1973. p. 38-68.

206. Kwiatkowski TJ, Jr., Bosco DA, Leclerc AL, Tamrazian E, Vanderburg CR, Russ C, et al. Mutations in the FUS/TLS gene on chromosome 16 cause familial amyotrophic lateral sclerosis. Science 2009;323(5918):1205-8.

207. Lawyer T, Jr., Netsky MG. Amyotrophic lateral sclerosis. AMA Arch Neurol Psychiatry 1953;69(2):171-92.

208. Lazarus JA, Todor JI. Age differences in the magnitude of associated movement. Dev Med Child Neurol 1987;29(6):726-33.

209. Lee Y, Morrison BM, Li Y, Lengacher S, Farah MH, Hoffman PN, et al. Oligodendroglia metabolically support axons and contribute to neurodegeneration. Nature 2012;487(7408):443-8.

210. Lefaucheur J-P. Chapter 37 - Transcranial magnetic stimulation. In: Levin KH, Chauvel P, editors. Handb Clin Neurol. 160: Elsevier; 2019. p. 559-80.

211. Leigh PN. Chapter 13 Amyotrophic lateral sclerosis. In: Eisen AA, Shaw PJ, editors. Handb Clin Neurol. 82: Elsevier; 2007. p. 249-78.

212. Leigh PN, Abrahams S, Al-Chalabi A, Ampong MA, Goldstein LH, Johnson J, et al. The management of motor neurone disease. J Neurol Neurosurg Psychiatry 2003;74 Suppl 4(Suppl 4):iv32-iv47.

213. Leis AA, Ross MA, Emori T, Matsue Y, Saito T. The silent period produced by electrical stimulation of mixed peripheral nerves. Muscle Nerve 1991;14(12):1202-8.

214. Leis AA, Stokic DS, Fuhr P, Kofler M, Kronenberg MF, Wissel J, et al. Nociceptive fingertip stimulation inhibits synergistic motoneuron pools in the human upper limb. Neurology 2000;55(9):1305-9.

215. Lemon RN. Descending pathways in motor control. Annu Rev Neurosci 2008;31:195-218.

216. Lemon RN, Griffiths J. Comparing the function of the corticospinal system in different species: organizational differences for motor specialization? Muscle Nerve 2005;32(3):261-79.

217. Liochev SI, Fridovich I. Mutant Cu,Zn superoxide dismutases and familial amyotrophic lateral sclerosis: evaluation of oxidative hypotheses. Free Radic Biol Med 2003;34(11):1383-9.

218. Logigian EL, Plotkin GM, Shefner JM. The cutaneous silent period is mediated by spinal inhibitory reflex. Muscle Nerve 1999;22(4):467-72.

219. Lourenco G, Iglesias C, Marchand-Pauvert V. Effects produced in human arm and forearm motoneurones after electrical stimulation of ulnar and median nerves at wrist level. Exp Brain Res 2007;178(2):267-84.

220. Macdonell RA, Shapiro BE, Chiappa KH, Helmers SL, Cros D, Day BJ, et al. Hemispheric threshold differences for motor evoked potentials produced by magnetic coil stimulation. Neurology 1991;41(9):1441-4.

221. Mackenzie IRA. Neuropathology of primary lateral sclerosis. Amyotroph Lateral Scler Frontotemporal Degener 2020;21(sup1):47-51.

222. Magladery JW, McDougal DB, Jr. Electrophysiological studies of nerve and reflex activity in normal man. I. Identification of certain reflexes in the electromyogram and the conduction velocity of peripheral nerve fibers. Bull Johns Hopkins Hosp 1950;86(5):265-90.

223. Magladery JW, Porter WE, Park AM, Teasdall RD. Electrophysiological studies of nerve and reflex activity in normal man. IV. The two-neurone reflex and identification of certain action potentials from spinal roots and cord. Bull Johns Hopkins Hosp 1951;88(6):499-519.

224. Magne VA, Adde L, Hoare B, Klingels K, Simon-Martinez C, Mailleux L, et al. Assessment of mirror movements in children and adolescents with unilateral cerebral palsy: reliability of the Woods and Teuber scale. Dev Med Child Neurol 2021;63(6):736-42.

225. Magrane J, Manfredi G. Mitochondrial function, morphology, and axonal transport in amyotrophic lateral sclerosis. Antioxid Redox Signal 2009;11(7):1615-26.

226. Manconi FM, Syed NA, Floeter MK. Mechanisms underlying spinal motor neuron excitability during the cutaneous silent period in humans. Muscle Nerve 1998;21(10):1256-64.

227. Maragakis NJ, de Carvalho M, Weiss MD. Therapeutic targeting of ALS pathways: Refocusing an incomplete picture. Ann Clin Transl Neurol 2023:10.1002/acn3.51887. Advance online publication.

228. Masrori P, Van Damme P. Amyotrophic lateral sclerosis: a clinical review. Eur J Neurol 2020;27(10):1918-29.

229. Matsumoto G, Stojanovic A, Holmberg CI, Kim S, Morimoto RI. Structural properties and neuronal toxicity of amyotrophic lateral sclerosis-associated Cu/Zn superoxide dismutase 1 aggregates. J Cell Biol 2005;171(1):75-85.

230. Maudrich T, Kenville R, Lepsien J, Villringer A, Ragert P, Steele CJ. Mirror Electromyografic Activity in the Upper and Lower Extremity: A Comparison between Endurance Athletes and Non-Athletes. Front Hum Neurosci 2017;11:485.

231. Mayston MJ, Harrison LM, Quinton R, Stephens JA, Krams M, Bouloux PM. Mirror movements in X-linked Kallmann's syndrome. I. A neurophysiological study. Brain 1997;120 (Pt 7):1199-216.

232. Mayston MJ, Harrison LM, Stephens JA. A neurophysiological study of mirror movements in adults and children. Ann Neurol 1999;45(5):583-94.

233. Mazzini L, Balzarini C, Gareri F, Brigatti M. H-reflex changes in the course of amyotrophic lateral sclerosis. Electroencephalogr Clin Neurophysiol 1997;104(5):411-7.

234. Mazzocchio R, Rossi A. Further evidence for Renshaw inhibition in man. A combined electrophysiological and pharmacological approach. Neurosci Lett 1989;106(1-2):131-6.

235. Mazzocchio R, Rossi A. Recurrent inhibition. Neurology 1996;47(6):1606-8.

236. Mazzocchio R, Rossi A. Role of Renshaw cells in amyotrophic lateral sclerosis. Muscle Nerve 2010;41(4):441-3.

237. Mazzocchio R, Rossi A, Rothwell JC. Depression of Renshaw recurrent inhibition by activation of corticospinal fibres in human upper and lower limb. J Physiol 1994;481 (Pt 2)(Pt 2):487-98.

238. McDonald JH. Handbook of Biological Statistics. 3rd ed. Baltimore, Maryland: Sparky House Publishing, 2014.

239. McGown A, McDearmid JR, Panagiotaki N, Tong H, Al Mashhadi S, Redhead N, et al. Early interneuron dysfunction in ALS: insights from a mutant sod1 zebrafish model. Ann Neurol 2013;73(2):246-58.

240. McGraw KO, Wong SP. Forming inferences about some intraclass correlation coefficients. Psychol Methods 1996;1(1):30.

241. McKay KA, Smith KA, Smertinaite L, Fang F, Ingre C, Taube F. Military service and related risk factors for amyotrophic lateral sclerosis. Acta Neurol Scand 2021;143(1):39-50.

242. Mead RJ, Shan N, Reiser HJ, Marshall F, Shaw PJ. Amyotrophic lateral sclerosis: a neurodegenerative disorder poised for successful therapeutic translation. Nat Rev Drug Discov 2023;22(3):185-212.

243. Mehta P, Horton DK, Kasarskis EJ, Tessaro E, Eisenberg MS, Laird S, et al. CDC Grand Rounds: National Amyotrophic Lateral Sclerosis (ALS) Registry Impact, Challenges, and Future Directions. MMWR Morb Mortal Wkly Rep 2017;66(50):1379-82.

244. Meister S, Wolters A, Walter U, Benecke R, Wittstock M. Mirror Movements in Amyotrophic Lateral Sclerosis. Klinische Neurophysiologie 2011;42(01).

245. Menon P, Yiannikas C, Kiernan MC, Vucic S. Regional motor cortex dysfunction in amyotrophic lateral sclerosis. Ann Clin Transl Neurol 2019;6(8):1373-82.

246. Menzies FM, Cookson MR, Taylor RW, Turnbull DM, Chrzanowska-Lightowlers ZM, Dong L, et al. Mitochondrial dysfunction in a cell culture model of familial amyotrophic lateral sclerosis. Brain 2002;125(Pt 7):1522-33.

247. Merton PA, Morton HB. Stimulation of the cerebral cortex in the intact human subject. Nature 1980;285(5762):227.

248. Meyer BU, Röricht S, Gräfin von Einsiedel H, Kruggel F, Weindl A. Inhibitory and excitatory interhemispheric transfers between motor cortical areas in normal humans and patients with abnormalities of the corpus callosum. Brain 1995;118 (Pt 2):429-40.

249. Meyer BU, Roricht S, Woiciechowsky C. Topography of fibers in the human corpus callosum mediating interhemispheric inhibition between the motor cortices. Ann Neurol 1998;43(3):360-9.

250. Miller RG, Mitchell JD, Lyon M, Moore DH. Riluzole for amyotrophic lateral sclerosis (ALS)/motor neuron disease (MND). Cochrane Database Syst Rev 2007(1):CD001447.

251. Miller TM, Cudkowicz ME, Genge A, Shaw PJ, Sobue G, Bucelli RC, et al. Trial of Antisense Oligonucleotide Tofersen for SOD1 ALS. N Engl J Med 2022;387(12):1099-110.

252. Mills CK. UNILATERAL ASCENDING PARALYSIS AND UNILATERAL DESCENDING PARALYSIS.THEIR CLINICAL VARIETIES AND THEIR PATHOLOGIC CAUSES. Jama 1906;XLVII(20):1638-45.

253. Mills KR. The natural history of central motor abnormalities in amyotrophic lateral sclerosis. Brain 2003;126(Pt 11):2558-66.

254. Mills KR. Magnetic stimulation and central conduction time. In: Eisen A, editor. Handbook of Clinical Neurophysiology. 4: Elsevier; 2004. p. 283-93.

255. Millul A, Beghi E, Logroscino G, Micheli A, Vitelli E, Zardi A. Survival of patients with amyotrophic lateral sclerosis in a population-based registry. Neuroepidemiology 2005;25(3):114-9.

256. Miranda PC. Physics of effects of transcranial brain stimulation. Handb Clin Neurol 2013;116:353-66.

257. Misiaszek JE. The H-reflex as a tool in neurophysiology: its limitations and uses in understanding nervous system function. Muscle Nerve 2003;28(2):144-60.

258. Mitchell JD, O'Brien M R, Joshi M. Audit of outcomes in motor neuron disease (MND) patients treated with riluzole. Amyotroph Lateral Scler 2006;7(2):67-71.

259. Mizuno Y, Tanaka R, Yanagisawa N. Reciprocal group I inhibition on triceps surae motoneurons in man. J Neurophysiol 1971;34(6):1010-7.

260. Morin C, Pierrot-Deseilligny E. [Spinal mechanism of the antispastic action of TRH in patients with amyotrophic lateral sclerosis]. Rev Neurol (Paris) 1988;144(11):701-3.

261. Mousavi S-AJ, Zamani B, Shahmiri SS, Rohani M, Shahidi GA, Mostafapour E, et al. Pulmonary function tests in patients with amyotrophic lateral sclerosis and the association between these tests and survival. Iran J of Neurol 2014;13(3):131.

262. Nagelkerke NJD. A note on a general definition of the coefficient of determination. Biometrika 1991;78(3):691-2.

263. Nakamura H, Kitagawa H, Kawaguchi Y, Tsuji H. Intracortical facilitation and inhibition after transcranial magnetic stimulation in conscious humans. J Physiol 1997;498 (Pt 3)(Pt 3):817-23.

264. Neary D, Snowden JS, Mann DM. Cognitive change in motor neurone disease/amyotrophic lateral sclerosis (MND/ALS). J Neurol Sci 2000;180(1-2):15-20.

265. Neumann DA, Kelly ER, Kiefer CL, Martens K, Grosz CM. Kinesiology of the Musculoskeletal System: Foundations for Rehabilitation: Elsevier, 2017.

266. Neumann M, Sampathu DM, Kwong LK, Truax AC, Micsenyi MC, Chou TT, et al. Ubiquitinated TDP-43 in frontotemporal lobar degeneration and amyotrophic lateral sclerosis. Science 2006;314(5796):130-3.

267. Nieto-Gonzalez JL, Moser J, Lauritzen M, Schmitt-John T, Jensen K. Reduced GABAergic inhibition explains cortical hyperexcitability in the wobbler mouse model of ALS. Cereb Cortex 2011;21(3):625-35.

268. Nihei K, McKee AC, Kowall NW. Patterns of neuronal degeneration in the motor cortex of amyotrophic lateral sclerosis patients. Acta Neuropathol 1993;86(1):55-64.

269. Oldfield RC. The assessment and analysis of handedness: the Edinburgh inventory. Neuropsychologia 1971;9(1):97-113.

270. Ottaviani D, Tiple D, Suppa A, Colosimo C, Fabbrini G, Cincotta M, et al. Mirror movements in patients with Parkinson's disease. Mov Disord 2008;23(2):253-8.

271. Özyurt MG, Topkara B, İşak B, Türker KS. Amyotrophic lateral sclerosis weakens spinal recurrent inhibition and post-activation depression. Clin Neurophysiol 2020;131(12):2875-86.

272. Paillard J. Réflexes et régulations d'origine proprioceptive chez l'homme: étude neuro-physiologique et psychophysiologique. Paris: Arnette Paris; 1955.

273. Patrikios JS. Contribution a l'etude des formes cliniques et de l'anatomie pathologique de la sclerose lateral amytrophique. Paris: Faculté de Médecine, Université de Paris; 1918.

274. Pavey N, Menon P, van den Bos MAJ, Kiernan MC, Vucic S. Cortical inhibition and facilitation are mediated by distinct physiological processes. Neurosci Lett 2023;803:137191.

275. Pierrot-Deseilligny E. Electrophysiological assessment of the spinal mechanisms underlying spasticity. Electroencephalogr Clin Neurophysiol Suppl 1990;41:264-73.

276. Pierrot-Deseilligny E. Propriospinal transmission of part of the corticospinal excitation in humans. Muscle Nerve 2002;26(2):155-72.

277. Pierrot-Deseilligny E, Burke D. The Circuitry of the Human Spinal Cord. Cambridge: Cambridge University Press, 2012.

278. Pierrot-Deseilligny E, Bussel B. Evidence for recurrent inhibition by motoneurons in human subjects. Brain Res 1975;88(1):105-8.

279. Pierrot-Deseilligny E, Bussel B, Sideri G, Cathala HP, Castaigne P. Effect of voluntary contraction on H reflex changes induced by cutaneous stimulation in normal man. Electroencephalogr Clin Neurophysiol 1973;34(2):185-92.

280. Pierrot-Deseilligny E, Mazevet D. The monosynaptic reflex: a tool to investigate motor control in humans. Interest and limits. Neurophysiol Clin 2000;30(2):67-80.

281. Pierrot-Deseilligny E, Morin C, Bergego C, Tankov N. Pattern of group I fibre projections from ankle flexor and extensor muscles in man. Exp Brain Res 1981;42(3-4):337-50.

282. Pinto AC, Evangelista T, Carvalho M, Alves MA, Sales Luís ML. Respiratory assistance with a non-invasive ventilator (Bipap) in MND/ALS patients: survival rates in a controlled trial. J Neurol Sci 1995;129 Suppl:19-26.

283. Pinto S, Geraldes R, Vaz N, Pinto A, de Carvalho M. Changes of the phrenic nerve motor response in amyotrophic lateral sclerosis: longitudinal study. Clin Neurophysiol 2009;120(12):2082-5.

284. Pinto S, Gromicho M, Oliveira Santos MO, Swash M, De Carvalho M. Respiratory onset in amyotrophic lateral sclerosis: clinical features and spreading pattern. Amyotroph Lateral Scler Frontotemporal Degener 2023;24(1-2):40-4.

285. Pinto S, Pinto A, de Carvalho M. Phrenic nerve studies predict survival in amyotrophic lateral sclerosis. Clin Neurophysiol 2012;123(12):2454-9.

286. Porter R. The corticomotoneuronal component of the pyramidal tract: corticomotoneuronal connections and functions in primates. Brain Res 1985;357(1):1-26.

287. Portney LG. Foundations of clinical research: applications to evidence-based practice. 4th ed: FA Davis, 2020.

288. Pringle CE, Hudson AJ, Munoz DG, Kiernan JA, Brown WF, Ebers GC. Primary lateral sclerosis. Clinical features, neuropathology and diagnostic criteria. Brain 1992;115 (Pt 2):495-520.

289. Prout AJ, Eisen AA. The cortical silent period and amyotrophic lateral sclerosis. Muscle Nerve 1994;17(2):217-23.

290. Pugdahl K, Camdessanché JP, Cengiz B, de Carvalho M, Liguori R, Rossatto C, et al. Gold Coast diagnostic criteria increase sensitivity in amyotrophic lateral sclerosis. Clin Neurophysiol 2021;132(12):3183-9.

291. Pujia F, Serrao M, Brienza M, Vestrini E, Valente GO, Coppola G, et al. Effects of a selective serotonin reuptake inhibitor escitalopram on the cutaneous silent period: A randomized controlled study in healthy volunteers. Neuroscience Letters 2014;566:17-20.

292. Pupillo E, Messina P, Logroscino G, Beghi E, Group S. Long-term survival in amyotrophic lateral sclerosis: a population-based study. Ann Neurol 2014;75(2):287-97.

293. Ravits J, Appel S, Baloh RH, Barohn R, Brooks BR, Elman L, et al. Deciphering amyotrophic lateral sclerosis: what phenotype, neuropathology and genetics are telling us about pathogenesis. Amyotroph Lateral Scler Frontotemporal Degener 2013;14 Suppl 1(0 1):5-18.

294. Ravits JM, La Spada AR. ALS motor phenotype heterogeneity, focality, and spread: deconstructing motor neuron degeneration. Neurology 2009;73(10):805-11.

295. Raynor E, Shefner J. Recurrent inhibition is decreased in patients with amyotrophic lateral sclerosis. Neurology 1994;44(11):2148-53.

296. Renshaw B. Central effects of centripetal impulses in axons of spinal ventral roots. J Neurophysiol 1946;9(3):191-204.

297. Rivadeneyra-Domínguez E, Rodríguez-Landa JF. Cycads and their association with certain neurodegenerative diseases. Neurología (English Edition) 2014;29(9):517-22.

298. Robinson LR, Jantra P, MacLean IC. Central motor conduction times using transcranial stimulation and F wave latencies. Muscle Nerve 1988;11(2):174-80.

299. Rodi Z, Springer C. Influence of muscle contraction and intensity of stimulation on the cutaneous silent period. Muscle Nerve 2011;43(3):324-8.

300. Romaniello A, Truini A, Galeotti F, De Lena C, Willer JC, Cruccu G. Cutaneous silent period in hand muscle is evoked by laser stimulation of the palm, but not the hand dorsum. Muscle Nerve 2004;29(6):870-2.

301. Rosen DR, Siddique T, Patterson D, Figlewicz DA, Sapp P, Hentati A, et al. Mutations in Cu/Zn superoxide dismutase gene are associated with familial amyotrophic lateral sclerosis. Nature 1993;362(6415):59-62.

302. Rossi A, Mazzocchio R. Presence of homonymous recurrent inhibition in motoneurones supplying different lower limb muscles in humans. Exp Brain Res 1991;84(2):367-73.

303. Rossi P, Pierelli F, Parisi L, Perrotta A, Bartolo M, Amabile G, et al. Effect of painful heterotopic stimulation on the cutaneous silent period in the upper limbs. Clin Neurophysiol 2003;114(1):1-6.

304. Rossi S, Hallett M, Rossini PM, Pascual-Leone A. Safety, ethical considerations, and application guidelines for the use of transcranial magnetic stimulation in clinical practice and research. Clin Neurophysiol 2009;120(12):2008-39.

305. Rossini PM, Berardelli A, Deuschl G, Hallett M, Maertens de Noordhout AM, Paulus W, et al. Applications of magnetic cortical stimulation. The International Federation of Clinical Neurophysiology. Electroencephalography and clinical neurophysiology Supplement 1999;52:171-85.

306. Rossini PM, Burke D, Chen R, Cohen LG, Daskalakis Z, Di Iorio R, et al. Non-invasive electrical and magnetic stimulation of the brain, spinal cord, roots and peripheral nerves: Basic principles and procedures for routine clinical and research application. An updated report from an I.F.C.N. Committee. Clin Neurophysiol 2015;126(6):1071-107.

307. Rothstein JD. Current hypotheses for the underlying biology of amyotrophic lateral sclerosis. Ann Neurol 2009;65 Suppl 1(S1):S3-9.

308. Rothwell JC, Colebatch J, Britton TC, Priori A, Thompson PD, Day BL, et al. Physiological studies in a patient with mirror movements and agenesis of the corpus callosum. J Physiol 1991;438:34P.

309. Rothwell JC, Hallett M, Berardelli A, Eisen A, Rossini P, Paulus W. Magnetic stimulation: motor evoked potentials. The International Federation of Clinical Neurophysiology. Electroencephalogr Clin Neurophysiol Suppl 1999;52:97-103.

310. Rouiller EM, Babalian A, Kazennikov O, Moret V, Yu XH, Wiesendanger M. Transcallosal connections of the distal forelimb representations of the primary and supplementary motor cortical areas in macaque monkeys. Exp Brain Res 1994;102(2):227-43.

311. Ruddy KL, Leemans A, Carson RG. Transcallosal connectivity of the human cortical motor network. Brain Struct Funct 2017;222(3):1243-52.

312. Rudomin P, Schmidt RF. Presynaptic inhibition in the vertebrate spinal cord revisited. Exp Brain Res 1999;129(1):1-37.

313. Ryan M, Heverin M, McLaughlin RL, Hardiman O. Lifetime Risk and Heritability of Amyotrophic Lateral Sclerosis. JAMA Neurol 2019;76(11):1367-74.

314. Salamatina A, Yang JH, Brenner-Morton S, Bikoff JB, Fang L, Kintner CR, et al. Differential Loss of Spinal Interneurons in a Mouse Model of ALS. Neuroscience 2020;450:81-95.

315. Sale MV, Semmler JG. Age-related differences in corticospinal control during functional isometric contractions in left and right hands. J Appl Physiol (1985) 2005;99(4):1483-93.

316. Salerno A, Georgesco M. Double magnetic stimulation of the motor cortex in amyotrophic lateral sclerosis. Electroencephalogr Clin Neurophysiol 1998;107(2):133-9.

317. Sangari S, Iglesias C, El Mendili MM, Benali H, Pradat PF, Marchand-Pauvert V. Impairment of sensory-motor integration at spinal level in amyotrophic lateral sclerosis. Clin Neurophysiol 2016;127(4):1968-77.

318. Sangari S, Peyre I, Lackmy-Vallee A, Bayen E, Pradat PF, Marchand-Pauvert V. Transient increase in recurrent inhibition in amyotrophic lateral sclerosis as a putative protection from neurodegeneration. Acta Physiol (Oxf) 2022;234(4):e13758.

319. Sasaki S, Iwata M. Mitochondrial alterations in the spinal cord of patients with sporadic amyotrophic lateral sclerosis. J Neuropathol Exp Neurol 2007;66(1):10-6.

320. Saxena S, Caroni P. Selective neuronal vulnerability in neurodegenerative diseases: from stressor thresholds to degeneration. Neuron 2011;71(1):35-48.

321. Schieppati M, Poloni M, Nardone A. Voluntary muscle release is not accompanied by H-reflex inhibition in patients with upper moto neuron lesions. Neurosci Lett 1985;61(1-2):177-81.

322. Schott GD, Wyke MA. Congenital mirror movements. J Neurol Neurosurg Psychiatry 1981;44(7):586-99.

323. Sehm B, Perez MA, Xu B, Hidler J, Cohen LG. Functional neuroanatomy of mirroring during a unimanual force generation task. Cereb Cortex 2010;20(1):34-45.

324. Serrao M, Parisi L, Pierelli F, Rossi P. Cutaneous afferents mediating the cutaneous silent period in the upper limbs: evidences for a role of low-threshold sensory fibres. Clin Neurophysiol 2001;112(11):2007-14.

325. Shahani BT, Young RR. Studies of the Normal Human Silent Period. In: Desmedt, J.E., editor. New developments in electromyography and clinical neurophysiology. Basel: Karger; 1973. p. 589-602.

326. Shaw PJ, Eggett CJ. Molecular factors underlying selective vulnerability of motor neurons to neurodegeneration in amyotrophic lateral sclerosis. J Neurol 2000;247 Suppl 1:I17-27.

327. Shefner JM, Al-Chalabi A, Baker MR, Cui LY, de Carvalho M, Eisen A, et al. A proposal for new diagnostic criteria for ALS. Clin Neurophysiol 2020;131(8):1975-8.

328. Shefner JM, Logigian EL. The mixed nerve silent period in normal subjects and patients with amyotrophic lateral sclerosis. Electromyogr Clin Neurophysiol 1998;38(8):505-10.

329. Sherrington C. Inhibition as a Coordinative Factor. Nobel Lecture. https://www.nobelprize.org/prizes/medicine/1932/sherrington/lecture/1932.

330. Shibuya K, Park SB, Geevasinga N, Huynh W, Simon NG, Menon P, et al. Threshold tracking transcranial magnetic stimulation: Effects of age and gender on motor cortical function. Clin Neurophysiol 2016a;127(6):2355-61.

331. Shibuya K, Park SB, Geevasinga N, Menon P, Howells J, Simon NG, et al. Motor cortical function determines prognosis in sporadic ALS. Neurology 2016b;87(5):513-20.

332. Shibuya K, Simon NG, Geevasinga N, Menon P, Howells J, Park SB, et al. The evolution of motor cortical dysfunction in amyotrophic lateral sclerosis. Clin Neurophysiol 2017;128(6):1075-82.

333. Siciliano G, Manca ML, Sagliocco L, Pastorini E, Pellegrinetti A, Sartucci F, et al. Cortical silent period in patients with amyotrophic lateral sclerosis. J Neurol Sci 1999;169(1-2):93-7.

334. Simon NG, Lin CS, Lee M, Howells J, Vucic S, Burke D, et al. Segmental motoneuronal dysfunction is a feature of amyotrophic lateral sclerosis. Clin Neurophysiol 2015;126(4):828-36.

335. Smeyers J, Banchi EG, Latouche M. C9ORF72: What It Is, What It Does, and Why It Matters. Front Cell Neurosci 2021;15:661447.

336. Sommer M, Tergau F, Wischer S, Reimers CD, Beuche W, Paulus W. Riluzole does not have an acute effect on motor thresholds and the intracortical excitability in amyotrophic lateral sclerosis. J Neurol 1999;246 Suppl 3:Iii22-6.

337. Spencer PS, Lagrange E, Camu W. ALS and environment: Clues from spatial clustering? Rev Neurol (Paris) 2019;175(10):652-63.

338. Statland JM, Barohn RJ, McVey AL, Katz JS, Dimachkie MM. Patterns of Weakness, Classification of Motor Neuron Disease, and Clinical Diagnosis of Sporadic Amyotrophic Lateral Sclerosis. Neurol Clin 2015;33(4):735-48.

339. Stefan K, Kunesch E, Benecke R, Classen J. Effects of riluzole on cortical excitability in patients with amyotrophic lateral sclerosis. Ann Neurol 2001;49(4):536-9.

340. Stephens B, Guiloff RJ, Navarrete R, Newman P, Nikhar N, Lewis P. Widespread loss of neuronal populations in the spinal ventral horn in sporadic motor neuron disease. A morphometric study. J Neurol Sci 2006;244(1-2):41-58.

341. Stetkarova I, Kofler M. Differential effect of baclofen on cortical and spinal inhibitory circuits. Clinical Neurophysiology 2013;124(2):339-45.

342. Swash M. Why are upper motor neuron signs difficult to elicit in amyotrophic lateral sclerosis? J Neurol Neurosurg Psychiatry 2012;83(6):659-62.

343. Swash M. MUNIX in the clinic in ALS: MUNE comes of age. Clin Neurophysiol 2017;128(3):482-3.

344. Swash M, Burke D, Turner MR, Grosskreutz J, Leigh PN, de Carvalho M, et al. Occasional essay: Upper motor neuron syndrome in amyotrophic lateral sclerosis. J Neurol Neurosurg Psychiatry 2020;91(3):227-34.

345. Takei K, Watanabe K, Yuki S, Akimoto M, Sakata T, Palumbo J. Edaravone and its clinical development for amyotrophic lateral sclerosis. Amyotroph Lateral Scler Frontotemporal Degener 2017;18(sup1):5-10.

346. Tankisi H, Nielsen CS, Howells J, Cengiz B, Samusyte G, Koltzenburg M, et al. Early diagnosis of amyotrophic lateral sclerosis by threshold tracking and conventional transcranial magnetic stimulation. Eur J Neurol 2021;28(9):3030-9.

347. Tankisi H, Pia H, Strunge K, Howells J, Cengiz B, Samusyte G, et al. Three different short-interval intracortical inhibition methods in early diagnosis of amyotrophic lateral sclerosis. Amyotroph Lateral Scler Frontotemporal Degener 2023;24(1-2):139-47.

348. Tergau F, Wanschura V, Canelo M, Wischer S, Wassermann EM, Ziemann U, et al. Complete suppression of voluntary motor drive during the silent period after transcranial magnetic stimulation. Exp Brain Res 1999;124(4):447-54.

349. Thakore NJ, Pioro EP. Laughter, crying and sadness in ALS. J Neurol Neurosurg Psychiatry 2017;88(10):825-31.

350. Tian D, Izumi S-i, Suzuki E. Modulation of Interhemispheric Inhibition between Primary Motor Cortices Induced by Manual Motor Imitation: A Transcranial Magnetic Stimulation Study. Brain Sciences 2021;11:266.

351. Tohgi H, Abe T, Yamazaki K, Murata T, Ishizaki E, Isobe C. Remarkable increase in cerebrospinal fluid 3-nitrotyrosine in patients with sporadic amyotrophic lateral sclerosis. Ann Neurol 1999;46(1):129-31.

352. Tomsic M. Assessing cognitive decline in ALS: Portuguese adaptation of the Edinburgh Cognitive and Behavioural ALS Screen (ECAS). University of Lisbon; 2015.

353. Triggs WJ, Calvanio R, Levine M. Transcranial magnetic stimulation reveals a hemispheric asymmetry correlate of intermanual differences in motor performance. Neuropsychologia 1997;35(10):1355-63.

354. Triggs WJ, Macdonell RA, Cros D, Chiappa KH, Shahani BT, Day BJ. Motor inhibition and excitation are independent effects of magnetic cortical stimulation. Ann Neurol 1992;32(3):345-51.

355. Triggs WJ, Menkes D, Onorato J, Yan RS, Young MS, Newell K, et al. Transcranial magnetic stimulation identifies upper motor neuron involvement in motor neuron disease. Neurology 1999;53(3):605-11.

356. Turner MR, Barohn RJ, Corcia P, Fink JK, Harms MB, Kiernan MC, et al. Primary lateral sclerosis: consensus diagnostic criteria. J Neurol Neurosurg Psychiatry 2020;91(4):373-7.

357. Turner MR, Kiernan MC. Does interneuronal dysfunction contribute to neurodegeneration in amyotrophic lateral sclerosis? Amyotroph Lateral Scler 2012;13(3):245-50.

358. Turner MR, Wicks P, Brownstein CA, Massagli MP, Toronjo M, Talbot K, et al. Concordance between site of onset and limb dominance in amyotrophic lateral sclerosis. J Neurol Neurosurg Psychiatry 2011;82(8):853-4.

359. Uchida A, Sasaguri H, Kimura N, Tajiri M, Ohkubo T, Ono F, et al. Non-human primate model of amyotrophic lateral sclerosis with cytoplasmic mislocalization of TDP-43. Brain 2012;135(Pt 3):833-46.

360. Ugawa Y, Hanajima R, Kanazawa I. Interhemispheric facilitation of the hand area of the human motor cortex. Neurosci Lett 1993;160(2):153-5.

361. Uncini A, Kujirai T, Gluck B, Pullman S. Silent period induced by cutaneous stimulation. Electroencephalogr Clin Neurophysiol 1991;81(5):344-52.

362. Urban PP, Solinski M, Best C, Rolke R, Hopf HC, Dieterich M. Different short-term modulation of cortical motor output to distal and proximal upper-limb muscles during painful sensory nerve stimulation. Muscle Nerve 2004;29(5):663-9.

363. Uttner I, Mai N, Esslinger O, Danek A. Quantitative evaluation of mirror movements in adults with focal brain lesions. Eur J Neurol 2005;12(12):964-75.

364. Valero-Cabré A, Amengual JL, Stengel C, Pascual-Leone A, Coubard OA. Transcranial magnetic stimulation in basic and clinical neuroscience: A comprehensive review of fundamental principles and novel insights. Neurosci Biobehav Rev 2017;83:381-404.

365. Valls-Sole J, Alvarez R, Tolosa ES. Vibration-induced presynaptic inhibition of the soleus H reflex is temporarily reduced by cortical magnetic stimulation in human subjects. Neuroscience Letters 1994;170(1):149-52.

366. Valls-Solé J, Pascual-Leone A, Wassermann EM, Hallett M. Human motor evoked responses to paired transcranial magnetic stimuli. Electroencephalogr Clin Neurophysiol 1992;85(6):355-64.

367. Van Deerlin VM, Leverenz JB, Bekris LM, Bird TD, Yuan W, Elman LB, et al. TARDBP mutations in amyotrophic lateral sclerosis with TDP-43 neuropathology: a genetic and histopathological analysis. Lancet Neurol 2008;7(5):409-16.

368. van den Bos MAJ, Higashihara M, Geevasinga N, Menon P, Kiernan MC, Vucic S. Pathophysiological associations of transcallosal dysfunction in ALS. Eur J Neurol 2021;28(4):1172-80.

369. Van den Bos MAJ, Menon P, Howells J, Geevasinga N, Kiernan MC, Vucic S. Physiological Processes Underlying Short Interval Intracortical Facilitation in the Human Motor Cortex. Front Neurosci 2018;12:240.

370. Vardy AN, Daffertshofer A, Ridderikhoff A, Beek PJ. Differential after-effects of bimanual activity on mirror movements. Neurosci Lett 2007;416(2):117-22.

371. Vermeiren Y, Janssens J, Van Dam D, De Deyn PP. Serotonergic Dysfunction in Amyotrophic Lateral Sclerosis and Parkinson's Disease: Similar Mechanisms, Dissimilar Outcomes. Front Neurosci 2018;12:185.

372. Verschueren A, Grapperon AM, Delmont E, Attarian S. Prevalence of spasticity and spasticity-related pain among patients with Amyotrophic Lateral Sclerosis. Revue Neurologique 2021;177(6):694-8.

373. Vidovic M, Muschen LH, Brakemeier S, Machetanz G, Naumann M, Castro-Gomez S. Current State and Future Directions in the Diagnosis of Amyotrophic Lateral Sclerosis. Cells 2023;12(5):736.

374. Vucic S, Cheah BC, Kiernan MC. Defining the mechanisms that underlie cortical hyperexcitability in amyotrophic lateral sclerosis. Exp Neurol 2009;220(1):177-82.

375. Vucic S, Cheah BC, Yiannikas C, Kiernan MC. Cortical excitability distinguishes ALS from mimic disorders. Clin Neurophysiol 2011;122(9):1860-6.

376. Vucic S, Ferguson TA, Cummings C, Hotchkin MT, Genge A, Glanzman R, et al. Gold Coast diagnostic criteria: Implications for ALS diagnosis and clinical trial enrollment. Muscle Nerve 2021;64(5):532-7.

377. Vucic S, Kiernan MC. Novel threshold tracking techniques suggest that cortical hyperexcitability is an early feature of motor neuron disease. Brain 2006;129(Pt 9):2436-46.

378. Vucic S, Kiernan MC. Abnormalities in cortical and peripheral excitability in flail arm variant amyotrophic lateral sclerosis. J Neurol Neurosurg Psychiatry 2007;78(8):849-52.

379. Vucic S, Kiernan MC. Cortical excitability testing distinguishes Kennedy's disease from amyotrophic lateral sclerosis. Clin Neurophysiol 2008;119(5):1088-96.

380. Vucic S, Kiernan MC. Utility of transcranial magnetic stimulation in delineating amyotrophic lateral sclerosis pathophysiology. Handb Clin Neurol 2013;116:561-75.

381. Vucic S, Nicholson GA, Kiernan MC. Cortical hyperexcitability may precede the onset of familial amyotrophic lateral sclerosis. Brain 2008;131(Pt 6):1540-50.

382. Vucic S, Nicholson GA, Kiernan MC. Cortical excitability in hereditary motor neuronopathy with pyramidal signs: comparison with ALS. J Neurol Neurosurg Psychiatry 2010;81(1):97-100.

383. Vucic S, Stanley Chen KH, Kiernan MC, Hallett M, Benninger DH, Di Lazzaro V, et al. Clinical diagnostic utility of transcranial magnetic stimulation in neurological disorders. Updated report of an IFCN committee. Clin Neurophysiol 2023;150:131-75.

384. Vucic S, Ziemann U, Eisen A, Hallett M, Kiernan MC. Transcranial magnetic stimulation and amyotrophic lateral sclerosis: pathophysiological insights. J Neurol Neurosurg Psychiatry 2013;84(10):1161-70.

385. Wainger BJ, Macklin EA, Vucic S, McIlduff CE, Paganoni S, Maragakis NJ, et al. Effect of Ezogabine on Cortical and Spinal Motor Neuron Excitability in Amyotrophic Lateral Sclerosis: A Randomized Clinical Trial. JAMA Neurol 2021;78(2):186-96.

386. Welniarz Q, Dusart I, Gallea C, Roze E. One hand clapping: lateralization of motor control. Front Neuroanat 2015;9:75.

387. Werhahn KJ, Kunesch E, Noachtar S, Benecke R, Classen J. Differential effects on motorcortical inhibition induced by blockade of GABA uptake in humans. J Physiol 1999;517 (Pt 2)(Pt 2):591-7.

388. Wijesekera LC, Leigh PN. Amyotrophic lateral sclerosis. Orphanet J Rare Dis 2009;4:3.

389. Wilke S, Groenveld D, Grittner U, List J, Flöel A. cSPider – Evaluation of a Free and Open-Source Automated Tool to Analyze Corticomotor Silent Period. PLoS One 2016;11(6):e0156066.

390. Wittstock M, Meister S, Walter U, Benecke R, Wolters A. Mirror movements in amyotrophic lateral sclerosis. Amyotroph Lateral Scler 2011;12(6):393-7.

391. Wittstock M, Wilde N, Grossmann A, Kasper E, Teipel S. Mirror Movements in Amyotrophic Lateral Sclerosis: A Combined Study Using Diffusion Tensor Imaging and Transcranial Magnetic Stimulation. Front Neurol 2020;11:164.

392. Wittstock M, Wolters A, Benecke R. Transcallosal inhibition in amyotrophic lateral sclerosis. Clin Neurophysiol 2007;118(2):301-7.

393. Wolf J, Safer A, Wohrle JC, Palm F, Nix WA, Maschke M, et al. Factors predicting one-year mortality in amyotrophic lateral sclerosis patients--data from a population-based registry. BMC Neurol 2014;14:197.

394. Woods BT, Teuber HL. Mirror movements after childhood hemiparesis. Neurology 1978;28(11):1152-7.

395. World Medical A. World Medical Association Declaration of Helsinki: ethical principles for medical research involving human subjects. Jama 2013;310(20):2191-4.

396. Writing Group On Behalf Of The Edaravone Als 19 Study G. Open-label 24-week extension study of edaravone (MCI-186) in amyotrophic lateral sclerosis. Amyotroph Lateral Scler Frontotemporal Degener 2017;18(sup1):55-63.

397. Xiao S, McLean J, Robertson J. Neuronal intermediate filaments and ALS: a new look at an old question. Biochim Biophys Acta 2006;1762(11-12):1001-12.

398. Xu L, Liu T, Liu L, Yao X, Chen L, Fan D, et al. Global variation in prevalence and incidence of amyotrophic lateral sclerosis: a systematic review and meta-analysis. J Neurol 2020;267(4):944-53.

399. Yamauchi H, Fukuyama H, Ouchi Y, Nagahama Y, Kimura J, Asato R, et al. Corpus callosum atrophy in amyotrophic lateral sclerosis. J Neurol Sci 1995;134(1-2):189-96.

400. Yokota T, Yoshino A, Inaba A, Saito Y. Double cortical stimulation in amyotrophic lateral sclerosis. J Neurol Neurosurg Psychiatry 1996;61(6):596-600.

401. Zanette G, Tamburin S, Manganotti P, Refatti N, Forgione A, Rizzuto N. Changes in motor cortex inhibition over time in patients with amyotrophic lateral sclerosis. J Neurol 2002a;249(12):1723-8.

402. Zanette G, Tamburin S, Manganotti P, Refatti N, Forgione A, Rizzuto N. Different mechanisms contribute to motor cortex hyperexcitability in amyotrophic lateral sclerosis. Clin Neurophysiol 2002b;113(11):1688-97.

403. Zarei S, Carr K, Reiley L, Diaz K, Guerra O, Altamirano PF, et al. A comprehensive review of amyotrophic lateral sclerosis. Surg Neurol Int 2015;6:171.

404. Zhao J, Wang X, Huo Z, Chen Y, Liu J, Zhao Z, et al. The Impact of Mitochondrial Dysfunction in Amyotrophic Lateral Sclerosis. Cells 2022;11(13).

405. Zheng X, Wang S, Huang J, Lin J, Yang T, Xiao Y, et al. Physical activity as risk factor in amyotrophic lateral sclerosis: a systematic review and meta-analysis. J Neurol 2023;270(5):2438-50.

406. Ziemann U. Pharmacology of TMS. Suppl Clin Neurophysiol 2003;56:226-31.

407. Ziemann U. Cortical threshold and excitability measurements. In: Eisen A, editor. Handbook of Clinical Neurophysiology. 4: Elsevier; 2004. p. 317-35.

408. Ziemann U, Netz J, Szelényi A, Hömberg V. Spinal and supraspinal mechanisms contribute to the silent period in the contracting soleus muscle after transcranial magnetic stimulation of human motor cortex. Neurosci Lett 1993;156(1-2):167-71.

409. Ziemann U, Rothwell JC, Ridding MC. Interaction between intracortical inhibition and facilitation in human motor cortex. J Physiol 1996;496 (Pt 3)(Pt 3):873-81.

410. Ziemann U, Winter M, Reimers CD, Reimers K, Tergau F, Paulus W. Impaired motor cortex inhibition in patients with amyotrophic lateral sclerosis. Evidence from paired transcranial magnetic stimulation. Neurology 1997;49(5):1292-8.

411. Zou ZY, Zhou ZR, Che CH, Liu CY, He RL, Huang HP. Genetic epidemiology of amyotrophic lateral sclerosis: a systematic review and meta-analysis. J Neurol Neurosurg Psychiatry 2017;88(7):540-9.

11. Appendix

Study III – Supplementary materials

Code for the 3 kHz Sampling Frequency

```
a1 = readtable('EMGMON__001_R.txt');% Reads the text file containing the EMG signal of the muscle contracting.
x1 = a1{: ,:} ';
abs11 = abs(x1); % Obtaining the signal 's absolute value
a2 = readtable('EMGMON__001_C.txt'); % Reads the text file of the corresponding contralateral muscle.
x2 = a2{: ,:} ';
abs21 = abs(x2); % Obtaining the signal 's absolute value


% Studying of the signal corresponding to the Muscle Contraction
window = 150; % Window utilised for the Root Mean Square
envelope11 = sqrt(movmean((abs11.^2) ,window)); % Performing of the Root Mean Square on the data , obtaining its envelope
diferenca11 = zeros(1 ,29999); % Initialization of a Vector with the same size as the data
for i1=1:29999 % For cycle which lets us store the differences between subsequent data points, which is later needed
diferenca11(1,i1) = envelope11(1,i1+1) -envelope11(1,i1);
end
absdiferenca11 = abs(diferenca11); % Absolute value of said difference
MCD1 = mean(absdiferenca11 (1:29999) ); % Mean of the absolute value of the differences between subsequent points
EMG1 = mean(abs11(1 ,1:29999)); % Mean of the absolute value of the EMG signal
thresholdA1=EMG1+(2.66*MCD1); % Calculating the first Threshold needed
envelope12 = sqrt(movmean((abs21.^2) ,window));

% Finding the Beginning of the EMG Signal

% Point from where the signal goes above ThresholdA , and the contraction is already happening
encontrado11 = false; % Initialization of a Boolean variable as False , which stores whether the desired point has been obtained
for i1 = 1:30000 % For cycle that ranges from 1 to the number of data points registered
if envelope11(1,i1)>thresholdA1 && encontrado11 == false % If the said envelope 's data point value is larger then ThresholdA , and if the Boolean Variable is still False , it will continue its search
thresholdB1 = mean(envelope11(1 ,1:i1)); % Computation of an intermediary Threshold based on the Envelope Values
thresholdC1 = thresholdB1 +2.66*MCD1; % Obtaining the Final Threshold needed
posicaoi1 = i1; % Variable to Store the Position being studied
encontrado41 = false; % Initialization of new Boolean Variable needed , which indicates the necessary conditions have been met
for l1 = posicaoi1:posicaoi1+300 % For cycle that ranges between the Data point stored previously (posicaoi1) and the 300 points that succeed it, to make sure the script does not get stuck on a random artifact of the signal
if envelope11(1,l1)<thresholdA1 && encontrado41 == false % If there is a point that goes below ThresholdA on the 300 points that succeed posicaoi1
encontrado41 = true; % Variable changes to the value True , not entering this if-clause until the cycle finishes running. end
end
```

```
if encontrado41 == false % If there is a point that goes below the ThresholdA mark on those 300 points that follow , this is not the point we want , therefore , we must study the next one, until we find one that meets the criteria
encontrado11 = true; % Enables the initial for cycle to continue its search
end
end
end

%Finding out where the Contraction is actually Starting
encontrado21 = false; % New Boolean variable initialized , to store whether or not the value corresponding to the beginning of the signal candidate has already been found
for j1 = 1:posicaoi1 % For cycle that ranges from 1 to the position obtained previously (point where the signal is bigger then ThresholdA)
posicaoj1 = 1;
if envelope11(1,j1)>thresholdC1 && encontrado21 == false % If the envelope value corresponding to j1 position goes above the ThresholdC , and a value meeting those criteria is yet to be found
posicaoj1 = j1;
encontrado21 = true; % If the envelope value corresponding to j1 position goes above the ThresholdC , and a value meeting those criteria is yet to be found
end
end
encontrado31 = false; % New Boolean Variable Initialized , to store whether or not there is a data point on the envelope that returns to a value below ThresholdC , which would make that point the start to the signal
for k1 = posicaoi1:-1:posicaoj1 % For cycle which ranges from posicaoj (where the signal is already bigger than ThresholdC) to posicaoi1
(where the signal goes below ThresholdA). This search is done backwards
if envelope11(1,k1)<thresholdC1 && encontrado31 == false % If a data point is found on that interval which goes below ThresholdC
comecosinal1 = k1; % Storing of that point as the beginning of the contraction of the Muscle
encontrado31 = true; % Making the script able to ignore this if clause , as the point desired has already been obtained
end
end
if encontrado31 == false % If no point in that range of indexes goes below ThresholdC again
comecosinal1 = posicaoj1; % The contraction begins on the posicaoj1 (where its corresponding value is the first point to be bigger than ThresholdC) , stored previously
end

% Finding the End of the EMG Signal
encontrado61 = false; % Initialization of a boolean variable that dictates whether or not the data point that represents the end of the Contraction has been found
for m1 = posicaoi1 :30000 % For cycle that ranges from posicaoi1 (where the signal goes below ThresholdA) and the last position of a existing data point (30000)
  if envelope11(1,m1) < thresholdA1 && encontrado61 == false % If the corresponding data point comes back to a value below ThresholdA
posicaom1 = m1; % Sinalization of said point as the candidate to represent the end of the contraction
encontrado81 = false; % Storing of a new Boolean variable that indicates if the necessary conditions are met or not
if posicaom1+1000 < 30000 % If the corresponding data point to our stored position plus 1000 is still within the limits of the number of data points
for o1 = posicaom1:posicaom1+1000 % For cycle which covers all those 1000 positions of data points and the position of the data point being studied
if envelope11(1,o1) > thresholdA1 && encontrado81 == false % If a data point with a position greater than the one being studied (over its next 1000 positions) goes once again below ThresholdA
encontrado81 = true; % The conditions are not met, and the Boolean variable encontrado81 is changed to True
end
end
if encontrado81 == false % If the conditions are met
```

```
encontrado61 = true; % The data point chosen is correct , representing the end of the contraction. encontrado61 is changed to True , meaning the final data point has been found. The first if clause never runs again , and the for cycle ends
end
end
end
end

% Converting the positions to the corresponding latency , bearing in mind the sampling frequency utilised
temposinal1 = (comecosinal1 /3000); % Start of the contraction
disp('Active Muscle Latency (in s):');
disp(temposinal1);


mean1 = trapz(envelope11(comecosinal1:posicaom1)); % Performance of a Trapezoidal Numeric Integration of the RMS values
mean2 = trapz(envelope12(comecosinal1:posicaom1)); % Performance of a Trapezoidal Numeric Integration of the RMS values
disp('Active Muscle Amplitude');
disp(mean1);
percentage1 = (mean2/mean1)*100; % Signal percentage that exists on the the original contraction versus its corresponding mirror movement
disp('Mirror Muscle Amplitude (in percentage):');
disp(percentage1);

% Plotting of the 4 graphs , both signals and its corresponding envelopes
ax1 = subplot(2 ,2 ,1);
plot(abs11);
xline(comecosinal1);
xline(posicaom1);
title('Active Muscle - Absolute Value of EMG');
ax2 = subplot(2 ,2 ,2);
plot(envelope11);
yline(thresholdA1);
yline(thresholdC1);
xline(comecosinal1);
xline(posicaom1);
title('Active Muscle - RMS');
ax3 = subplot(2 ,2 ,3);
plot(abs21);
xline(comecosinal1);
xline(posicaom1);
title('Mirror Muscle - Absolute Value of EMG');
ax4 = subplot(2 ,2 ,4);
plot(envelope12);
xline(comecosinal1);
xline(posicaom1);
title('Mirror Muscle - RMS');
linkaxes([ax1 ax3]);
linkaxes([ax2 ax4]);
```

Code for the 24 kHz Sampling Frequency

```
a1 = readtable('EMGMON__001_R.txt'); % Reads the text file containing the EMG signal of the muscle contracting.
x1 = a1{: ,:} ';
abs11 = abs(x1); % Obtaining the signal 's absolute value
a2 = readtable('EMGMON__001_C.txt'); % Reads the text file of the corresponding contralateral muscle.
x2 = a2{: ,:} ';
abs21 = abs(x2); % Obtaining the signal 's absolute value


% Studying of the signal corresponding to the Muscle Contraction
window = 1200; % Window utilised for the Root Mean Square
envelope11 = sqrt(movmean((abs11.^2) ,window)); % Performing of the Root Mean Square on the data , obtaining its envelope
diferenca11 = zeros(1 ,239999); % Initialization of a Vector with the same size as the data
for i1=1:239999 % For cycle which lets us store the differences between subsequent data points , which is later needed
diferenca11(1,i1) = envelope11(1,i1+1) -envelope11(1,i1);
end
absdiferenca11 = abs(diferenca11); % Absolute value of said difference
MCD1 = mean(absdiferenca11 (1:239999) ); % Mean of the absolute value of the differences between subsequent points
EMG1 = mean(abs11(1 ,1:239999)); % Mean of the absolute value of the EMG signal
thresholdA1=EMG1+(2.66*MCD1); % Calculating the first Threshold needed
envelope12 = sqrt(movmean((abs21.^2) ,window));

% Finding the Beginning of the EMG Signal

% Point from where the signal goes above ThresholdA , and the contraction is already happening
encontrado11 = false; % Initialization of a Boolean variable as False , which stores whether the desired point has been obtained
for i1 = 1:240000 % For cycle that ranges from 1 to the number of data points registered
if envelope11(1,i1)>thresholdA1 && encontrado11 == false % If the said envelope 's data point value is larger then ThresholdA , and if the Boolean Variable is still False , it will continue its search
thresholdB1 = mean(envelope11(1 ,1:i1)); % Computation of an intermediary Threshold based on the Envelope Values
thresholdC1 = thresholdB1 +2.66*MCD1; % Obtaining the Final Threshold needed
posicaoi1 = i1; % Variable to Store the Position being studied
encontrado41 = false; % Initialization of new Boolean Variable needed , which indicates the necessary conditions have been met
for l1 = posicaoi1:posicaoi1+2400 % For cycle that ranges between the Data point stored previously (posicaoi1) and the 2400 points that succeed it, to make sure the script does not get stuck on a random artifact of the signal
if envelope11(1,l1)<thresholdA1 && encontrado41 == false % If there is a point that goes below ThresholdA on the 2400 points that succeed posicaoi1
encontrado41 = true; % Variable changes to the value True , not entering this if-clause until the cycle finishes running.
end
end
if encontrado41 == false % If there is a point that goes below the ThresholdA mark on those 2400 points that follow , this is not the point we want , therefore , we must study the next one, until we find one that meets the criteria
encontrado11 = true; % Enables the initial for cycle to continue its search
end
end
end

```

```
%Finding out where the Contraction is actually Starting
encontrado21 = false; % New Boolean variable initialized , to store whether or not the value
        corresponding to the beginning of the signal candidate has already been found
for j1 = 1:posicaoi1 % For cycle that ranges from 1 to the position obtained previously (point where
        the signal is bigger then ThresholdA)
posicaoj1 = 1;
if envelope11(1,j1)>thresholdC1 && encontrado21 == false % If the envelope value
        corresponding to j1 position goes above the ThresholdC , and a value meeting those
        criteria is yet to be found
posicaoj1 = j1; % Storing of that position on a new variable
encontrado21 = true; % Boolean variable is now True , which means this if clause will not run again
unnecessarily
end
end
encontrado31 = false; % New Boolean Variable Initialized , to store whether or not there is a data point
        on the envelope that returns to a value below ThresholdC , which would make that point the start
        to the signal
for k1 = posicaoi1:-1:posicaoj1 % For cycle which ranges from posicaoj (where the signal is already
        bigger than ThresholdC) to posicaoi1
        (where the signal goes below ThresholdA). This search is done backwards
if envelope11(1,k1)<thresholdC1 && encontrado31 == false % If a data point is found on that interval
which goes below ThresholdC
comecosinal1 = k1; % Storing of that point as the beginning of the contraction of the Muscle
encontrado31 = true; % Making the script able to ignore this if clause , as the point desired has already
been obtained
end
end
if encontrado31 == false % If no point in that range of indexes goes below ThresholdC again
comecosinal1 = posicaoj1; % The contraction begins on the posicaoj1 (where its corresponding value is
        the first point to be bigger than ThresholdC) , stored previously
end

% Finding the End of the EMG Signal
encontrado61 = false; % Initialization of a boolean variable that dictates whether or not the data point
        that represents the end of the Contraction has been found
for m1 = posicaoi1 :240000 % For cycle that ranges from posicaoi1 (where the signal goes below
        ThresholdA) and the last position of a existing data point (240000)
if envelope11(1,m1) < thresholdA1 && encontrado61 == false % If the corresponding
data point comes back to a value below ThresholdA
posicaom1 = m1; % Sinalization of said point as the candidate to represent the end of the
contraction
encontrado81 = false; % Storing of a new Boolean variable that indicates if the necessary conditions are
met or not
if posicaom1+8000 < 240000 % If the corresponding data point to our stored position plus 8000 is still
within the limits of the number of data points
for o1 = posicaom1:posicaom1+8000 % For cycle which covers all those 8000 positions of data points
        and the position of the data point being studied
if envelope11(1,o1) > thresholdA1 && encontrado81 == false % If a data point with a position greater
        than the one being studied (over its next 8000 positions) goes once again below ThresholdA
encontrado81 = true; % The conditions are not met, and the Boolean variable encontrado81 is
changed to True
end
end
if encontrado81 == false % If the conditions are met encontrado61 = true; % The data point chosen is
correct , representing the end of the contraction. encontrado61 is changed to True , meaning the final data
point has been found. The first if clause never runs again , and the for cycle ends
end
end
end
end

% Converting the positions to the corresponding latency , bearing in mind the sampling
```

```
        frequency utilised
temposinal1 = (comecosinal1 /24000); % Start of the contraction
disp('Active Muscle Latency (in s):');
disp(temposinal1);


mean1 = trapz(envelope11(comecosinal1:posicaom1)); % Performance of a Trapezoidal
        Numeric Integration of the RMS values
mean2 = trapz(envelope12(comecosinal1:posicaom1)); % Performance of a Trapezoidal
        Numeric Integration of the RMS values
disp('Active Muscle Amplitude');
disp(mean1);
percentage1 = (mean2/mean1)*100; % Signal percentage that exists on the the original contraction
versus its corresponding mirror movement
disp('Mirror Muscle Amplitude (in percentage):');
disp(percentage1);

% Plotting of the 4 graphs , both signals and its corresponding envelopes
ax1 = subplot(2 ,2 ,1);
plot(abs11);
xline(comecosinal1);
xline(posicaom1);
title('Active Muscle - Absolute Value of EMG');
ax2 = subplot(2 ,2 ,2);
plot(envelope11);
yline(thresholdA1);
yline(thresholdC1);
xline(comecosinal1);
xline(posicaom1);
title('Active Muscle - RMS');
ax3 = subplot(2 ,2 ,3);
plot(abs21);
xline(comecosinal1);
xline(posicaom1);
title('Mirror Muscle - Absolute Value of EMG');
ax4 = subplot(2 ,2 ,4);
plot(envelope12);
xline(comecosinal1);
xline(posicaom1);
title('Mirror Muscle - RMS');
linkaxes([ax1 ax3]);
linkaxes([ax2 ax4]);
```